THE JOURNAL
OF
CHEMICAL PHYSICS

VOLUME 10 OCTOBER, 1942 NUMBER 10

The Double Minimum Problem Applied to Potassium Hydrogen Fluoride

GEORGE GLOCKLER AND GEORGE E. EVANS
University of Iowa, Iowa City, Iowa

(Received July 20, 1942)

The doublet character of the infra-red absorption line at 2.67μ of solid potassium hydrogen fluoride is due to the "tunnel effect." The proton has two potential minima between the fluorine nuclei in the FHF^- ion. The distance of a minimum to the center of the ion is 0.26A. The height of the potential hill is 33,400 calories.

THE infra-red absorption line of solid potassium hydrogen fluoride at 2.67μ has been found to have doublet character by Buswell, Maycock, and Rodebush.[1] The two lines are located at 2.649μ (3775.0 cm^{-1}) and 2.729μ (3664.4 cm^{-1}). Buswell *et al.* suggested that this doublet nature might be due to the "tunnel effect" on the supposition that the proton may oscillate between two potential minima located between the two fluorine nuclei and equidistant from a plane at right angles to the figure axis of the FHF^- ion at its midpoint.

A similar case in the ammonia molecule has been studied by several authors[2-4] with a variety of potential energy expressions. The values of the total energy given by Wall and Glockler have been applied to the present case, after having solved them for all possible values of the parameter q. This quantity is given by

$$q^2=(4\pi^2\mu\nu_0 l^2)/h, \tag{1}$$

where μ is (1/38+1/1.008) or 0.982, ν_0 is the average fundamental frequency (3719.7 cm^{-1}), l is the distance from the center of the ion to the potential minimum, and h is Planck's constant. For the purpose of calculation the following abbreviations have been used:

$$A=4q^2/(\pi)^{\frac{1}{2}}\int_0^{-q}\exp(-n^2)dn;$$

$$B=4/(\pi)^{\frac{1}{2}}q\cdot\exp(-q^2);$$

$$C=\exp(-q^2);$$

$$D=(1-2q^2)\exp(-q^2).$$

$$W_{OS}/h\nu_0=\tfrac{1}{2}[1+(2q^2-A-B)/(1+C)]; \tag{2}$$

$$W_{OA}/h\nu_0=\tfrac{1}{2}[1+(2q^2-A)/(1-C)]; \tag{3}$$

$$W_{IS}/h\nu_0=\tfrac{3}{2}[1+(2q^2-A-Bq^2)/(3-3D)]; \tag{4}$$

$$W_{IA}/h\nu_0=\tfrac{3}{2}[1+(2q^2-A-2B+Bq^2)/(3+3D)]. \tag{5}$$

The calculated values are shown in Fig. 1. The doublet separation is given by

$$\Delta h\nu_0=W_{IA}-W_{IS}+W_{OA}-W_{OS} \tag{6}$$

and is plotted as a function of q in Fig. 2. From this graph a value of q can be found from the experimental doublet separation $\Delta h\nu_0/h\nu_0=(3775.0-3664.4)/3719.7=0.03$. In the present case q is 2.7. From Eq. (1), which can be written

$$l=5.805q/(\mu\nu_0)^{\frac{1}{2}}, \tag{1a}$$

the distance (l) from the center to the potential minimum is found to be 0.26 angstrom.

[1] A. M. Buswell, R. L. Maycock, and W. H. Rodebush, J. Phys. Chem. **8**, 362 (1940).
[2] F. Hund, Zeits. f. Physik **43**, 805 (1927).
[3] D. M. Dennison, Rev. Mod. Phys. **3**, 280 (1931).
[4] See F. T. Wall and G. Glockler, J. Chem. Phys. **5**, 314 (1937) for further literature references.

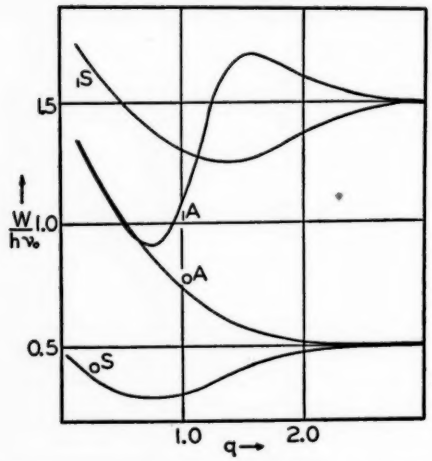

FIG. 1. Energy states (W) for double minimum problem. S=symmetric and A=antisymmetric levels; ν_0=fundamental frequency; q=coordinate. (Applicable for values of the parameter q greater than about 2.)

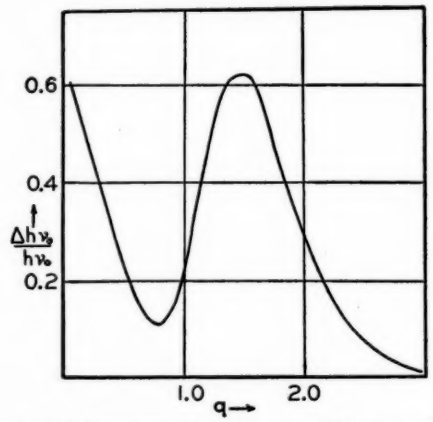

FIG. 2. Doublet separation in tunnel effect. ν_0=fundamental frequency; q=coordinate. (Applicable for values of the parameter q greater than about 2.)

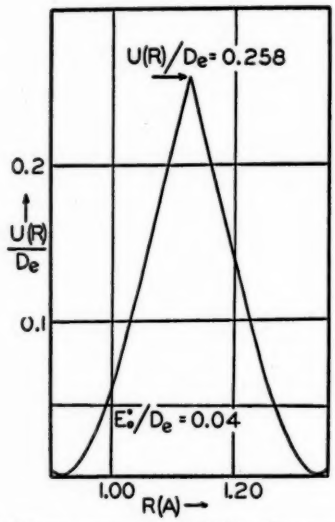

FIG. 3. Two Morse curves for HF. The F atom centers are 2.25A apart as in FHF^-. D_e=6.4 ev.

In order for the whole consideration to be valid this distance must check reasonably well with the dimensions of the FHF^- ion as obtained from other sources. The following information has been found on the size of this ion. Bozorth[5] studied the diffraction of x-rays from potassium hydrogen fluoride and found the F−F distance to be 2.25 angstroms. He could not obtain the H−F distance since protons usually do not scatter x-rays sufficiently to be observed. The distance from the center of the ion to a fluorine nucleus is then 1.13A. Another value may be obtained from the application of the theory of small vibrations to the triatomic FHF^- ion. The line at 2.67μ is considered to be the asymmetric frequency:

$$\nu_3=[(k.p)/m]^{\frac{1}{2}}=3719.7\ \text{cm}^{-1},$$

where k=force constant, m=mass of fluorine atom, M=mass of hydrogen, and $p=(2m+M)/m$. The simple valency force field has been used.[6] The force constant calculated is 0.4 megadyne per cm. An application of Badger's rule[7] to the hydrides of the first row of the periodic table shows that the rule holds very well and permits the calculation of the H−F distance in FHF^- from the force constant. The value[8] obtained is 1.15A which is, however, the distance from the center of the ion to a fluorine nucleus, because it is assumed in the application of the theory of small vibrations that the hydrogen atom resides midway between the fluorine nuclei and nothing in this calculation indicates two potential minima. Hence the half-distance between the fluorine atoms is 1.13A from crystal structure study and 1.15A from spectroscopy via the theory of small vibrations. The average of 1.14A will be taken for the next consideration. Since the distance from the center of the ion to the potential minimum has been estimated to be 0.26A, the H−F distance is 0.88A. This value does not seem unreasonable when compared with the H−F distance in monomeric hydrogen

[5] R. M. Bozorth, J. Am. Chem. Soc. **45**, 2128 (1923).
[6] K. W. F. Kohlrausch, *Der Smekal-Raman Effekt* (*Ergänzungsband*) (Julius Springer, Berlin, 1938), p. 64.
[7] R. M. Badger, J. Chem. Phys. **2**, 128 (1934); **3**, 710 (1935).
[8] Unpublished results.

fluoride, 0.92A, obtained from its band spectroscopy.[9] Another way of making the comparison is to say that the distance (l) from the ion center to the potential minimum would be 0.22A (1.14−0.92) if the proton remains at the same equilibrium distance from the fluorine nucleus in the FHF^- ion as in HF. These various possibilities are summarized in Table I. It appears that these values check sufficiently well to warrant the belief that the doublet under consideration is due to the "tunnel effect." It is to be expected in FHF^- and a further calculation of the potential hill also favors this view. The height of the potential barrier can be obtained from

$$V_{x=0}=\tfrac{1}{2}(h\nu_0 q^2)=38{,}750 \text{ cal./mole},$$

with $\nu_0=3719.7$ cm^{-1} and $q=2.7$. The zero-point energy is one-half the fundamental frequency ν_3 multiplied by Planck's constant and amounts to 5316 calories. The barrier has a value of 33,400 calories. This quantity can be compared with the potential hill formed when two Morse curves for HF are approached in such a way as to make the F−F distance 2.25A (see Fig. 3). The height calculated is 38,065 calories/mole. For the Morse curve[10] the data on HF given by Herzberg[9] were used. The heat of dissociation of HF is 6.4 ev and $\omega_e=4141.305$ cm^{-1}. The zero-point energy is calculated to be 5918 cal./mole. Hence the potential hill intervening is 32,150 calories/mole. This height is of the same order as the barrier in FHF^- as was to be expected. The problem of the FHF^- ion has been discussed by Pauling.[11]

TABLE I.

		Distance	Remarks
a	½ (F–F)	1.13A	Crystal structure of KHF_2
b	H–F	1.15	$k=0.4$ megadyne/cm from 3719.7 cm^{-1} and Badger's rule (Really ½ (F–F) distance!)
c	½ (F–F)	1.14	Average: *a* and *b*
d	H–F	0.92	In HF monomer (band spectra)
e	*l*	0.22	*c* minus *d*
f	*l*	0.26	Tunnel effect
g	H–F	0.88	HF distance in FHF^-; *c* minus *f*.

[9] G. Herzberg, *Molecular Spectra and Molecular Structure* (Prentice-Hall, Inc., New York, 1939), p. 488.

[10] Reference 9, pp. 108–9.

[11] L. Pauling, *The Nature of the Chemical Bond* (Cornell University Press, Ithaca, New York, 1940), second edition, chapter 9.

OCTOBER, 1942 JOURNAL OF CHEMICAL PHYSICS VOLUME 10

The Elimination of Errors due to Electrode Polarization in Measurements of the Dielectric Constants of Electrolytes

THOMAS M. SHAW
Western Regional Research Laboratory, Bureau of Agricultural Chemistry and Engineering, U. S. Department of Agriculture, Albany, California

(Received July 6, 1942)

An investigation was made of the errors resulting from electrode polarization in measurements of the dielectric constants of solutions containing electrolytes. The applicability of two methods, one used by Fricke and Curtis and the other by Oncley, to eliminate these errors, was considered. There is introduced a modification of Oncley's method, which was found applicable at higher electrolyte concentrations than Oncley's method. The relative effectiveness of the modified method and that of Fricke and Curtis was tested by employing the two methods to correct experimental data obtained for aqueous solutions of glycine containing various amounts of electrolytes. The measurements were made at frequencies ranging from 10 to 5000 kc, and at conductivities ranging from 0.29×10^{-4} to 1.74×10^{-4} ohm^{-1} cm^{-1}. The corrected values of the dielectric constant were compared with known values in the literature and found to be in good agreement. The limitations of the methods are considered and the usefulness of the methods in cases where the dielectric constant varies with frequency is discussed.

I. INTRODUCTION

THE polarization of dielectric constant cell electrodes is an important source of error in the determination of the dielectric properties of dilute electrolyte solutions. This phenomenon becomes increasingly important as the frequency is lowered and as the conductivity of the solution is raised. Where precise dielectric constant

determinations are desired steps must be taken either to reduce the magnitude of the polarization to the point where it may be neglected or appropriate correction measures must be employed. It is a common practice to reduce the amount of polarization by using platinized electrodes and for many purposes this procedure constitutes an acceptable solution to the difficulty.

For measurements on biological systems platinized electrodes have several disadvantages. They require frequent rechecking because of the instability of the platinization and they may effect, catalytically, a change in the system under investigation.[1] Furthermore, even though platinized electrodes are used, for precise measurements at low frequencies electrode polarization may still be significant. For these reasons the elimination of electrode polarization errors for bare platinum electrodes was investigated.

Aqueous solutions of glycine, containing known amounts of electrolytes, were studied. Two methods were employed to correct the experimental data for electrode polarization. As a test of the effectiveness of the polarization correction methods the dielectric constants calculated from the experimental measurements were compared with known values.

II. ELECTRODE POLARIZATION CORRECTION METHODS

The problem of correcting dielectric cell capacitance measurements for electrode polarization capacity is complicated by the fact that the frequency dependence of the polarization capacitance is not definitely known. Although it varies with the kind of electrodes and with the solution used, the polarization capacitance C_p, for limited ranges of frequency, can usually be expressed by an equation of the form

$$C_p = M\nu^{-m}, \tag{1}$$

where ν is the frequency, and M and m are empirical constants.[2]

When the capacitance of a dielectric cell is measured it is usually represented electrically in terms of an equivalent parallel capacitance C. This capacitance is thus a measure of both the electrode polarization capacitance and the capacitance of the solution contained between the cell electrodes. In general the dielectric constant of the solution depends on the frequency of measurement,[3] and this of course causes a corresponding dependence of the capacitance of the solution contained between the cell electrodes. Since the polarization capacitance of the electrodes is also frequency dependent, as Eq. (1) indicates, the variation of the cell capacitance with changes in frequency may be exceedingly complex.

Two methods have been used to treat the problem of electrode polarization effects in the measurement of dielectric constants of solutions. The first method to be discussed was described by Fricke and Curtis,[4] and was used in a study of the dielectric properties of suspensions. In their work platinized electrodes were used but the method, in principle, is applicable to either bare or platinized electrodes. The second method was described by Oncley[5] and was used in studies of the dielectric properties of protein solutions using a cell with sandblasted platinum electrodes.

In the method described by Fricke and Curtis measurements of the capacitance of the dielectric cell are made for two different spacings of the cell electrodes. When this is done the dielectric constant of the solution can be obtained without knowing the absolute value of the polarization capacitance. The latter appears only as a parameter in the calculations, and is eliminated.

The dielectric constant ϵ of the solution is calculated from the measured capacitances C_1 and C_2, corresponding to the electrode spacings d_1 and d_2, by means of the equation[6]

$$\epsilon = [d_2^2(C_2 - C_0) - d_1^2(C_1 - C_0)]/[K(d_2 - d_1)]. \tag{2}$$

Here C_0 and K are constants for the particular dielectric cell. Their significance and evaluation are discussed in Section III of this paper.

Oncley's method, referred to previously, makes use of an empirical equation to correct for electrode polarization. The dielectric constant is

[1] J. W. Mehl and C. L. A. Schmidt, J. Gen. Physiol. **18**, 467 (1935).
[2] I. Wolfe, Phys. Rev. **27**, 755 (1926).
[3] P. Debye, *Polar Molecules* (Chemical Catalogue Company, New York, New York, 1929).
[4] H. Fricke and H. J. Curtis, J. Phys. Chem. **41**, 729 (1937).
[5] J. L. Oncley, J. Am. Chem. Soc. **60**, 1115 (1938).
[6] A derivation of this equation and a statement of the conditions under which it is valid are given in the Appendix to this paper.

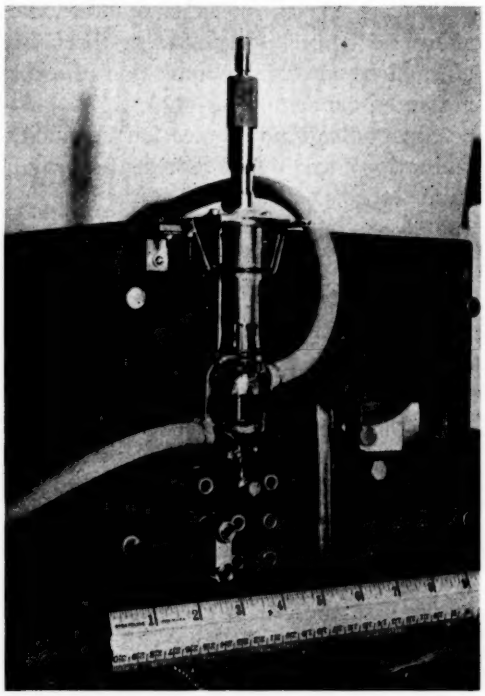

FIG. 1. Photograph of micrometer type cell showing lead and switching arrangement.

calculated by means of the equation,[6]

$$\epsilon=(C-C_0-AG^2\nu^{-\frac{1}{2}})d/K, \qquad (3)$$

where C is the observed cell capacitance for an electrode spacing d, C_0 and K are constants of the cell, and $AG^2\nu^{-\frac{1}{2}}$ is the correction term for polarization. In the correction term, G is the cell conductance, ν is the frequency, and A is a constant for the solution under consideration. The value of A is the slope of the straight line obtained when $(C-C_0)$ is plotted against $G^2\nu^{-\frac{1}{2}}$ in a frequency region where the dielectric constant does not vary. When measurements are extended to a region where the dielectric constant varies with frequency, it is assumed that the same value of A still prevails.

Oncley found that the polarization term $AG^2\nu^{-\frac{1}{2}}$ allowed accurate corrections for electrode polarization to be made only for frequencies greater than 25 kc. For lower frequencies it was found that the simple correction term $AG^2\nu^{-\frac{1}{2}}$ was not valid and the curves were no longer linear.

In a recent paper Smiley and Smith[7] have reported a study of electrode polarization in the frequency range 1 to 30 kc. These authors conclude from their studies, as reported by Ferry and Oncley,[8] that at frequencies less than 25 kc the correction term $AG^2\nu^{-\frac{1}{2}}$ is not applicable.

To meet this difficulty at low frequencies, Ferry and Oncley[8] assumed that the polarization correction could be considered as the sum of two terms: one, a function of the conductivity of the solution, and the other, a function of the nature of the solute. The difference in polarization of two solutions of equal conductivity was then found proportional to $\nu^{-\frac{1}{2}}$. Accordingly, then, polarization corrections could be made by comparing the unknown solution with a known salt solution of equal conductivity. With this method, Oncley and Ferry have made corrections for polarization in protein solutions with conductivities ranging up to 40×10^{-6} ohm^{-1} cm^{-1} at frequencies as low as 10 kc.

It will be shown later, in the present paper, that Oncley's original correction scheme can be retained and the use of a comparison solution avoided, even at frequencies as low as 10 kc and for conductivities of the order 200×10^{-6} ohm^{-1} cm^{-1}.

III. EXPERIMENTAL

Apparatus

The cell used in this investigation is shown in Fig. 1. This cell is of the micrometer type with two circular platinum sheet electrodes, one mounted on the spindle of a micrometer screw, and the other fixed. This type of cell is especially useful for making electrode polarization corrections according to Fricke's method. The electrode spacing may be varied from 0.05 to 10.0 mm with a precision of setting equal to ±0.002 mm. The temperature of the cell was controlled to within ±0.1°C by circulating mineral oil from a thermostat through the glass jacket enclosing the cell. The volume of solution ordinarily used is 2 ml.

By mounting the cell on the condenser used as a capacitance standard, as shown in Fig. 1, several advantages were derived. Short direct leads resulted in a low value of lead inductance, and a rigid and easily reproduced cell mounting resulted in constant lead capacitances.

[7] W. G. Smiley and A. K. Smith, J. Am. Chem. Soc. **64**, 624 (1942).

[8] J. D. Ferry and J. L. Oncley, J. Am. Chem. Soc. **63**, 272 (1941).

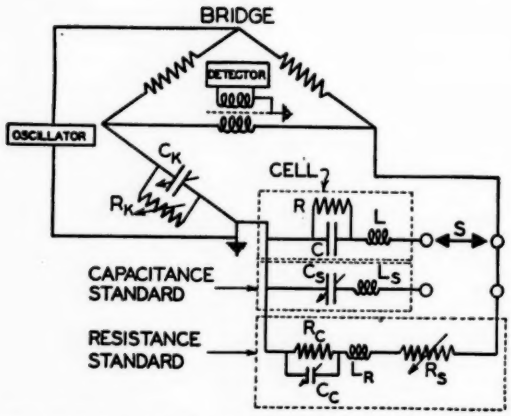

FIG. 2. Schematic diagram of bridge circuit arranged for substitution measurements. Components used in set-up are: *Bridge*, General Radio Type 516-CS1; *Oscillator*, General Radio Type 684A; *Detector*, Sargent Radio Model 11VA and Dumont Oscilloscope Type 168 equipped with General Radio Type 814 Amplifier and 8 Type 814P filters; *Capacitance Standard*, General Radio Precision Condenser, Type 722D; *Resistance Standard*, General Radio Decade Resistance Box equipped with inductance compensating network, R_C, C_C (see reference 8). *Cell*, see Fig. 1.

A bridge substitution method was used to determine the capacitance and the resistance of the cell. At each of the various frequencies employed, a precision variable condenser was substituted for the cell by means of the switch S, indicated in Fig. 2, which is a schematic diagram of the circuit used. After the substitution the bridge was rebalanced by adjustment of the precision condenser and an inductance-compensated resistance box.[9] The various items of equipment making up the circuit have been identified on the diagram. It should be noted that in the electrical set-up employed in this paper all lead inductances are measured from the terminals of the precision condenser. The latter may then be considered as the reference terminals of the system.

The use of a substitution method effectively eliminates from the measurements errors which arise from the bridge proper. The further errors which must be considered are those due to the inductances L, L_S, L_R, of the leads between the capacitance and resistance standards and the cell. These inductances affect both the cell resistance and capacitance obtained by the substitution method. In the work reported in this paper only the low frequency measurements of resistance are used, for which lead inductance effects are negligible. The following discussion is therefore directed to the elimination of errors in the measured capacitances.

The effect of lead inductances on a capacitance determination may be represented by the equation

$$C_S = C + \Delta C_a + \Delta C_b + \Delta C_c + \Delta C_d + \Delta C_e, \quad (4)$$

where C_S is the capacitance setting of the precision condenser, C is the true terminal capacitance of the cell, and the delta terms are capacitance errors to be described below.

The series inductance L of the cell contributes capacitance errors, ΔC_a and ΔC_b. This inductance is in series with the unknown capacitance C of the cell and gives rise to the capacitance increment $\Delta C_a = [C - C/(1-\omega^2 LC)]$ for a frequency $\nu = \omega/2\pi$. Further, since L is in series with the resistance R of the cell, it gives rise to a capacitance increment $\Delta C_b = (-L/R^2)$. The equations expressing the delta terms are valid when $R^2 \gg \omega^2 L$, which condition holds for the frequencies and resistance values involved here. A detailed treatment of lead errors is given by Davies.[10]

The inductance of the standard condenser L_S behaves in a manner similar to L. At high frequencies the capacitance of the standard condenser is increased by an amount $\Delta C_c = [C_S - C_S/(1-\omega^2 L_S C_S)]$. Because the standard condenser has a high parallel resistance, the correction ΔC_d, due to the condenser resistance being in series with L_S, is very small and can be completely neglected in the work discussed here.

The inductance L_R of the standard resistor R_S gives rise to an effective capacitance $C_e = (-L_R/R_S^2)$. In making a substitution measurement of the cell capacitance, the initial bridge balance is obtained with the standard resistance set at its maximum value, equal to 260.2 ohms. After the cell is removed from the circuit and the standard condenser substituted for it, R_S is reduced from its maximum value to another value, which depends on the cell resistance. Hence the effective capacitance C_e of the standard resistor changes during a given cell capacitance measurement and may cause large

[9] J. L. Oncley, J. Phys. Chem. **44**, 1103 (1940).

[10] R. M. Davies, Phil. Mag. **20**, 75 (1935).

errors if ignored. This effective capacitance *change* ΔC_e was reduced to less than ± 0.7 $\mu\mu$f for frequencies between 5000 and 10 kc by means of a modification of the inductance compensation scheme described by Oncley.[9] A description of the method used to evaluate the capacitance errors in the resistance standard is being prepared for publication.

For the cell shown in Fig. 1, L was found to be 0.11×10^{-6} henry. This value was calculated from measurements of the variation in effective capacitance of the cell at high frequencies. This value of L is sufficiently small that the capacitance ΔC_b may be neglected for all values of the cell resistance R used in the present measurements. For a minimum value of R equal to 450 ohms, the maximum value of ΔC_b is approximately 0.5 $\mu\mu$f. This value is slightly less than the maximum capacitance error of the standard resistor R_S, mentioned above, and it has therefore been neglected.

The capacitances ΔC_a and ΔC_c remain to be considered. These were caused to cancel each other effectively by adjusting L_s to equal L.[8]

Calibration of the Cell

Calibration measurements were made with water and dilute aqueous potassium chloride solutions as standards of known dielectric constant. A frequency of 1000 kc was used in order to avoid electrode polarization. Measurements were made of the parallel capacitance of the cell for a series of electrode spacings between 0.0200 and 0.6000 cm. The cell capacitance C is given by the equation[11]

$$C=C_0+K\epsilon/d, \qquad (5)$$

where C_0 is the distributed capacitance, K is *approximately* equal to the electrode area divided by 4π, ϵ is the dielectric constant of the cell contents, and d is the electrode spacing. The constants C_0 and K were evaluated from straight line graphs of C plotted as function of $1/d$. The average values obtained were $C_0=3.5\pm0.5$ $\mu\mu$f and $K=0.1700\pm0.0005$ $\mu\mu$f cm. They were used in reducing the capacitance measurements, for the glycine solutions, to dielectric constants as discussed subsequently.

[11] K. S. Cole and H. J. Curtis, Rev. Sci. Inst. **8**, 333 (1937).

Materials

Glycine was chosen for the dielectric constant measurements for two reasons. First, the dielectric constants of aqueous glycine solutions are known with considerable accuracy[12] for all obtainable concentrations of the material. They serve, therefore, as convenient standards to evaluate the adequacy of the methods for making polarization corrections. Second, glycine solutions were to be used as solvents in a study of the dielectric properties of lactoglobulin in this laboratory over the same frequency range employed in the present investigation and it was desirable, therefore, to know the behavior of the cell when filled with glycine solutions.

The glycine was obtained from the Eastman Kodak Company and was recrystallized once from 90 percent methanol. The solutions studied contained 0.5, 1.5, and 2.5 moles of glycine per liter. In order to vary the conductivity of the solutions, they were made up to contain from 0.0001 to 0.0015 mole per liter of potassium chloride. In this way the conductivity of the solutions was caused to vary from 29×10^{-6} to 174×10^{-6} ohm^{-1} cm^{-1}.

IV. RESULTS

Tables I, II, and III summarize the results for nine solutions of glycine. For the sake of

TABLE I. Summary of cell capacitances and dielectric constants for glycine solutions. Electrode polarization corrections made by the Fricke and Curtis method.

1	2	3	4	5	6	7	8	9	10
	Observed capacitance, $\mu\mu$f								
	$(C-C_0)$			$(C-C_0)$			Dielectric constant ϵ		
	Electrode spacing, d								
	d =0.123 cm		d = 0.173 cm	d =0.273 cm			[Eq. (2)]		
Frequency in kc	Solution[a]								
	D	E	F	D	E	F	D	E	F
5000	158.4	158.5	112.6	71.4	71.7	71.8	114.7	115.5	116.8
1000	158.2	159.0	113.5	71.1	71.5	71.3	113.9	114.6	113.0
500	158.8	158.3	113.6	71.1	71.5	71.9	113.6	115.0	115.5
100	159.5	160.7	115.9	71.2	72.0	72.7	113.5	115.1	114.9
50	160.6	166.9	121.3	71.5	73.2	74.6	113.6	114.9	113.8
40	161.5	171.2	124.8	71.7	74.1	75.9	113.7	115.0	113.3
30	163.2	179.6	131.4	72.0	75.7	78.6	113.6	114.7	113.5
20	166.8	201.7	149.0	72.9	80.4	85.9	114.1	115.3	114.5
10	185.7	306.3	232.0	76.7	102.3	120.2	114.0	117.2	118.8

[a] Solutions D, E, F contain 1.5 M glycine and have conductivities of 55.7, 139, and 174×10^{-6} ohm^{-1} cm^{-1}, respectively. Conductivities were brought to these values by the addition of KCl.

[12] J. Wyman, Jr. and T. L. McMeekin, J. Am. Chem. Soc. **55**, 915 (1933).

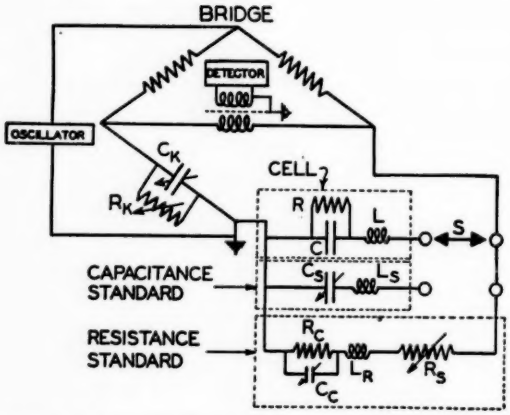

FIG. 2. Schematic diagram of bridge circuit arranged for substitution measurements. Components used in set-up are: *Bridge*, General Radio Type 516-CS1; *Oscillator*, General Radio Type 684A; *Detector*, Sargent Radio Model 11VA and Dumont Oscilloscope Type 168 equipped with General Radio Type 814 Amplifier and 8 Type 814P filters; *Capacitance Standard*, General Radio Precision Condenser, Type 722D; *Resistance Standard*, General Radio Decade Resistance Box equipped with inductance compensating network, R_C, C_C (see reference 8). *Cell*, see Fig. 1.

A bridge substitution method was used to determine the capacitance and the resistance of the cell. At each of the various frequencies employed, a precision variable condenser was substituted for the cell by means of the switch S, indicated in Fig. 2, which is a schematic diagram of the circuit used. After the substitution the bridge was rebalanced by adjustment of the precision condenser and an inductance-compensated resistance box.[9] The various items of equipment making up the circuit have been identified on the diagram. It should be noted that in the electrical set-up employed in this paper all lead inductances are measured from the terminals of the precision condenser. The latter may then be considered as the reference terminals of the system.

The use of a substitution method effectively eliminates from the measurements errors which arise from the bridge proper. The further errors which must be considered are those due to the inductances L, L_S, L_R, of the leads between the capacitance and resistance standards and the cell. These inductances affect both the cell resistance and capacitance obtained by the substitution method. In the work reported in this paper only the low frequency measurements of resistance are used, for which lead inductance effects are negligible. The following discussion is therefore directed to the elimination of errors in the measured capacitances.

The effect of lead inductances on a capacitance determination may be represented by the equation

$$C_S = C + \Delta C_a + \Delta C_b + \Delta C_c + \Delta C_d + \Delta C_e, \quad (4)$$

where C_S is the capacitance setting of the precision condenser, C is the true terminal capacitance of the cell, and the delta terms are capacitance errors to be described below.

The series inductance L of the cell contributes capacitance errors, ΔC_a and ΔC_b. This inductance is in series with the unknown capacitance C of the cell and gives rise to the capacitance increment $\Delta C_a = [C - C/(1-\omega^2 LC)]$ for a frequency $\nu = \omega/2\pi$. Further, since L is in series with the resistance R of the cell, it gives rise to a capacitance increment $\Delta C_b = (-L/R^2)$. The equations expressing the delta terms are valid when $R^2 \gg \omega^2 L$, which condition holds for the frequencies and resistance values involved here. A detailed treatment of lead errors is given by Davies.[10]

The inductance of the standard condenser L_S behaves in a manner similar to L. At high frequencies the capacitance of the standard condenser is increased by an amount $\Delta C_c = [C_S - C_S/(1-\omega^2 L_S C_S)]$. Because the standard condenser has a high parallel resistance, the correction ΔC_d, due to the condenser resistance being in series with L_S, is very small and can be completely neglected in the work discussed here.

The inductance L_R of the standard resistor R_S gives rise to an effective capacitance $C_e = (-L_R/R_S^2)$. In making a substitution measurement of the cell capacitance, the initial bridge balance is obtained with the standard resistance set at its maximum value, equal to 260.2 ohms. After the cell is removed from the circuit and the standard condenser substituted for it, R_S is reduced from its maximum value to another value, which depends on the cell resistance. Hence the effective capacitance C_e of the standard resistor changes during a given cell capacitance measurement and may cause large

[9] J. L. Oncley, J. Phys. Chem. **44**, 1103 (1940).

[10] R. M. Davies, Phil. Mag. **20**, 75 (1935).

errors if ignored. This effective capacitance *change* ΔC_e was reduced to less than ± 0.7 $\mu\mu$f for frequencies between 5000 and 10 kc by means of a modification of the inductance compensation scheme described by Oncley.[9] A description of the method used to evaluate the capacitance errors in the resistance standard is being prepared for publication.

For the cell shown in Fig. 1, L was found to be 0.11×10^{-6} henry. This value was calculated from measurements of the variation in effective capacitance of the cell at high frequencies. This value of L is sufficiently small that the capacitance ΔC_b may be neglected for all values of the cell resistance R used in the present measurements. For a minimum value of R equal to 450 ohms, the maximum value of ΔC_b is approximately 0.5 $\mu\mu$f. This value is slightly less than the maximum capacitance error of the standard resistor R_S, mentioned above, and it has therefore been neglected.

The capacitances ΔC_a and ΔC_c remain to be considered. These were caused to cancel each other effectively by adjusting L_s to equal L.[8]

Calibration of the Cell

Calibration measurements were made with water and dilute aqueous potassium chloride solutions as standards of known dielectric constant. A frequency of 1000 kc was used in order to avoid electrode polarization. Measurements were made of the parallel capacitance of the cell for a series of electrode spacings between 0.0200 and 0.6000 cm. The cell capacitance C is given by the equation[11]

$$C=C_0+K\epsilon/d, \qquad (5)$$

where C_0 is the distributed capacitance, K is *approximately* equal to the electrode area divided by 4π, ϵ is the dielectric constant of the cell contents, and d is the electrode spacing. The constants C_0 and K were evaluated from straight line graphs of C plotted as function of $1/d$. The average values obtained were $C_0=3.5\pm0.5$ $\mu\mu$f and $K=0.1700\pm0.0005$ $\mu\mu$f cm. They were used in reducing the capacitance measurements, for the glycine solutions, to dielectric constants as discussed subsequently.

[11] K. S. Cole and H. J. Curtis, Rev. Sci. Inst. **8**, 333 (1937).

Materials

Glycine was chosen for the dielectric constant measurements for two reasons. First, the dielectric constants of aqueous glycine solutions are known with considerable accuracy[12] for all obtainable concentrations of the material. They serve, therefore, as convenient standards to evaluate the adequacy of the methods for making polarization corrections. Second, glycine solutions were to be used as solvents in a study of the dielectric properties of lactoglobulin in this laboratory over the same frequency range employed in the present investigation and it was desirable, therefore, to know the behavior of the cell when filled with glycine solutions.

The glycine was obtained from the Eastman Kodak Company and was recrystallized once from 90 percent methanol. The solutions studied contained 0.5, 1.5, and 2.5 moles of glycine per liter. In order to vary the conductivity of the solutions, they were made up to contain from 0.0001 to 0.0015 mole per liter of potassium chloride. In this way the conductivity of the solutions was caused to vary from 29×10^{-6} to 174×10^{-6} ohm^{-1} cm^{-1}.

IV. RESULTS

Tables I, II, and III summarize the results for nine solutions of glycine. For the sake of

TABLE I. Summary of cell capacitances and dielectric constants for glycine solutions. Electrode polarization corrections made by the Fricke and Curtis method.

1	2	3	4	5	6	7	8	9	10
	Observed capacitance, $\mu\mu$f								
	$(C-C_0)$			$(C-C_0)$			Dielectric constant ϵ		
	Electrode spacing, d								
	$d=0.123$ cm		$d=0.173$ cm	$d=0.273$ cm			[Eq. (2)]		
Frequency in kc	D	E	F	Solution[a] D	E	F	D	E	F
5000	158.4	158.5	112.6	71.4	71.7	71.8	114.7	115.5	116.8
1000	158.2	159.0	113.5	71.1	71.5	71.3	113.9	114.6	113.0
500	158.8	158.3	113.6	71.1	71.5	71.9	113.6	115.0	115.5
100	159.5	160.7	115.9	71.2	72.0	72.7	113.5	115.1	114.9
50	160.6	166.9	121.3	71.5	73.2	74.6	113.6	114.9	113.8
40	161.5	171.2	124.8	71.7	74.1	75.9	113.7	115.0	113.3
30	163.2	179.6	131.4	72.0	75.7	78.6	113.6	114.7	113.5
20	166.8	201.7	149.0	72.9	80.4	85.9	114.1	115.3	114.5
10	185.7	306.3	232.0	76.7	102.3	120.2	114.0	117.2	118.8

[a] Solutions D, E, F contain 1.5 M glycine and have conductivities of 55.7, 139, and 174×10^{-6} ohm^{-1} cm^{-1}, respectively. Conductivities were brought to these values by the addition of KCl.

[12] J. Wyman, Jr. and T. L. McMeekin, J. Am. Chem. Soc. **55**, 915 (1933).

TABLE II. Summary of corrected capacitances and dielectric constants for glycine solutions. Polarization corrections according to modification of the Oncley method.

1	2	3	4	5	6	7	8	9	10	11	12	13
	Corrected capacitance, C' $\mu\mu f$ [Eq. (6)]						Dielectric constant, ϵ					
	Electrode spacing, d						Electrode spacing, d					
	d =0.123 cm			d =0.173 cm			d =0.123 cm			d =0.173 cm		
	Solution[a]											
Frequency in kc	D	E	F	D	E	F	D	E	F	D	E	F
5000	158.4	158.5	[b]	112.8	113.3	112.6	114.6	114.7	[b]	114.8	115.3	114.6
1000	158.1	159.0		113.1	113.8	113.4	114.4	115.0		115.1	115.8	115.4
500	158.7	158.3		113.0	113.8	113.4	114.8	114.5		115.0	115.8	115.4
100	159.0	157.8		113.2	113.7	113.5	115.0	114.2		115.2	115.7	115.5
50	158.8	157.6		113.3	113.4	113.6	114.9	114.0		115.3	115.4	115.6
40	158.9	157.7		113.3	113.4	113.6	115.0	114.1		115.3	115.4	115.6
30	159.0	157.5		113.3	113.2	113.1	115.0	114.0		115.3	115.2	115.1
20	159.0	157.8		113.5	112.7	113.6	115.0	114.2		115.5	114.7	115.6
10	158.7	163.3[c]		113.5	113.9	113.5	114.8	118.1[c]		115.5	116.0	115.5

[a] Solutions D, E, F contain 1.5 M glycine and have conductivities of 55.7, 139, and 174 $\times 10^{-6}$ ohm^{-1} cm^{-1}, respectively. Conductivities were brought to these values by the addition of KCl.
[b] Measurements not made for solution F at this electrode spacing.
[c] This value is probably in error; not included in averages in Table III.

brevity, detailed data are presented only for the solutions of the 1.5 M glycine.

In Table I, columns 2–7, are shown observed capacitances for three solutions of 1.5 M glycine of different conductivities and for two values of electrode spacing. In columns 8–10 appear the dielectric constants of the solutions calculated from the values of C by means of Eq. (2) according to the method of Fricke and Curtis. The capacitance values in columns 2–7 show clearly the regular increase due to electrode polarization that occurs with decreasing frequency and increasing conductivity. For the solutions of highest conductivity the polarization becomes so large that at low frequencies the observed capacitances are approximately twice the high frequency values. At the three highest frequencies no polarization effects are apparent. The capacitance variations that occur at these frequencies are within the limits of experimental error.

The dielectric constants shown in columns 8–10 should be free from electrode polarization effects if the Fricke and Curtis method is valid. The agreement manifest between the values of ϵ for solutions of different conductivity at high and low frequencies shows this to be the case. No significant trends with frequency or conductivity are apparent, the values of ϵ for the lower frequencies and higher conductivities being in good agreement with the values for the higher frequencies and lower conductivities, where electrode polarization is negligible. Average values from columns 8–10 of Table I are summarized in Table III, together with similar data for 0.5 and 2.5 M glycine, for comparison with the results obtained by an application of a

TABLE III. Comparison of dielectric constants of glycine solutions showing effectiveness of methods used to correct for electrode polarization.

1	2	3	4	5	6	7
Solution			Dielectric constant, ϵ			
			Results of present work			
			Fricke and Curtis method		Modified Oncley method	
Glycine moles/liter	Conductivity at 10 kc ohm^{-1} cm^{-1} $\times 10^6$	Accepted value[d]	Mean[a]	Average deviation	Mean[a]	Average deviation
(A) 0.5	29.0		90.9	±0.11	92.2[b] 91.4	±0.06 ±0.07
(B) 0.5	75.4	91.74	91.5	±0.27	91.7 92.1	±0.16 ±0.14
(C) 0.5	135		91.9	±0.19	91.6 91.8	±0.43 ±0.30
(D) 1.5	55.7		113.8	±0.28	114.8 115.2	±0.17 ±0.18
(E) 1.5	139	114.52	115.2	±0.48	114.3 115.5	±0.26 ±0.31
(F) 1.5	174		114.9	±1.42	—[c] 115.3	— ±0.27
(G) 2.5	60.4		139.3	±0.61	136.7 137.4	±0.08 ±0.11
(H) 2.5	99.7	137.30	138.2	±0.24	138.1 138.3	±0.06 ±0.24
(I) 2.5	140		138.1	±1.07	137.2 138.5	±0.44 ±0.22

[a] Mean of 9 values over frequency range 10 to 5000 kc.
[b] In this column the upper figure is for d =0.123 cm; lower figure is for d =0.173 cm.
[c] No measurements were made for d =0.123 cm.
[d] Values for dielectric constant from J. Wyman, Jr., Phys. Rev. 35, 623 (1930) (water); J. Wyman, Jr., and T. L. McMeekin, J. Am. Chem. Soc. 55, 913 (1933) (glycine).

modification of Oncley's method to the same experimental data.

In Table II are presented the results obtained when a modification of Oncley's method is used to correct the experimental data for electrode polarization. Oncley's method was modified in order to be able to make corrections at low frequencies without introducing the additional complication of the comparison method that Ferry and Oncley[8] found necessary. When values of the observed capacitance C are plotted as a function of $G^2\nu^{-1.5}$ or simply $\nu^{-1.5}$, because G^2 changes very little in the frequency region concerned,[13] curves of the type shown in Fig. 3 are obtained. These curves are linear at all except the highest conductivities for frequencies down to about 25 kc. Below this frequency the curves are no longer linear. This behavior was noted by Ferry and Oncley and resulted in their adoption of a comparison method, mentioned previously.

In an effort to avoid the additional complication introduced by the comparison method, tests

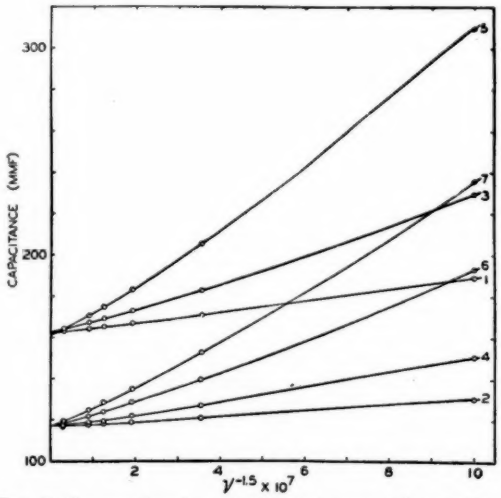

FIG. 3. Curves showing relation between cell capacitance C and frequency ν to -1.5 power for 1.5 molar glycine solutions of varying conductivity σ and for different dielectric cell electrode spacings d.

Curve 1, $\sigma = 55.7\times10^{-6}$ ohm^{-1} cm^{-1}, $d = 0.123$ cm.
Curve 2, $\sigma = 55.7\times10^{-6}$ ohm^{-1} cm^{-1}, $d = 0.173$ cm.
Curve 3, $\sigma = 91.4\times10^{-6}$ ohm^{-1} cm^{-1}, $d = 0.123$ cm.
Curve 4, $\sigma = 91.4\times10^{-6}$ ohm^{-1} cm^{-1}, $d = 0.173$ cm.
Curve 5, $\sigma = 139\times10^{-6}$ ohm^{-1} cm^{-1}, $d = 0.123$ cm.
Curve 6, $\sigma = 139\times10^{-6}$ ohm^{-1} cm^{-1}, $d = 0.173$ cm.
Curve 7, $\sigma = 174\times10^{-6}$ ohm^{-1} cm^{-1}, $d = 0.173$ cm.

[13] In all the experiments here reported the total change in conductance amounts to a decrease of 1 percent or less for the frequency range 10 kc to 500 kc.

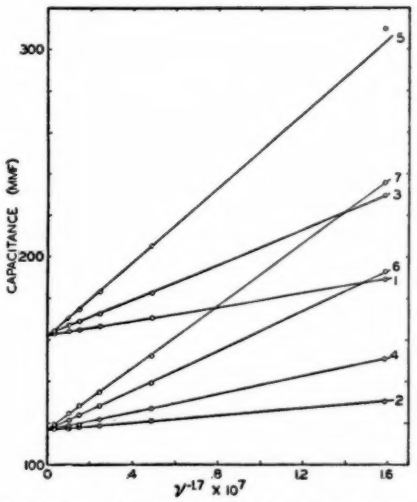

FIG. 4. Curves showing relation between dielectric cell capacitance C and frequency ν to -1.7 power for 1.5 molar glycine solutions of varying conductivity σ and for different dielectric cell electrode spacings d.

Curve 1, $\sigma = 55.7\times10^{-6}$ ohm^{-1} cm^{-1}, $d = 0.123$ cm.
Curve 2, $\sigma = 55.7\times10^{-6}$ ohm^{-1} cm^{-1}, $d = 0.173$ cm.
Curve 3, $\sigma = 91.4\times10^{-6}$ ohm^{-1} cm^{-1}, $d = 0.123$ cm.
Curve 4, $\sigma = 91.4\times10^{-6}$ ohm^{-1} cm^{-1}, $d = 0.173$ cm.
Curve 5, $\sigma = 139\times10^{-6}$ ohm^{-1} cm^{-1}, $d = 0.123$ cm.
Curve 6, $\sigma = 139\times10^{-6}$ ohm^{-1} cm^{-1}, $d = 0.173$ cm.
Curve 7, $\sigma = 174\times10^{-6}$ ohm^{-1} cm^{-1}, $d = 0.173$ cm.

were made in the present work to see if the adoption of a different frequency dependence would yield straight lines. By successive trials it was found that when values of C were plotted as a function of $\nu^{-1.7}$, straight lines resulted. This behavior was found not only for the glycine solutions, for which data are reported here, but in addition for aqueous solutions of potassium chloride with concentrations ranging from zero to 0.002 N. Typical curves of C *versus* $\nu^{-1.7}$ are shown in Fig. 4.

The fact that graphs of C *versus* $\nu^{-1.7}$ are linear would appear to indicate that the constant m in Eq. (1) is equal to 0.3[14] for the lower frequencies, at least, rather than 0.5 as was assumed by Oncley.[5] That m varies with the frequency is well known. For example, Wolfe[2] reported m to be approximately 0.5 in the upper portion and approximately 0.3 in the lower portion of a frequency range of 0.2 kc to 200 kc. The present results, however, seem to indicate that m is not critical for high frequencies and for low conductivities, and that m = either 0.5 or 0.3 represents the data adequately. At the very low frequencies,

[14] See Appendix 2.

however, as a comparison of Figs. 3 and 4 shows, the smaller value of m is essential.

The values of C', the corrected capacitance of the cell, which appear in columns 2–7 of Table II, were therefore obtained according to the equation

$$C' = (C - C_0 - S\nu^{-1.7}). \quad (6)$$

The constant S was obtained from the straight lines resulting when C was plotted against $\nu^{-1.7}$. The values of C' are seen to be independent of frequency and conductivity. The excellent agreement between high and low frequency values confirms the use of Eq. (6) for the elimination of the polarization effects which occur at the lower frequencies.

The dielectric constants which appear in columns 8–13 of Table II were calculated according to the relation $\epsilon = C'd/K$.

Averages of the values in columns 8–13 have been assembled in Table III for comparison with the results obtained by the method of Fricke and Curtis.

An inspection of Table III reveals that the Fricke and Curtis method and the modified Oncley method are equally adequate to eliminate polarization effects. The dielectric constants obtained by an application of these methods to the experimental data are seen to agree well with the values of Wyman and McMeekin.[12] This is true for solutions with conductivities ranging from 0.29 to 1.74×10^{-4} ohm^{-1} cm^{-1}. No dependence of the dielectric constant on the conductivity of the solution is apparent. The differences between the "mean" and "accepted" values is about the same for the two methods. With one exception these differences are of an order of magnitude consistent with the uncertainty in the cell constants.

The quantities listed as "average deviations" in columns 5 and 7 represent deviations among the values for different frequencies. In most instances these deviations are much less for the modified Oncley method than for the method of Fricke and Curtis. They probably reflect errors arising from incomplete compensation of the lead inductance in the standard resistor, as mentioned earlier. The greater deviation in the case of the results with the Fricke and Curtis method is to be expected since twice as many observations, each subject to the same uncertainty, enter into the calculations, as a comparison of Eqs. (2) and (6) shows.

V. CONCLUSIONS

The data presented demonstrate that errors due to electrode polarization in dielectric constant measurements may be eliminated equally well by the application of the Fricke and Curtis method or the modification of Oncley's method, described in the present paper. This conclusion applies, of course, only for the frequency range and conductivity range investigated. There appears to be no reason why the Fricke and Curtis method cannot be extended to much lower frequencies and to higher conductivities. On the other hand the extension of the modified Oncley method is questionable. Since the frequency dependence of the polarization is known to vary with the frequency, it is quite likely that for a precise correction of the polarization at lower frequencies it would be necessary to take this fact into account.

Of the two methods for eliminating polarization errors, there is no doubt of the more general utility of the Fricke and Curtis method. This is true despite the fact that the dielectric constants obtained with their method are less precise than the values obtained with the modification of Oncley's method. The greater utility arises from the fact that the Fricke and Curtis method can be used to eliminate polarization effects in measurements made at a single frequency only. Oncley's method or the present modification of it, on the other hand, requires measurements for at least two frequencies; moreover, these must lie outside of the dispersion region of the material under investigation. This latter limitation is particularly important in studies of proteins or other high molecular weight compounds where the dielectric constant may show dispersion over an extremely wide range of frequencies. In those instances where this limitation does not apply, Oncley's method would appear preferable on the basis of increased precision and because it may be used for measurements made with a simple cell having fixed electrodes.

APPENDIX 1

Derivation of Eq. (2)

It is desired to find an equation expressing the dielectric constant of a solution in a dielectric constant cell with

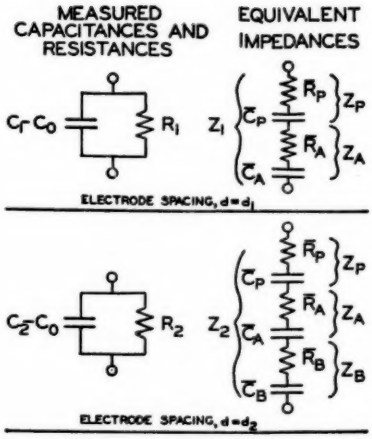

FIG. 5. Schematic diagram showing relation between measured capacitances and resistances and equivalent impedances. C_1, R_1, measured parallel capacitance and resistance of cell for electrode spacing d_1; C_2, R_2, measured parallel capacitance and resistance of cell for electrode spacing d_2; and C_0, distributed capacitance of cell.

Z_p = impedance of electrodes;
Z_A = impedance of solution defined by electrode spacing d_1;
Z_B = increase in impedance of solution due to change in electrode spacing from d_1 to d_2;
Z_1 = total impedance of cell for electrode spacing d_1;
Z_2 = total impedance of cell for electrode spacing d_2.

Dashed quantities are equivalent series capacitance and resistance components of corresponding impedances.

polarized electrodes in terms of the measured resistance and capacitance of the cell. Referring to Fig. 5, where the symbols are defined, it can be seen that the impedance of the element of solution, Z_B, of length (d_2-d_1) is given by,

$$Z_B = Z_2 - Z_1. \tag{7}$$

Making use of the well-known relations between the capacitance and resistance of series and parallel equivalent circuits, substitution for the impedances in Eq. (7) yields,

$$\omega^2 C_B R_B^2/(1+\omega^2 C_B^2 R_B^2) = [\omega^2(C_2-C_0)R_2^2]/[1+\omega^2(C_2-C_0)^2R_2^2] - [\omega^2(C_1-C_0)R_1^2]/[1+\omega^2(C_1-C_0)^2R_1^2] \tag{8}$$

and

$$R_B/(1+\omega^2 C_B^2 R_B^2) = R_2/[1+\omega^2(C_2-C_0)^2R_2^2]) - R_1/[1+\omega^2(C_1-C_0)^2R_1^2]. \tag{9}$$

Now for the conditions, which hold for all measurements reported in this paper where the polarization is significant,

$$\omega^2(C_1-C_0)^2R_1^2 \ll 1, \quad \omega^2(C_2-C_0)^2R_2^2 \ll 1,$$

and

$$\omega^2 C_B^2 R_B^2 \ll 1, \tag{10}$$

it follows that,

$$C_B = [(C_2-C_0)R_2^2 - (C_1-C_0)R_1^2]/(R_2-R_1)^2 \tag{11}$$

and

$$R_B = (R_2-R_1). \tag{12}$$

Equation (11) may be simplified further. Jones and Christian[15] have shown that the equivalent series resistances of a cell of the type used here may be expressed,

$$\bar{R}_1 = (d_1/A\sigma) + \bar{R}_P \tag{13}$$

and

$$\bar{R}_2 = (d_2/A\sigma) + \bar{R}_P, \tag{14}$$

where A is the area of the cell electrodes and σ is the specific conductivity of the solution. For the conditions (10), $\bar{R}_1 = R_1$ and $\bar{R}_2 = R_2$. Thus Eqs. (13) and (14) may be substituted in Eq. (11) with the result,

$$C_B = [d_2^2(C_2-C_0) - d_1^2(C_1-C_0)]/(d_2-d_1)^2. \tag{15}$$

Now it follows from the theory for a parallel plate condenser that

$$C_B = \epsilon K/(d_2-d_1), \tag{16}$$

where K is a constant. The elimination of C_B from Eqs. (15) and (16) yields finally,

$$\epsilon = [d_2^2(C_2-C_0) - d_1^2(C_1-C_0)]/K(d_2-d_1). \tag{2}$$

This equation also holds for frequencies where electrode polarization is negligible but for which the condition expressed in (10) is not satisfied. When the electrode polarization is negligible, $(C_1-C_0) = K'/d_1$, $(C_2-C_0) = K'/d_2$, $C_B = K'/(d_2-d_1)$, $R_1 = K''d_1$, $R_2 = K''d_2$, and $R_B = K''(d_2-d_1)$, where for a given cell and solution K' and K'' are constants. If these values are substituted in Eqs. (8) and (9), then

$$C_B = C_1 \cdot C_2/(C_1-C_2). \tag{17}$$

This equation may be used interchangeably with Eq. (2) when electrode polarization effects are absent.

APPENDIX 2

Derivation of Eq. (3)

The cell is assumed to be represented by a measured parallel capacitance $(C-C_0)$ and measured parallel conductance $G = (1/R)$, as Fig. 5 indicates. These quantities are related to the series polarization capacitance $\bar{C}_p$ of the electrodes, and the series capacitance $\bar{C}$ of the solution in the cell by the following equation,

$$(C-C_0) = \{G^2/\omega^2[\bar{C}\cdot\bar{C}_p/(\bar{C}+\bar{C}_p)]\}, \tag{18}$$

which can be obtained by a process similar to that used in Appendix 1, for the condition, $R^2(C-C_0)^2\omega^2 \ll 1$. Assuming that the polarization capacitance may be represented by $\bar{C}_p = M\nu^{-m}$ [Eq. 1] by substitution is obtained,

$$(C-C_0) = (G^2\nu^{-(2-m)}/4\pi^2 M) + (G^2/4\pi^2\nu^2\bar{C}). \tag{19}$$

When $R^2C^2\omega^2 \ll 1$ then $\bar{C} = G^2/4\pi^2\nu^2 C$, which when substituted in Eq. (19) yields

$$C' = C - C_0 - AG^2\nu^{-(2-m)}, \tag{20}$$

where C' is the cell capacitance corrected for electrode polarization. Now, making use of the equation for a parallel plate condenser, $\epsilon = C'd/K$, Eq. (20) becomes

$$\epsilon = [C - C_0 - AG^2\nu^{-(2-m)}]d/K, \tag{3}$$

which, for $m = 0.5$, is the desired equation.

[15] G. Jones and S. M. Christian, J. Am. Chem. Soc. **57**, 272 (1935).

Counting of Free Alkyl Radicals. Application to the Photolysis of Acetone

MILTON H. FELDMAN, JOHN E. RICCI, AND MILTON BURTON
Department of Chemistry, New York University, New York, New York

(Received July 27, 1942)

Long, heavy lead mirrors are deposited in a reaction tube, and metal is transported therefrom by free radicals according to the Paneth method. The lead alkyl is collected and the lead determined by a micro-method. Assuming that all the alkyl radicals are mirror-active and that all the lead is transported as PbR_4, the number of radicals can be estimated. The method is applied to work on the photolysis of acetone at 2537A. It is shown that the difference in apparent half-lives of radicals produced at 45°C (1.1×10^{-2} sec.) and at 100°C (8×10^{-3} sec.) may be explained on the basis of the instability of free acetyl. The actual concentration of methyl radicals in the flowing gas in the experiments reported is estimated to be $\sim2\times10^{-3}$ mole percent or 1.7×10^{-12} mole per cc, immediately past the irradiated zone.

INTRODUCTION

ALTHOUGH methods of absorption spectroscopy have been used for determining the concentrations of such free radicals as OH[1] and CN,[2] such methods are not in general available for the estimation of the more complicated free radicals represented by the alkyls.[3] Given an adequate method of measuring the metal transported, the classical mirror methods of Paneth and his co-workers[4] would seem to be applicable.

One method which has been used to count alkyl radicals is to deposit a tellurium mirror of known weight in a tube and to remove it according to the Paneth method. The time required to remove the mirror completely has been used to estimate the free radical concentration;[5] however, this method is in error for it is implicitly assumed in the calculation that every radical strikes the mirror at least once in passing it, no matter how much the mirror area may be reduced. Paneth, Hofeditz, and Wunsch[6] have picked up lead from a large mirror in a similar way and have thermally decomposed the lead tetramethyl so formed in another portion of the reaction tube. After the section containing the lead deposit is cut out of the tube, the sample may be removed and estimated by turbidimetric methods. Although Paneth and his co-workers did not specifically use the method for the estimation of free radicals, it is interesting to note that their paper shows that at least 82 percent of the free radicals produced were active in removing mirrors; the general inference which may be drawn from their work is that very probably every methyl radical which strikes a mirror reacts with it. In a similar method,[7] the lead deposited was measured by its radioactivity. The latter method is very sensitive, but it is not readily susceptible to quantitative techniques. Furthermore, like the other deposition method, it is not quite satisfactory because the decomposition of the lead alkyl changes the rest of the system under investigation.

In the modification of the Paneth method described in this report, the lead is removed from a long heavy mirror by free radicals and collected as lead alkyl which is then converted to lead nitrate and estimated by microanalytical techniques. In this way, 25μg, or $\sim1.2\times10^{-7}$ mole of Pb is conveniently measured. The number of free radicals involved may then be calculated on the basis of the assumption that all the lead is transported as PbR_4. The application of this technique is illustrated in work on the half-life of radicals from the photolysis of acetone.

EXPERIMENTS AND DISCUSSION

Apparatus and Method

The apparatus, with the exception of a collection bulb M, shown in Fig. 1, is in all es-

[1] O. Oldenberg, J. Chem. Phys. **2**, 713 (1934).
[2] J. U. White, J. Chem. Phys. **8**, 459 (1940). Cf. G. Kistiakowsky and H. Gershinowitz, *ibid.*, **1**, 432 (1933).
[3] Cf. O. Oldenberg, J. Phys. Chem. **41**, 293 (1937).
[4] See F. O. Rice and K. K. Rice, *The Aliphatic Free Radicals* (Johns Hopkins Press, Baltimore, 1935) for references.
[5] J. S. A. Forsythe, Trans. Faraday Soc. **37**, 312 (1941).
[6] Paneth, Hofeditz and Wunsch, J. Chem. Soc. 372 (1935).
[7] Burton, Ricci, and Davis, J. Am. Chem. Soc. **62**, 265 (1940).

sentials similar to that described in previous publications from this laboratory.[8] The same careful, high vacuum techniques and methods of purifying and handling acetone are employed. A departure is in the actual deposition of the lead mirrors in the quartz reaction tube: (a) the final deposit is much heavier than that in the usual mirror technique, and (b) the length of the mirror in the tube (it covers the cylindrical surface completely and heavily) is fixed to exceed a definite amount. In this work, as will be shown, 17–20 mm was the necessary minimum length.

The methods of illumination (at 2537A with a spiral quartz mercury resonance lamp) and of starting and stopping runs were as already described.[8] Temperatures in the irradiated zone were controlled manually to within 1.5° with an electric fan. Asbestos housing was required to give better control at 100°C. The temperature of the rest of the reaction tube was between 20° and 25°C, depending on the room temperature. All experiments were conducted at an input pressure of acetone (into the reaction tube) of 2.1 mm Hg. Previous calibration showed that under such pressure and at room temperature in the reaction system, the streaming velocity of acetone through the 0.54-cm internal diameter quartz tube of length set at ~75 cm was 3.0 $(\pm.1)\times10^3$ cm/sec.

Collection of Lead

For the determination of the quantity of lead picked up by methyl radicals during the course of a run, the condensable products were collected in the bulb L kept at liquid nitrogen temperature. After isolation from the system this mixture was warmed to 35–40°C and distilled into a second trap M at −196°C, containing about 1 cc of a mixture (in equal volumes) of bromine and carbon tetrachloride, previously evacuated and stored at this temperature. This second trap was then shut off and warmed for five minutes at 0–25°C, to allow the bromine to convert the lead tetramethyl to lead bromide, a procedure similar to that used by Leighton and

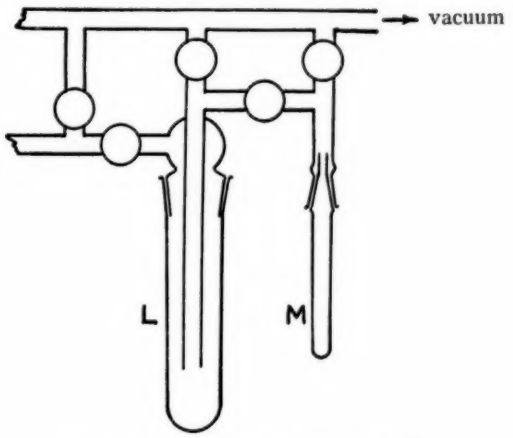

FIG. 1. Arrangement for removing PbR_4.

Mortensen[9] and others for similar purposes, such as the determination of lead in lead tetraethyl for gasoline.[10] The volatile substances (including carbon tetrachloride and excess of bromine) were then all distilled back, slowly and carefully to avoid bumping, at room temperature, into the original trap L now cooled again to −196°, leaving behind just the lead bromide corresponding to the lead picked up in the run. More rapid distillation at higher termperature sometimes resulted in bumping of the mixture and loss of sample; and more prolonged treatment with bromine produced, evidently by reaction with acetone, an oily material very difficult to separate from the lead bromide.

Analytical Method

For the analytical determination of the lead bromide thus obtained, the contents of the trap M were transferred, after heating with 15 cc of very dilute HNO_3 (~0.3 percent), to a 125-cc separatory funnel, the trap being washed out with a further 15-cc portion of water.

The lead in the solution was determined by the dithizone method using approximately the procedure described by Moskowitz,[11] all reagents and apparatus being prepared essentially according to his directions. After adjustment of the pH of the aqueous solution to 8.5–10, using

[8] Cf. May, Taylor, and Burton, J. Am. Chem. Soc. **63**, 249 (1941).

[9] P. A. Leighton and R. A. Mortensen, J. Am. Chem. Soc. **58**, 453 (1936).

[10] K. Dosios and J. Pierri, Zeits. f. anal. Chemie **81**, 214 (1930).

[11] S. Moskowitz, J. Ind. Hyg. Toxicol. **20**, 457 (1938).

phenol red and concentrated NH_4OH, two extractions of the lead as lead dithizonate are carried out. The first extraction uses 8 cc of dithizone-chloroform solution and 5 cc of chloroform, the water layer being further washed with a 2-cc portion of chloroform. In the second extraction, 4 cc of the same dithizone solution and 5 cc of chloroform are used, followed again by washing. The amount of dithizone used represents altogether approximately a threefold excess. The combined chloroform solution, containing the lead dithizonate together with excess of dithizone, is now treated with successive 100-cc portions of 0.5 percent aqueous KCN for the removal of the excess of dithizone. The complete removal of this reagent is indicated when a fresh portion of KCN solution remains colorless after shaking with the chloroform layer. Complete removal was further verified in some cases by testing the final KCN layer with 1 cc of chloroform and 2 drops of lead nitrate solution equivalent to 1μg of lead. The lead dithizonate is next decomposed by treatment with about 100 cc of 1 percent HCl, which removes the lead and leaves the green dithizone in the chloroform.

This free dithizone, equivalent to the lead being determined, is now titrated with standard lead nitrate solution containing 10μg of Pb per cc, freshly prepared from a solution of 1000μg/cc. The separated chloroform-dithizone layer is treated with 50–60 cc of fresh KCN solution, so that the dithizone is distributed in both phases, its concentration being actually very much higher in the aqueous KCN than in the chloroform layer. To this two-phase system is now added about three-fourths of the required lead, estimated after a preliminary titration of a similar sample or from the result of a similar run. The red lead dithizonate formed enters the chloroform and the excess dithizone remains practically entirely in the KCN layer. After removal then of the main chloroform layer, the KCN solution is finally titrated with small portions (1 cc chloroform and 1μg of Pb) until the fresh chloroform portion is no longer colored pink after vigorous shaking with the KCN layer.

The procedure was tested on known quantities of lead (5–50μg) in the form of lead nitrate solution. On 17 such tests the error ranged from -1.5 to -5μg, averaging $-3.2\pm1.5\mu$g, with no clear correlation between the error and the amount of lead involved. With a correction of $+3.2\mu$g, the lead determinations should be expected to be correct within an uncertainty of about $\pm1.5\mu$g. As a further test, a sample of lead tetramethyl obtained by fractional distillation of an old sample of some material furnished by the Ethyl Corporation[12] was analyzed by the procedure described, including freezing out in trap *L*, distillation over to the bromine trap *M*, and removal of volatile substances and subsequent analysis of the lead bromide. For five aliquots of presumably 28.5μg taken, the result obtained, including the correction of 3.2μg, was $26.6\pm1.0\mu$g. The deficiency may have been caused by low purity of the lead tetramethyl, but it seems to indicate that the determinations are easily within 10 percent and probably within 5 percent of the truth. Further evidence of their dependability, or at least of their relative consistency, is found in the consistency of the results obtained in the determination of the half-life of the methyl radicals produced in the photochemical decomposition of acetone in the experiments described below.

In order that the results obtained should have quantitative significance, the conditions of operation were standardized and evaluated in various respects.

Duplication of Results

Blank experiments (without illumination, or in the absence of a sensitive mirror) indicated that no lead was picked up beyond the limits of experimental error ($\sim1.5\mu$g). On the other hand, Table I indicates that under fixed conditions of illumination, and with a sufficiently long mirror, at a fixed distance from the irradiated zone, the amount of lead picked up in a given time was invariable within the limits of experimental error. Furthermore, the same table shows that for fixed conditions of illumination, rate of flow, and mirror position, the amount of lead picked up was proportional to the time of illumination.

[12] We are indebted to Dr. G. Calingaert of the Ethyl Corporation for the gift of this material.

TABLE I. Effect of mirror length and number of mirrors on lead pick-up; photolysis at 45°C.

Exp. No.	Mirror length mm	Mirror distance* cm	Time, min.	Pb μg
14	19.5	0	5	25
15	24	0	5	24.5
58	>32	0	7.5	35
63	>32	0	3	15
28	2 mirrors, >32	0, 12	5	28.8
30	2 mirrors, >32	0, 12	5	30.5

* Mirror distance is the distance between nearest edges of irradiated zone and mirror.

Mirror Length

From Table I it is also seen that for the rather short, fixed time (5 min.) used in the experiments described below, the amount of lead picked up from mirrors $\geq$32 mm in length was not greater than that from the shorter mirrors (19.5 and 24 mm). Similar experiments with mirrors at a distance of 18.5 cm from the irradiated zone showed, in agreement with these figures, that a mirror about 17–20 mm long was sufficient to stop all radicals. The actual mirrors used in the acetone experiments here reported were all between 32 and 38 mm long, easily sufficient to stop all mirror-active particles passing over such a surface.

Stray Pick-Up

An interesting aspect of this and other work using this method is the possibility that a considerable contribution to the lead pick-up during a run is from the stray or "shadow" mirror left in the length of the reaction tube during successive mirror depositions. Consequently, an experiment was run in which a mirror was driven up the tube toward the acetone inlet before the irradiated zone. Under these conditions the only lead that could be picked up during a run would have to come from the "shadow mirror." It was established that the amount of lead so picked up was negligible (i.e., $<\sim 1.5\mu g$).

Effect of Second Mirror

A corollary experiment is to lay down two heavy standard mirrors, one near the irradiated zone and the other some distance away. As indicated above, it had already been established that the first mirror was able to stop all mirror-active particles. Nevertheless when an additional standard mirror was placed further down the tube at a sufficient distance, increased pick-up was detected in the 45° photolysis, as shown in runs 28 and 30, in Table I. The explanation is simple. Evidence adduced by Spence and Wild[13] and Herr and Noyes,[14] as well as in this work, indicates that at least part of the reaction proceeds via

$$(CH_3)_2CO \xrightarrow{h\nu} CH_3 + CH_3CO. \qquad (1)$$

The acetyl radical is fairly stable below 60° and breaks up slowly either in the gas phase or on the wall. Apparently it does not itself react with metal mirrors.[15] Given time, however, it decomposes (i.e., as it passes down the reaction tube) in the over-all reaction:

$$CH_3CO \rightarrow CH_3 + CO \qquad (2)$$

and the additional free methyl radicals so produced can pick up lead in detectable quantities from the second mirror. A similar experiment with photolysis at 100° (in connection with further work under way on the decomposition of acetone) indicates, as expected, no such additional pick-up of lead at the second mirror.

Half-Life Experiments

It follows, of course, that the so-called half-life of methyl radicals as determined on radicals obtained from the photolysis of acetone at low temperatures (below 60°) is illusory and represents an average of two different effects: a disappearance of methyl radicals during their passage down the reaction tube, presumably giving ethane, and a production of methyl radicals from reaction (2).

For this reason, it was decided to illustrate the sensitivity of this analytical method of measuring the Paneth effect by half-life experiments on acetone photolyzed at 45°, at which temperature the CH_3CO radicals have considerable persistence, and at 100°, at which temperature the CH_3CO radicals produced by reaction (1) de-

[13] R. Spence and W. Wild, J. Chem. Soc. 352 (1937).
[14] D. S. Herr and W. A. Noyes, Jr., J. Am. Chem. Soc. **62**, 2052 (1940).
[15] Cf. T. G. Pearson and R. H. Purcell, J. Chem. Soc. 1151 (1935) for the cases of As, Sb, and Te.

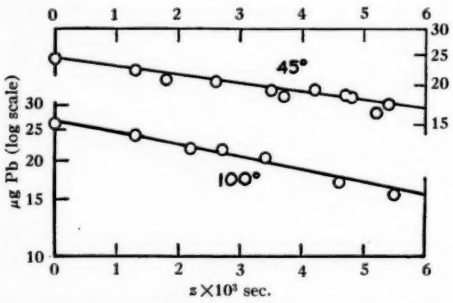

FIG. 2. The logarithm of the active concentration of radicals (measured by the quantity of lead picked up) as a function of the time of transport. Upper curve, photolysis of acetone at 45°; lower curve, at 100°.

compose via (2) presumably as rapidly as they are formed.

All the individual points obtained in this way are listed in Table II and plotted in Fig. 2. In Fig. 2, z represents the time in seconds taken by radicals to go from the irradiated zone to the mirror; z is calculated according to the formula of Paneth and Lautsch.[16] The vertical axis represents the activity of the radicals in terms of the number of μg of lead picked up. The apparent half-life calculated from the curve is 1.1 $(\pm 0.1)\times 10^{-2}$ sec. for the radicals obtained from acetone photolyzed at 45° and 8 $(\pm 0.5)\times 10^{-3}$ sec. for those produced at 100°C. These values are larger than any previously reported. The value for the half-life of methyls from the thermal decomposition of lead tetramethyl in H_2 as a carrier gas, reported by Paneth and Lautsch,[16] is $5.8-8.8\times 10^{-3}$ sec. at pressures of 2 and 2.5 mm, but with no correlation with the pressure. Any comparison of such half-life values, except as determined in the same apparatus and with the same technique, is probably unjustified, and it would seem that no absolute significance is to be attached to the values themselves. In the present experiments for example, a small but systematic error in the determination of the lead transported would have a definite effect on the half-life calculated. The difference in slopes here reported, however, (Fig. 2) indicates a real difference between the radicals produced at the different temperatures, the lower half-life value at 100° being expected, as explained above.

The lower value for the number of μg of lead picked up at "zero distance" in the 45° experiments as compared to the 100° experiments is to be attributed, of course, to the fact that not all the acetyl radicals are immediately decomposed at the lower temperature. No direct comparison with the corresponding 100° value (lead pick-up) may be made, however, because the concentrations of acetone in the irradiated zone, and hence the amounts of decomposition per unit time, are different in the two sets of experiments.

The slopes of the lines, however, are properly comparable for it was found that a change in temperature of the irradiated zone from 25° to 100° was without effect on the weight of acetone transported per unit time. It may finally be remarked that if the points plotted in these graphs had been averages of a number of widely divergent determinations (as is usually the case in Paneth mirror experiments) the distinction between the slopes of the two lines would not have been justifiable.

Steady State Concentration of Radicals

The actual concentration of free methyl radicals at any point in the tube may be calculated from the amount of lead picked up in a given time at that point and the quantity of gas passing that point in the same time. In illustration, assuming a temperature of 300°K and a pressure of ~1.5 mm in the gas flowing by at

TABLE II. Half-life measurements; all runs 5 minutes.

Temp. °C	Exp. No.	Dist. from illumination, cm	Time of transport, $z\times 10^3$ sec.	Pb picked up, μg
45	104	0	0	24.0
	103	6	1.3	22.2
	102	8.5	1.8	20.8
	101	12.2	2.6	20.5
	100	15.	3.2	22.2
	107	17.	3.5	19.2
	99	18.	3.7	18.4
	98	21.5	4.2	19.3
	106	24.5	4.7	18.5
	97	25.5	4.8	18.2
	96	29.	5.2	16.2
	105	31	5.4	17.2
100	115	0	0	26.1
	114	6	1.3	24.0
	113	10	2.2	21.9
	112	12.5	2.7	21.8
	111	16.7	3.4	20.6
	110	24.2	4.6	17.1
	108	32	5.5	15.7

[16] H. Paneth and W. Lautsch, Ber. **64**, 2708 (1931).

zero distance from the irradiated zone, the volume of gas passing this point in 5 minutes is found (from the streaming velocity) to be 2.7×10^{5} cc: the number of moles of CH_3 picked up in that time at that point is $4\times24\times10^{-6}/207$ or 4.6×10^{-7}. The concentration of CH_3 is therefore 1.7×10^{-12} mole per cc, or 2.1×10^{-13} mole percent in the gas.

Other examples of the usefulness of this method of counting free radicals will be given in forthcoming papers on the mechanism of the photolysis of propionaldehyde and of acetone.

OCTOBER, 1942 JOURNAL OF CHEMICAL PHYSICS VOLUME 10

Contact Angles at Liquid-Liquid-Air Interfaces*

WILLIAM FOX
Department of Chemistry, Columbia University, New York, New York
(Received June 15, 1942)

Angles at the points of contact of a number of liquid-liquid-air systems were measured. A new method of measuring the interfacial tension is presented. The work of adhesion between the phases is determined. A new theory of spreading is offered.

MEASUREMENTS of contact angles at liquid-liquid-solid and liquid-solid-air interfaces have been made by a number of workers. Difficulties due to poor reproducibility of solid surfaces and due to the effects of adsorbed and condensed layers on solid phases, however, markedly affect the experimental results.[1,2] Notwithstanding these difficulties the measurements of contact angles have been of considerable value in both scientific and industrial investigations.

In view of the importance of this work it is perhaps surprising that no one has made use of the corresponding phenomenon at liquid-liquid-air interfaces. This phenomenon can be easily investigated by bringing an air bubble to a liquid-liquid interface and measuring the contact angles of the system. The surfaces involved are definite and reproducible. No condensed layers of an extraneous phase can be present under the condition of the experiment. In addition the systems involve surface energies for which values are known or can be determined. (The surface energies of solids cannot readily be determined.)

Such measurements at liquid-liquid-air interfaces can be used to determine the interfacial tension free from inexact assumptions concerning the value of the contact angles, and also to determine the values for the work of adhesion and the work of spreading of different phases. It is with this valuable and thermodynamically sound tool for the study of the energy relations at liquid-liquid interfaces that this paper will be concerned.

The method used is similar to that of Taggart *et al.* applied previously only to the measurement of contact angles at liquid-solid-air interfaces.[3] An air bubble is brought by means of a curved pipette to a hollow glass tube (3-mm inside diameter) sealed to a glass rod. The air bubble is then brought down to the interface of the two liquids and the angles of contact at the points where the interfaces meet are determined. This simple apparatus can be easily refined in some such manner as indicated by Bartell[2] to allow for convenient measurement on either side of the interface. Photographs were made of the air bubble, the contact angles being determined by direct measurement with a protractor either upon the photograph itself or upon the ground glass focusing screen. The contact angles are sharply defined and reproducible, and are the same on approaching the interface

* Publication assisted by the Ernest Kempton Adams Fund for Physical Research of Columbia University.
[1] N. K. Adam, *Physics and Chemistry of Surfaces*, p. 180.
[2] F. E. Bartell and P. H. Cardwell, J. Am. Chem. Soc. 494 (1942); 1530 (1942); 1641 (1942).
[3] Taggart, Taylor, and Ince, Trans. A.I.M.E. **87**, 285 (1930).

from either direction. Measurements made at different times agree with each other within the experimental precision of the measurement.

Equilibrium at the interfaces of the systems studied was obtained quickly and did not change with time. This is not unexpected as at the immediate vicinity of the surfaces of discontinuity the phases are quickly saturated with each other. It should be noted also that as predicted by the Gibbs relation all the interfaces (liquid 1-air, liquid 2-air, and liquid 1-liquid 2) will be richer in the material for which $-\partial\sigma/\partial c$ is greatest.

The only factors that can affect the angles are those which change the relations of the three interfacial tensions. As distortion of the air bubble at the interface can have no effect on the value of the interfacial tensions it is not possible for distortion to change the values of the angles. Therefore the size of the bubble and the manner in which it is held against the interface do not affect the values obtained.

Consider a system where the air bubble makes a definite contact angle with the liquid-liquid interface. On bringing an air bubble to a water-aniline interface equilibrium is established definitely and suddenly. When the points of contact of the three interfaces are in equilibrium the following relations may be written.[4] (See Fig. 1.)

$$\sigma_{w,an}+\sigma_{w,A}\cos\theta+\sigma_{an,A}\cos\phi=\sigma_p=0; \quad (1)$$

$$\sigma_{w,A}\sin\theta-\sigma_{an,A}\sin\phi=\sigma_p=0. \quad (2)$$

From (1) and (2) we get

$$d\sigma_{an,w}=-\sigma_{w,A}[\sin(\theta+\phi)/\cos\phi]d\theta$$

$$-[\cos(\theta-\phi)/\cos\phi]d\sigma_{w,A}-\left[\frac{\cos 2\phi}{\cos\phi}\right]d\sigma_{an,A}. \quad (3)$$

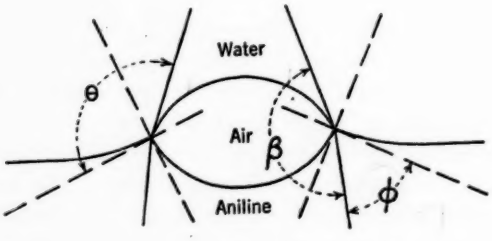

FIG. 1.

[4] σ = interfacial tension; w = water; an = aniline; A = air; $\sigma_p=0$ = tension at the points of contact at equilibrium.

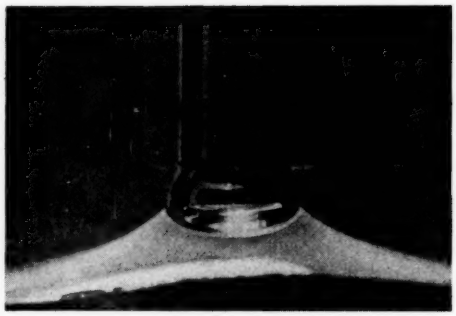

FIG. 2. Water-air-aniline; temperature 22°C.

Angle θ shall always be the angle measured through the top liquid, angle ϕ the angle through the bottom liquid, and angle β the angle through the gas phase.

Equation (3) will be discussed further in another paper.

The experimental procedure employed was to measure angle θ and then to calculate angles ϕ and β by the use of Eq. (2). Angles ϕ and β should not be measured directly as the image of the aniline-air interface is distorted by the curvature of the interfaces and by the difference in the refractive index of the different phases.

Reference to the photographs (Figs. 2 and 3) of the aniline-water-air systems[5] show that $\theta=131.1\pm3.0°$.[6]

An air bubble when released below the interface in the aniline phase will rise to the interface and (if not too large) be held there showing the same relations of the angles within the experimental precision of the measurement.

It was observed that over a range of temperature from 20° to 50° there was no measurable change in the values of the angles.[7,8]

Since a change in temperature over this range had no measurable effect on the values of the angles, we may therefore use the angles observed to determine the interfacial energies over the range of temperature for which the angles are constant.

[5] The aniline was practically colorless. C. P. Bakers analyzed.

[6] Result of twenty measurements. Mean = 131.1° a.d. 3.0°.

[7] Investigations are now being made with systems in the region of critical mixing.

[8] I. W. Wark and H. B. Cox [Trans. A.I.M.E. **112**, 189 (1934)] report no measurable change in contact angles at liquid-solid-air interfaces for ΔT of 10 degrees.

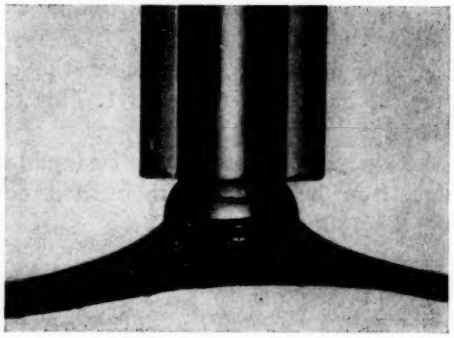

FIG. 3. Water-air-aniline; temperature 33°C.

By Eq. (2) using the surface tension values of Reynolds,[9]

$$0=\sigma_{w,A}\sin\theta-\sigma_{an,A}\sin\phi,$$

$$\sin\phi=\frac{46.4}{42.2}\sin\theta$$

$$\phi=56°,$$

and by Eq. (1)

$$0=\sigma_{an,A}\cos\phi+\sigma_{w,A}\cos\theta+\sigma_{an,w},$$

$$\sigma_{an,w_{26°C}}=6.9\pm0.6\ \text{erg/cm}^2.$$

This value although precise only to about 9 percent differs from the result predicted by Antonow's rule (which rests on the assumption that $\theta=180°$ and $\phi=0°$) by about 64 percent and from the value of Reynolds (who neglects consideration of the angle that the interface makes with the third phase) by about 44 percent.

In the case of the benzene-water-air (also ether-water-air) system the air bubble when brought down to the interface through the benzene is not held at the interface. If pressed against the interface the bubble will tend to distort and force the interface down. On the other hand when the bubble is brought up to the interface from the water layer the benzene enfolds the air bubble, i.e., the air bubble goes into the benzene layer immediately. If an air bubble is brought below the interface into the water layer and a drop of benzene placed in contact with the air bubble, the benzene spreads out over the gas phase replacing the water in contact with the air so that the angle of the benzene-water interface against the benzene-air interface is 0° and that of the water-air interface against the benzene-air and the benzene-water interfaces is 180°. This behavior can be interpreted to mean that the air bubble is more easily "wetted" by the benzene than by water.

Considering the contact angles as the angles that the tangents to the curve (benzene-air and water-air) make with the liquid-liquid interface we have at the points of contact (Fig. 4) $\theta=0°$ and $\phi=180°$ and by Eq. (1)

$$0=\sigma_{B,w}+\sigma_{B,A}\cos 0°+\sigma_{w,A}\cos 180°$$

and

$$\sigma_{B,\omega}=\sigma_{w,A}-\sigma_{B,A}. \qquad (4)$$

The same relationship holds for the ether-water-air system. These results are those predicted by Antonow's rule. Antonow's rule is an empirical equation found to hold true for a number of systems. It can be seen that Antonow's rule is a special case resulting when $\theta=0°$ and $\phi=180°$ and Eq. (1) reduces to Eq. (4).

For the nitrobenzene-water (Fig. 5), carbon tetrachloride-water, chloroform-water, and malonic ester-water systems with air we have the condition that $\theta=180°$ and $\phi=0°$. Applying Eq. (1) we see that in all these cases (R=organic liquid)

$$\sigma_{R,w}=\sigma_{w,A}-\sigma_{R,A}$$

and Antonow's rule will also hold.

In all these systems an air bubble (if not too large) when released below the interface in the organic liquid will rise to the interface and be held there showing the same relations as above within the experimental precision of the measurement.

WORK OF ADHESION OF THE GAS PHASE AT THE INTERFACE OF TWO LIQUIDS

The work of adhesion between a gas and a liquid, both in contact with another liquid, at

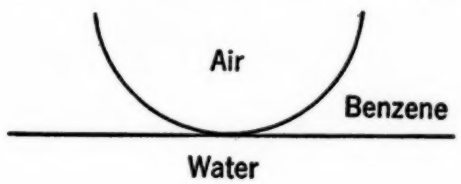

FIG. 4.

[9] W. C. Reynolds, Trans. Chem. Soc. **119**, 461 (1921).

constant temperature and pressure is numerically equal to the free energy required to separate the gas phase from the liquid phase. This value can now be determined. Let 1 represent the top liquid; 2 the bottom liquid; σ_i the initial tension at the point of contact; $\sigma_e=0$, the equilibrium tension at the points of contact.

As the air bubble is brought down to the interface, at the moment of contact $\theta_i=0°$; $\phi_i=180°$; $\beta_i=180°$.

(a) $$\sigma_i=\sigma_{2,A}+\sigma_{1,2}\cos\phi_i+\sigma_{1,A}\cos\beta_i,$$
$$\sigma_i=\sigma_{2,A}-\sigma_{1,A}-\sigma_{1,2}.$$

At equilibrium

(b) $$\sigma_e=0=\sigma_{1,2}+\sigma_{1,A}\cos\theta_e+\sigma_{2,A}\cos\phi_e.$$

Solving for

$$\sigma_{1,2}=-[\sigma_{1,A}\cos\theta_e+\sigma_{2,A}\cos\phi_e]$$

and substituting in (a) we get

$$\sigma_i=\sigma_{2,A}-\sigma_{1,A}+\sigma_{1,A}\cos\theta_e+\sigma_{2,A}\cos\phi_e. \quad (5)$$

Since $dG=VdP-SdT-Ad\sigma$

$$dG_{T,P}=-Ad\sigma,$$

$$\Delta G_{T,P}=-A(\sigma_e-\sigma_i),$$

and since

$$\sigma_e=0,$$

$$(\Delta G/A)_{T,P}=\sigma_i=-W/A=-\text{work of adhesion.}$$

In the benzene-water-air system and the ether-water-air system $\theta_e=0°$; $\phi_e=180°$; and $(\Delta G/A)_{T,P}=0$. The work of adhesion of the air bubble to the water in the presence of the organic liquid is zero and the air bubble will not be held by the water.

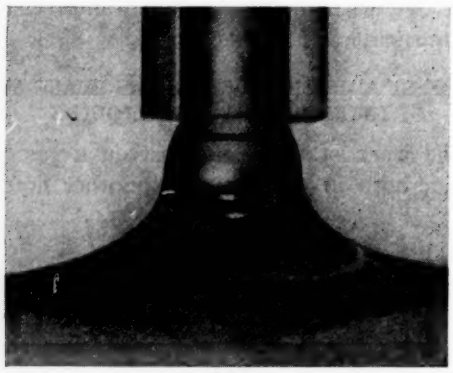

FIG. 5. Water-air-nitrobenzene; temperature 35°C.

It is also necessary to consider the energy holding the gas phase to liquid 1. This can be calculated in the following manner.

If the air bubble approaches the liquid-liquid interface from below at the moment of contact $\phi_i=0°$; $\beta_i=180°$; $\theta_i=180°$.

(c) $$\sigma_i=\sigma_{1,A}+\sigma_{2,A}\cos\beta_i+\sigma_{1,2}\cos\theta_i,$$

$$\sigma_i=\sigma_{1,A}-\sigma_{2,A}-\sigma_{1,2}.$$

At equilibrium

(d) $$\sigma_e=0=\sigma_{1,2}+\sigma_{2,A}\cos\phi_e+\sigma_{1,A}\cos\theta_e.$$

Solving for

$$-\sigma_{1,2}=\sigma_{2,A}\cos\phi_e+\sigma_{1,A}\cos\theta_e$$

and substituting in (c)

$$\sigma_i=\sigma_{1,A}-\sigma_{2,A}+\sigma_{2,A}\cos\phi_e+\sigma_{1,A}\cos\theta_e. \quad (6)$$

In the benzene-water-air and the ether-water-air systems $\phi_e=180°$; $\theta_e=0°$; $\beta_e=180°$ and from (6)

$$\sigma_i=-2(\sigma_{2,A}-\sigma_{1,A}).$$

$(\Delta G/A)_{T,P}$ will be negative and the gas phase will be held by the organic liquids (Table I).

In the carbon tetrachloride-water-air, nitrobenzene-water-air, chloroform-water-air and malonic ester-water-air systems $\theta_e=180°$; $\phi_e=0°$; $\beta_e=180°$. Applying Eq. (5)

$$\sigma_i=-2[\sigma_{1,A}-\sigma_{2,A}],$$

and from Eq. (6)

$$\sigma_i=0.$$

The air bubble will thus be held by the bottom liquid but not by the top liquid (Table I).

In the aniline-water-air system by Eq. (5)

$$(\Delta G/A)_{T,P}=-11.1 \text{ ergs/cm}^2$$

and by Eq. (6)

$$(\Delta G/A)_{T,P}=-2.7 \text{ ergs/cm}^2.$$

These values are equal to the free energy required to separate the gas phase from the aniline phase (saturated with water) and from the water phase (saturated with aniline), respectively (Table I).

TABLE I.*

Liquid 1 (saturated with liquid 2)	Liquid 2 (saturated with liquid 1)	Work of adhesion of liquid 1 (in contact with liquid 2) to air $=(-\Delta G/A)_{T,P}$	Work of adhesion of liquid 2 (in contact with liquid 1) to air $=(-\Delta G/A)_{T,P}$	Work of adhesion in air of liquid 1 to liquid 2 $=(-\Delta G/A)_{T,P}$	Temperature °C
Benzene	Water	68.8	0.0	57.6	19
Ether	Water	21.2	0.0	35.0	18
Water	Aniline	2.7	11.1	81.7	26
Water	Chloroform	0.0	66.8	52.8	18
Water	Carbon tetrachloride	0.0	87.0	53.4	17
Water	Nitrobenzene	0.0	49.4	86.4	18

* Units of Tables I and II =ergs/cm².
Values in Tables I and II based on surface tension data of Reynolds (see reference 9).

WORK OF ADHESION OF TWO-LIQUID PHASES AT A LIQUID-GAS INTERFACE

The work of adhesion between two liquids in contact with a gas phase at constant temperature and pressure is numerically equal to the free energy per unit area required to pull the liquids apart. This can also be calculated.

When a drop of the top liquid first touches the surface of the bottom liquid $\beta_i=0°$; $\theta_i=180°$; $\phi_i=180°$; and

(e) $$\sigma_i=\sigma_{2,1}+\sigma_{1,A}\cos\theta_i+\sigma_{2,1}\cos\phi_i,$$

$$\sigma_i=\sigma_{2,1}-\sigma_{1,A}-\sigma_{2,A}.$$

At equilibrium

(f) $$\sigma_e=0=\sigma_{2,1}+\sigma_{1,A}\cos\theta_e+\sigma_{2,A}\cos\phi_e.$$

Solving for

$$\sigma_{2,1}=-\sigma_{1,A}\cos\theta_e-\sigma_{2,A}\cos\phi_e,$$

and substituting in (e) we get[10]

$$\sigma_i=-\sigma_{1,A}-\sigma_{2,A}-[\sigma_{1,A}\cos\theta_e+\sigma_{2,A}\cos\phi_e]. \quad (7)$$

In the benzene-water-air and the ether-water-air systems $\theta_e=0°$; $\phi_e=180°$; $\beta_e=180°$; and from (7)

$$(\Delta G/A)_{T,P}=-2\sigma_{1,A}.$$

In the nitrobenzene-water-air, carbon tetrachloride-water-air, chloroform-water-air, and malonic ester-water-air systems $\theta_e=180°$; $\phi_e=0°$; $\beta_e=180°$. $(\Delta G/A)_{T,P}$ will therefore be equal to $-2\sigma_{2,A}$ (again twice the surface energy of the organic phase).

For the aniline-water-air system from Eq. (7) the work of adhesion of the two phases in the presence of air is found to be 81.7 ergs/cm² (Table I).

In the manner indicated above the value for the work of adhesion between any two liquids in the presence of a gas phase can be determined. The values thus obtained (Table I) do not agree with those given by Harkins[11] which are determined by measurements of the surface energies of the pure liquids, the interfacial tension between the saturated phases, and the application of the Dupré equation. If the surface tensions of each phase saturated with each other were determined, and the interfacial tension could be independently determined accurately, the application of the Dupré equation should then give the values as above calculated (Table I).

CONDITIONS WHICH WILL DETERMINE SPREADING

The theory of spreading which is commonly accepted states that spreading will occur if the work of adhesion between two phases is greater than the work of cohesion of the phase which is spreading.[12,13] From Eq. (7) we can see that for the organic liquid-water-air systems where the contact angles are 0° and 180° the work of adhesion will be equal to twice the surface tension of the liquid which has the lower surface

[10] Compare with the Dupré equation, $W=\sigma_{2,A}+\sigma_{1,A}-\sigma_{2,1}$.

[11] W. D. Harkins, J. Am. Chem. Soc., 356 (1917).
[12] W. D. Harkins, 6th Colloid Symposium Monograph, p. 23.
[13] W. D. Harkins, J. Chem. Phys. 9, 552 (1941).

TABLE II.

Liquid 1 (saturated with liquid 2)	Liquid 2 (saturated with liquid 1)	$(-\Delta G/A)_{T,P}$ liquid 1 spreading on liquid 2 in air	"Spreading coefficient" (Harkins) $t=20°C$	$(-\Delta G/A)_{T,P}$ liquid 2 spreading on liquid 1 in air	"Spreading coefficient" (Harkins) $t=20°C$	Temperature °C
Benzene	Water	57.6	8.86	−11.2	−78.92	19
Ether	Water	35.0	44.95	13.8	−66.35	18
Water	Aniline	70.6	−35.94	79.0	24.40	26
Water	Chloroform	−14.0	−78.25	52.8	12.99	18
Water	Carbon tetrachloride	−33.6	−89.35	53.4	2.83	17
Water	Nitrobenzene	37.0	−55.03	86.4	3.71	18

tension. Now the work of cohesion of a liquid in air is twice the surface tension. Therefore in considering the liquid with the lower surface tension as spreading, the "spreading coefficient" defined as *Wa-Wc* (for the cases above mentioned where the contact angles are 0° and 180°) will not be greater than zero. When the liquid with the greater surface tension is considered in spreading the "spreading coefficient" as defined will always be negative.

This "peculiar restriction" in the instances where the empirical relation expressed by Antonow actually does hold true is realized by the proponents of that theory, in answer to which they express great doubt that the Antonow relation is a valid one.

Consideration of what happens when a liquid spreads makes it evident that to explain spreading in a specific gas phase, we need only compare the work of adhesion of the gas to the liquid on which the spreading is to occur with the work of adhesion of the two liquids in the presence of that same gas phase. If the free energy change at constant temperature and pressure is negative the action will be spontaneous, and spreading will occur in that direction which will give a negative free energy change. A direct comparison of the values of the free energy change for the systems involved will then give a thermodynamically exact measure of the tendency and direction in which spreading will occur (Table II).

This theory is equally well applied to the phenomena at liquid-solid-air and liquid-liquid-solid interfaces.

SUMMARY

1. A method is presented whereby it is possible to determine the interfacial tension between two liquids from the surface tensions.

2. Antonow's rule is shown to be a special case of the equation

$$0=\sigma_{1,2}+\sigma_{1,A}\cos\theta+\sigma_{2,A}\cos\phi.$$

3. The Dupré equation is indicated as being a special case of the equation

$$\sigma_i=-\sigma_{1,A}-\sigma_{2,A}-[\sigma_{1,A}\cos\theta_e+\sigma_{2,A}\cos\phi_e].$$

4. The work of adhesion of a gas to each of the two liquids in contact with each other is calculated by the equations

$$\sigma_i=\sigma_{2,A}-\sigma_{1,A}+\sigma_{1,A}\cos\theta_e+\sigma_{2,A}\cos\phi_e$$

and

$$\sigma_i=\sigma_{1,A}-\sigma_{2,A}+\sigma_{2,A}\cos\phi_e+\sigma_{1,A}\cos\theta_e.$$

5. The work of adhesion of two liquids in contact with air is determined by the equation

$$\sigma_i=-\sigma_{1,A}-\sigma_{2,A}-[\sigma_{1,A}\cos\theta_e+\sigma_{2,A}\cos\phi_e].$$

6. A new theory of spreading is offered.

ACKNOWLEDGMENTS

The author wishes to express appreciation to Professor Arthur W. Thomas for his interest and guidance; also to thank Mr. Mario Castillo for generously making available his photographic equipment and Dr. Edward Adler for his careful review of the manuscript.

Contribution to Statistical Mechanics*

JOSEPH E. MAYER
Chemistry Department, Columbia University, New York, New York

(Received June 1, 1942)

The method of the grand partition function may be used to calculate distribution functions $F_n(z, \{\mathbf{n}\})$ proportional to the probability that n molecules in a system of fugacity z, and fixed temperature, occupy the position of their coordinates symbolized by $\{\mathbf{n}\}$. The method makes use of the distribution functions $F_n(0, \{\mathbf{n}\})$ at zero fugacity. The distribution functions may be written $F_n(z, \{\mathbf{n}\}) = \exp[-W_n(z, \{\mathbf{n}\})/kT]$, in which $W_n(z, \{\mathbf{n}\})$ is the potential of average force of n molecules at the fugacity z, which becomes equal to the ordinary potential energy at zero fugacity. The equations may be generalized to permit the calculation of the distribution functions at any fugacity assuming a knowledge of them at any other fugacity. Using methods previously employed for imperfect gases, the pressure, and also the density in molecules per unit volume, may be developed in a power series of difference of fugacity around any arbitrary fugacity. The coefficients of these developments are calculable at all fugacities by the same equations always employing the potentials of average force at the fugacity around which the development is made. The power series obtained represent functions which are regular on the real positive axis of fugacity except at the points characteristic of the phase transitions in the system.

INTRODUCTION

WE consider only systems of infinite extent in the volume space, the temperatures of which are fixed at T. The systems are one component systems, containing only one kind of molecule. Instead of using pressure P or density ρ for the independent variable of the system we shall find it convenient to use the fugacity, normalized in density units, for which the symbol z or y will be used. The definition of this fugacity may be written:

$$z = \lim_{\rho_0 = 0} [\rho_0 \exp(\mu - \mu_0)/kT], \tag{1}$$

in which μ is the chemical potential of the system, and μ_0 is the chemical potential at the density ρ_0. The density is expressed in molecules per unit volume, $\rho = \lim (N/V)$. According to this definition of z, as the fugacity is reduced to such a value that the system becomes a perfect gas the fugacity and density become equal:

$$\lim_{z=0} \left[\frac{z}{\rho}\right] = 1. \tag{2}$$

The individual molecule requires f coordinates for the description of its configuration, and three of these may always be chosen as the three cartesian coordinates, x, y, z, of the center of mass. The $f-3$ internal coordinates are either bounded between limits such as 0 and 2π, or the internal energy of the molecule is assumed to approach infinity as the value of the coordinate becomes large. The coordinates of the molecule i will be symbolized by

$$(i) = x_i, y_i, z_i, q_{1i}, \cdots, q_{(f-3)i}, \tag{3}$$

and the volume element, calculated in the f dimensional cartesian space by

$$d(i) = dx_i dy_i dz_i J\left[\frac{x}{q}\right] dq_{1i} \cdots dq_{(f-3)i}, \tag{4}$$

in which J is the Jacobian. The coordinates of n molecules will be indicated by

$$\{\mathbf{n}\} = (1), (2), \cdots, (i), \cdots, (n), \tag{5}$$

and the volume element by

$$d\{\mathbf{n}\} = d(1)d(2)\cdots d(i)\cdots d(n). \tag{6}$$

The distribution function $F_n(z, \{\mathbf{n}\})$, a function of the coordinates of n molecules, is defined by the statement that in an infinite system of fugacity z the probability that n molecules be at the position symbolized by $\{\mathbf{n}\}$, and in the element of configuration space $d\{\mathbf{n}\}$ is proportional to $F_n(z, \{\mathbf{n}\})d\{\mathbf{n}\}$:

$$F_n(z, \{\mathbf{n}\}) \text{ is proportional to probability of the configuration } \{\mathbf{n}\}, \tag{7}$$

and the normalization is so chosen that

$$\lim_{V=\infty} \left[\frac{1}{V^n} \int_V \int \cdots \int F_n(z, \{\mathbf{n}\}) d\{\mathbf{n}\}\right] = 1; \tag{8}$$

* Publication assisted by the Ernest Kempton Adams Fund for Physical Research of Columbia University.

the average value of the function F_n integrated over the internal coordinates of the molecules is unity in the $3n$-dimensional cartesian space of the coordinates of the centers of mass.

Functions $W_n(z, \{\mathbf{n}\})$ of the coordinates of n molecules in a system of fugacity z may be defined by the equation

$$-W_n(z, \{\mathbf{n}\})/kT = \ln F_n(z, \{\mathbf{n}\}). \quad (9)$$

These functions are actually the potentials of the average forces between n molecules in an infinite system of the fugacity z.

At zero fugacity the density is zero, and the n molecules are isolated in space. In a classical system the distribution function at zero density is proportional to the exponent of minus the potential energy divided by kT. We see, then, that for a classical system

$$W_n(0, \{\mathbf{n}\}) = U_n\{\mathbf{n}\} \quad \text{(classical)}. \quad (10)$$

If the deviations due to quantization from the classical equations are large the function $W_n(0, \{\mathbf{n}\})$ is generally a function of the temperature, but will still have such properties of the potential energy as will be made use of in this article. For convenience we shall refer to W_n at zero fugacity as the potential energy, but the use of the equations of this article is in no way restricted to classical systems.[1] For a quantum mechanical system the function $W_n(0, \{\mathbf{n}\})$ must be calculated by means of a Slatersum. An alternative and probably more satisfactory method of handling the case of a system of molecules having internal quantized degrees of freedom would be to replace the internal coordinates by the corresponding set of quantum numbers and replacing integration in the equations of this article by summation over the discrete values of the internal quantum numbers. In general the functions of the coordinates of the centers of mass may be handled as classical, but the functions would be different for different values of the internal quantum numbers.

In the succeeding section we shall construct an equation relating the distribution functions at two different fugacities, z and $y+z$.

[1] See, for instance, the analagous treatment of quantum mechanical systems by B. Kahn and G. E. Uhlenbeck, Physica **5**, 237 (1938), and by J. de Boer, Dissertation, Amsterdam (1940).

GENERALIZATION OF THE GRAND PARTITION FUNCTION

For reasons of brevity we introduce the symbol

$$\varphi(z) = P(z)/kT, \quad (11)$$

with $P(z)$ the pressure.

The probability $P_n(V, z, \{\mathbf{n}\})d\{\mathbf{n}\}$ that in an infinite system of fugacity z, there will be within the finite volume V exactly n and no more molecules, located at the position indicated by the symbol $\{\mathbf{n}\}$ (for which all n centers of mass are within V), and within the element $d\{\mathbf{n}\}$ of the configuration space, is known, from the theory of the grand partition function, to be given by

$$P_n(V, z, \{\mathbf{n}\}) = [\exp - V\varphi(z)]z^n F_n(0, \{\mathbf{n}\}). \quad (12)$$

The probability that there be exactly n molecules within V, without reference to their positions, is obtained by dividing the integral of this function over the volume V by $n!$, since integration covers $n!$ equivalent positions differing only in permutations of the identical molecules. The probability of having no molecules in V is $\exp - V\varphi(z)$. The sum of these probabilities over all n values, 0 to ∞, is unity. It follows that

$$\exp V\varphi(z) = \sum_{n=0}^{\infty} \frac{z^n}{n!} \int_V \int \cdots \int F_n(0, \{\mathbf{n}\})d\{\mathbf{n}\}, \quad (13)$$

which is one of the usual forms of the grand partition function.

The volume V must be macroscopically large so that the influence of surface effects is negligible. It is to be noted that the normalization of Eq. (8) applies only to the limit of infinite volume, and the integral of F_n over the finite volume V is not, in general, V^n.

For finite volumes V and real systems with short range repulsive forces the sum in (13) always converges, since the repulsive energy at short distances assures us that for sufficiently large values of n the integrand F_n approaches zero over the whole range of integration. Since the series is regular to infinite values of the fugacity, singularities in the pressure, indicative of phase transitions, appear only by going to the limit of infinite volume.[1]

The probability that in an infinite system of fugacity z, there be at the n points $\{\mathbf{n}\}$, in the element $d\{\mathbf{n}\}$, one molecule at each point, irrespective of the positions of other molecules in the system, is $[\rho(z)]^n F_n(z, \{\mathbf{n}\})d\{\mathbf{n}\}$. This probability will be equal to the sum of probabilities constructed in the following way. We enclose the n points by a singly connected volume V. The probability that there be a molecule at each of the n points, $\{\mathbf{n}\}$, and exactly m other molecules somewhere in V will be the integral of $P_{n+m}(V, z, \{\{\mathbf{n}\}+\{\mathbf{m}\}\})d\{\mathbf{n}+\mathbf{m}\}$ over all positions $\{\mathbf{m}\}$ within V divided by $m!$. The probability desired is the sum of these probabilities over all values of m:

$$[\rho(z)]^n F_n(z, \{\mathbf{n}\}) = \sum_{m=0}^{\infty} \int_V \int \cdots \times \int P_{n+m}(V, z, \{\mathbf{n}+\mathbf{m}\})d\{\mathbf{m}\}. \quad (14)$$

In order to obtain somewhat simpler appearing equations later we introduce

$$Q_n(z, \{\mathbf{n}\}) = \left[\frac{\rho(z)}{z}\right]^n F_n(z, \{\mathbf{n}\}), \quad (15)$$

and note that in view of Eq. (2),

$$Q_n(0, \{\mathbf{n}\}) = F_n(0, \{\mathbf{n}\}). \quad (15')$$

Introducing (15′) in (14), and using (15) and (12), one finds, with the completely arbitrary introduction of $\exp V\varphi(0) = 1$, since $\varphi(0) = 0$,

$$[\exp V\varphi(z)]Q_n(z, \{\mathbf{n}\}) = \sum_{m=0}^{\infty} \frac{z^m}{m!}[\exp V\varphi(0)] \times \int_V \int \cdots \int Q_{n+m}(0, \{\mathbf{n}+\mathbf{m}\})d\{\mathbf{m}\}. \quad (16)$$

The convention

$$Q_0(z) = 1 \quad (16')$$

is used. With (16′) Eq. (13) is seen to be a special case of (16).

For all finite values of V, and for real systems of molecules with short range forces and repulsion at short distances, the sum of (16) converges for the same reason discussed in connection with (13). Furthermore, for finite values of V, the functions $Q_n(z, \{\mathbf{n}\})$ for sufficiently large values of n are seen to approach zero in value for all values of the argument $\{\mathbf{n}\}$ within the volume V.

We form the permanently convergent sum

$$I_n\{\mathbf{n}\} = \sum_{m=0}^{\infty} \frac{(-z)^m}{m!}[\exp V\varphi(z)] \times \int_V \int \cdots \int Q_{n+m}(z, \{\mathbf{n}+\mathbf{m}\})d\{\mathbf{m}\}. \quad (17)$$

Into this the expression (16) for $Q_{n+m}(z, \{\mathbf{n}+\mathbf{m}\})$ is inserted:

$$I_n\{\mathbf{n}\} = \sum_{m=0}^{\infty} \sum_{k=0}^{\infty} \frac{z^{m+k}(-)^m}{m!k!}[\exp V\varphi(0)] \times \int_V \int \cdots \int Q_{n+m+k}(0, \{\mathbf{n}+\mathbf{m}+\mathbf{k}\})d\{\mathbf{m}+\mathbf{k}\}.$$

It is seen that for any given value of $m+k$ the sum of the coefficients is $(1-1)^{m+k}$ so that only the term $m=0$, $k=0$, remains. It follows that $I_n\{\mathbf{n}\} = [\exp V\varphi(0)]Q_n(0, \{\mathbf{n}\})$. One may write

$$[\exp V\varphi(0)]Q_n(0, \{\mathbf{n}\} = \sum_{m=0}^{\infty} \frac{(-z)^m}{m!}[\exp V\varphi(z)] \times \int_V \int \cdots \int Q_{n+m}(z, \{\mathbf{n}+\mathbf{m}\})d\{\mathbf{m}\}. \quad (18)$$

Let us now form $[\exp V\varphi(y+z)]Q_n(y+z, \{\mathbf{n}\})$, for the fugacity $y+z$, by inserting $y+z$ instead of z in the right-hand side of Eq. (16). Into this expression Eq. (18) for $[\exp V\varphi(0)]Q_{n+m}(0, \{\mathbf{n}+\mathbf{m}\})$ may be inserted. The resulting expression gives an explicit equation for the functions at the fugacity $y+z$ in terms of a double summation over numbers m and k of integrals of the functions at the fugacity z of $n+m+k$ molecules. For constant value of $m+k$ the coefficient is the sum of $(y+z)^m(-z)^k/m!k!$ over all values m with $m+k$ constant. The value of this sum is

$y^{m+k}/(m+k)!$. One obtains

$$[\exp V\varphi(y+z)]Q_n(y+z, \{\mathbf{n}\})$$

$$= \sum_{m=0}^{\infty} \frac{y^m}{m!}[\exp V\varphi(z)]$$

$$\times \int_V \int \cdots \int Q_{n+m}(z, \{\mathbf{n}+\mathbf{m}\})d\{\mathbf{m}\}. \quad (19)$$

Equation (19) might be regarded as a generalization of the equation of the grand partition function. The special case $z=0$ leads to Eq. (16). The case $y=-z$ leads to Eq. (18). The case $n=0$, with the convention (17) leads to an equation for the pressure $P=kT\varphi$, Eq. (11). In the usual formulation of the theory of the grand partition function the potential energy $U_n\{\mathbf{n}\}$ of n isolated molecules plays a singular role. In the formulation of Eq. (19) the fugacity zero, for which $W_n=U_n$, Eq. (10), is not singled out as exceptional, but the potentials of average force at any two different fugacities are connected.

For finite values of V, and for real systems with short range forces and repulsion on close approach, the sum of Eq. (19) is permanently convergent for all values of y. There are, consequently, no singularities in the functions φ or Q if these are calculated by using finite V values. There will, however, be enormously sharp breaks in the plot of these functions against y if macroscopic volumes are used. The equation implicitly assumes that the limit of infinite volume is used.

Equation (19) is entirely unsuitable, without transformation, for numerical solution, and for the same reason that the sharp breaks in the functions of y occur at large values of V, namely because for finite y and macroscopic values of V numerical convergence only sets in at enormously high terms: the largest term in the sum is that for which m is about 10^{23}. In the next section we shall show one method, of limited value, by which numerical computations may be attempted.

THE DEVELOPMENT OF Q_n AS A SUM OF SEPARABLE FUNCTIONS

The equations of the last section have been derived almost without reference to the form of the functions $Q_n(z, \{\mathbf{n}\})$ for different values of n. It was only necessary to assume the absolute convergence of the various sums appearing, which was assured by the assumption of a repulsive energy of sufficient magnitude.

In view of their definition in terms of probabilities, all the functions $Q_n(z, \{\mathbf{n}\})$ must be positive. It is seen from (19) that if the $Q_n(0, \{\mathbf{n}\})$ are all positive, then the $Q_n(z, \{\mathbf{n}\})$ will all be positive for real positive values of the fugacity. The functions at zero fugacity are generally regarded as defining the system, being themselves defined in terms of the potential energy $U_n\{\mathbf{n}\}$ by (10), (9), and (15′). As long as the potential energy is real the functions at zero fugacity are positive.

Most methods of attempting to obtain the properties of systems in the liquid state make implicit use of the assumption that the potentials of average force, $W_n(z\{\mathbf{n}\})$, and the distribution functions Q_n, at the fugacity z can undergo arbitrary small variations away from the equilibrium values, without leading to geometrical inconsistencies in their definitions as probabilities.

Some light may be shed on whether this is justifiable by a consideration of Eq. (19). Arbitrary functions $Q_n(z, \{\mathbf{n}\})$ could only represent a conceivable geometrical configuration of molecules at the fugacity z if the functions themselves were positive, and if the functions $Q_n(0, \{\mathbf{n}\})$, calculated from (19) with $y=-z$ were also positive. This condition is necessary and sufficient.

Now it can be independently shown that an arbitrary set of functions $F_n\{\mathbf{n}\}$ obeying conditions which will be set forth in the latter part of this section (namely, Eqs. (25), (26), and (27)) represents geometrically possible distribution functions of any finite numbers of molecules in an infinite system, provided the total density in the system is less than some value ρ_0, but are geometrically inconceivable as distribution functions if the density is assumed to exceed this value. The proof follows somewhat later.

The experimental functions $Q_n(z, \{\mathbf{n}\})$ in a real system obey Eq. (19) leading to functions $Q_n(0, \{\mathbf{n}\})$ of the real system, which are, of course, positive. Now suppose that we were to use Eq. (19) to calculate certain hypothetical functions, $Q_n(-\epsilon, \{\mathbf{n}\})$, $\epsilon>0$, for which ρ would have the negative value, $-\alpha$. As long as ϵ

remains small (but not necessarily infinitesimal), the functions $Q_n(-\epsilon, \{\mathbf{n}\})$ will remain positive; indeed, this will presumably be the case at least up to values of ϵ equal to the fugacity at which condensation occurs if the temperature is below the critical point. The functions $Q_n(z, \{\mathbf{n}\})$ of this system would then represent the distribution functions in another system for which the fugacity is $z+\epsilon$, and for which the distribution functions at zero fugacity were $Q(-\epsilon)$, and which would have a higher density than the first. It follows that the distribution functions of a real system are permissible geometrical representations of the distribution of molecules at a higher density than the real density of the system.

If we now only assume that the limiting density ρ_0, characteristic of the distribution functions, is a continuous function of the form of the functions $F_n\{\mathbf{n}\}$, then an arbitrary infinitesimal variation in the form of the actual distribution functions of a real system will not lead to functions which are geometrically unrealizable as probability functions for the distribution of molecules at the density of the system.

It remains necessary to prove that there is one limiting density ρ_0 for a given assumed set of distribution functions, $F_n\{\mathbf{n}\}$.

Such an assumed set of distribution functions must first obey the conditions imposed on any probability functions, that

$$\lim_{V=\infty}\left[\frac{1}{V}\int_V\int\cdots\int F_n\{\mathbf{n}\}d(i)\right] = F_{n-1}\{\{\mathbf{n}\}-(i)\}, \quad (20)$$

in which the division of the integral by V is required by the normalization of Eq. (8). The set of functions will obey (20) if

$$\lim_{r_{ni}=\infty}[F_{n+1}\{\{\mathbf{n}\}+(i)\}]=F_n\{\mathbf{n}\}F_1(i), \quad (21)$$

and the approach F_{n+1} to the product F_nF_1 is sufficiently rapid as the distance r_{ni} between the molecule i and the nearest member of the set $\{\mathbf{n}\}$ increases. This condition will be satisfied for finite values of n if the functions are constructed according to (25) and (26), as discussed later. If (27) is also satisfied we have a self-consistent scheme of constructing functions $F_n\{\mathbf{n}\}$, up to any finite value of n, which represent possible geometrical distributions of n molecules in an infinite space, and therefore at zero density.

We now ask whether such a set of functions, defined up to some given n, can represent the distribution of a set of n molecules in a system of volume V (n/V negligibly small) in which there are a total of N molecules with $N/V=\rho$. The question is equivalent to asking whether there exists a positive function $F_N\{\mathbf{N}\}$ of the coordinates $\{\mathbf{N}\}$ of all the molecules in the system for which

$$\frac{1}{V^{N-n}}\int_V\int\cdots\int F_N\{\mathbf{N}\}d\{\mathbf{N}-\mathbf{n}\}=F_n\{\mathbf{n}\}.$$

But if such a positive function does exist for N molecules there also exists one for $N-k$ molecules, namely, that obtained by integrating $F_N\{\mathbf{N}\}$ over the coordinates of k molecules, and dividing by V^k. Conversely if no such function exists for N, then no such function exists for a number of molecules greater than N. It is also trivial to see that for the type of distribution functions occurring in nature, namely, those for which repulsion between molecules exists, and $F_n\{\mathbf{n}\}$ approaches zero if two molecules are too close together, the upper limit N_0, for which such a positive distribution function can be found, is not, in general, infinity. It follows that for any arbitrarily defined set of distribution functions obeying (20), there exists a density $N_0/V=\rho_0$ such that the distribution functions represent a conceivable geometrical distribution of molecules in any system of density equal to or less than ρ_0, but not at higher densities.

We propose to seek solutions for the set of Eqs. (19) for which the distribution functions $Q_n(z, \{\mathbf{n}\}$ obey certain restricting conditions. The conditions themselves will be discussed first, and secondly whether the limitations are to be expected to be applicable to real systems.

We wish to seek only solutions for which the distribution functions of two distant subsets of molecules $\{\mathbf{n}\}$ and $\{\mathbf{m}\}$ are equal to the product of the distribution functions of the two subsets separately. If r_{nm} is used to signify the distance, in the three-dimensional cartesian space of the

centers of mass of the molecules, of the two nearest molecules belonging to different sets $\{\mathbf{m}\}$ and $\{\mathbf{n}\}$, then we wish to assume that always,

$$\lim_{r_{nm}=\infty}[Q_{n+m}(z,\{\mathbf{n}+\mathbf{m}\})]=Q_n(z,\{\mathbf{n}\})Q_m(z,\{\mathbf{m}\}). \quad (22)$$

We shall use the symbol $\{\nu\}_n$ to indicate the coordinates of a set of ν molecules, all of which are members of the set $\{\mathbf{n}\}$, and $\sum\{\nu\}_n$ to indicate summation over all possible subsets of the set $\{\mathbf{n}\}$ including the improper subset $\{\nu\}_n=\{\mathbf{n}\}$. Using the functions $W_n(z,\{\mathbf{n}\})$ defined by (9) we may formally define functions $w_\nu(z,\{\mathbf{v}\})$ by the equation

$$w_\nu(z,\{\mathbf{v}\})=\sum\{\mathbf{n}\}_\nu(-)^{\nu-n}W_n(z,\{\mathbf{n}\}_\nu, \quad (23)$$

for which the inverse is

$$W_n(z,\{\mathbf{n}\})=\sum\{\mathbf{v}\}_n w_\nu(z,\{\mathbf{v}\}_n), \quad (24)$$

in which the functions w_ν will be referred to as the component potentials of average force.

Taking the logarithm of (22), using (15) and (9), one sees that the assumption of Eq. (22) is equivalent to the assumption that

$$\lim_{r_{\nu\mu}=\infty}[w_{\nu+\mu}(z,\{\mathbf{v}+\mathbf{u}\})]=0, \quad (25)$$

namely, that the component potentials of average force approach zero in value if any one of the molecules of the set is far distant from all the other molecules of the set, or more generally, if the set breaks naturally into two or more distant subsets of molecules.

The use of Eq. (24) to represent the total potential of n molecules as a sum of terms each depending on the coordinates of a subset of the molecules alone, is usual at zero fugacity, for which the potential of average force is the true potential of the isolated molecules. For systems with van der Waals forces it is usually written with the drastic assumption that the total potential is the sum of the potentials of the single molecules $w_1(0,(i))$, plus the sum over all pairs of the mutual pair potentials $w_2(0,\{(i)+(j)\})$, which in our terminology would be assuming that $w_\nu=0$, $\nu\geq 3$. The assumption of Eq. (25) is essentially only that all forces fall to zero between distant molecules.

We wish, however, to make a more restrictive assumption than (25), namely, that the approach to zero is sufficiently rapid so that the integral

$$\lim_{V=\infty}\Big[\int_V\int\cdots\int[\exp -w_\nu(z,\{\mathbf{v}\})/kT-1]\times\prod_{i=1}^{i=\nu}[\exp -w_1(z,(i))/kT]d\{\mathbf{v}-\mathbf{1}\}, \quad (26)$$

remains finite even if the volume V over which the range of integration is extended approaches infinite limits. The assumption of finite values for (26) will not be valid for $w_2(0,\{(i)+(j)\})$ if the molecules i and j are charged. In all other cases of physical significance it appears to be likely that the assumption is justified.

We wish actually to assume that the terms w_ν of Eq. (24) converge very rapidly, and that terms with $\nu\geq 3$ are sufficiently unimportant that useful results may be obtained with their neglect. This assumption is in no way formally required, but any numerical computation involving the higher terms must necessarily be tedious, at least. Formally, however we shall have to assume that

$$\lim_{\nu=\infty}[w_\nu(z,\{\mathbf{v}\})]=0 \quad \text{(for all configurations } \{\mathbf{v}\}). \quad (27)$$

The assumptions of Eqs. (25), (26), and (27), will presumably be accepted as reasonable assumptions for systems composed of uncharged molecules at such temperatures and fugacities for which the liquid or gaseous phases are stable. The validity of the assumptions in the case that the crystalline phase is stable requires special consideration.

For a single crystal of fixed direction of the crystal axes, and with fixed phase of the lattice points along the axes, it appears to be natural to accept all three assumptions as valid for the distribution function. Such a crystal will be referred to as a fixed crystal. The function $w_1(z,(i))$ will be triply periodic in the coordinates of the center of mass of the molecule i. The periodicity of this function alone determines the long range order in the crystal. The function $w_2(z,\{(i)+(j)\})$ would also be expected to be triply periodic, with the same periodicity of the

lattice, in a rigid translation of the two centers of mass of the two molecules i and j together. (It might, however, conceivably be accidently invariant under such a translation.) The function w_2 determines the extent of the correlation between the positions of the two molecules, and must, in a real system, approach zero for large distances between the two molecules. It must also, in a real system, approach positively infinite values as the distance between the two molecules becomes small, assuring zero probability for the two molecules to be at the same position.

There seems, however, to be no simple way to insert boundary conditions into the grand ensemble upon which Eq. (19) is based, in such a way as to assure us that the solutions obtained would correspond to those of a fixed crystal. It is true that Kirkwood and Monroe[2] in their theory of fusion have obtained periodic solutions for w_1 by a method which is not essentially dissimilar to that which can be based on (19). However, the absence of satisfactory existence theorems for the type of non-linear integral equation which they were forced to solve, and the necessity which they faced of making several assumptions, may still leave possible doubt as to the validity of the result.

It might seem at first sight as though there were no difficulty. The solution expected from such an equation as (19) would correspond to the distribution functions for an ensemble of randomly oriented crystals with random phase of the lattice points for each orientation. Such a distribution function will be a linear combination of those corresponding to the fixed crystals. The solution of an integral equation derived by operating on (19) may well be expected to correspond to that of a fixed crystal with fixed but arbitrary axes and phase, so that the general solution would be a linear combination of these with all axes and phases. The difficulty arises in that the equations lead directly to the potentials of average force, and under the assumptions which we have made in Eqs. (25), (26), and (27).

The linear combination of *distribution functions* corresponding to an ensemble of fixed crystals will not correspond to a linear combination of potentials of average force, and the potentials of average force of such a linear combination will most certainly *not* obey the condition (22). None of the assumptions (25), (26), or (27) will be valid for the potentials of average force obtained from the distribution functions for an ensemble of crystals by Eq. (9).

We propose to show, however, that solutions corresponding to one single fixed crystal would be expected, if a system is assumed whose characteristics go over in the limit to those of the real system. It appears therefore to be probable, even aside from the success of Kirkwood and Monroe, that distribution functions corresponding to one fixed crystal, and obeying (25), (26), and (27), would be solutions to equations based on (19) and solved with the usual limits of accuracy in the treatment of the grand partition function.

Consider a real system, characterized by its component potentials $w_\nu(0, \{\nu\})$ at zero fugacity, for which the solutions of Eq. (19) at T and z would be expected to be functions corresponding to an ensemble of crystals with randomly oriented axes. The component potential $w_1(0, (i))$ of molecule i of this system is independent of the coordinates of the center of mass. Consider, now, a second system, consisting of a finite number N of molecules, but otherwise differing from the first only in an additive triply periodic term $w'_1(0, (i))$ in the component potentials of each of the single molecules, which has the periodicity of one of the fixed crystals of the equilibrium ensemble of the first system at T and z. The average value of w'_1 may be chosen as zero, and its amplitude as proportional to $N^{-1} \ln N$. The equilibrium configuration of this system will be that of a single fixed crystal, the orientation of which will be determined by the periodic external field, and the relative probability of this orientation to a random one will be proportional to some power of N, approaching infinity as the size of the system becomes infinite. Similarly the equilibrium configuration of a finite portion of volume V of this infinite system will be that of a single fixed crystal. But as the number N of molecules in the ensemble approaches infinity, the functions $Q_n(0, \{\mathbf{n}\})$ of any finite number n of molecules approach the same value as the corresponding functions of the

[2] John G. Kirkwood and Elizabeth Monroe, J. Chem. Phys. **9**, 514 (1941).

first system without the periodic external field. For solutions of (19) at finite values of V only functions Q_n with n finite enter. We must expect functions $Q_n(z, \{\mathbf{n}\})$ corresponding to a single fixed crystal to be *also* solutions of (19) for the original system, without the periodic field, as well as those not obeying the conditions (25), (26), and (27), corresponding to an ensemble of randomly oriented crystals.

The apparent contradiction of postulating two different solutions to (19), which in the form $z=0$, consists of a set of completely solved equations for the different $Q_n(y, \{\mathbf{n}\})$ functions of different n values, is resolved by the fact that the equation must always be solved by one of a number of various approximation methods. It is assumed that as V becomes large the influence of the surface is immaterial, and the "true" solutions are obtained without reference to the surface conditions.

Condition (27) assumes that the functions $Q_n(z, \{\mathbf{n}\})$ for large but finite values of n are completely determined in their functional dependence on the coordinates $\{\mathbf{n}\}$ by a finite (and numerically to a good approximation by a small) number of functions $w_\nu(z, \{\mathbf{v}\})$.

Functions $Q_n(z, \{\mathbf{n}\})$ obeying condition (22), and therefore also (25), may be conveniently written in various ways as sums of products of functions which are separable in the coordinates of subsets $\{\mathbf{v}\}_n$ of the set of molecules $\{\mathbf{n}\}$.

Condition (26) is required in order that the integral over the functions of the subsets converge.

For instance, we may write Q_n as the sum, $\sum\{k\{\mathbf{v}_i\}_n\}_u$, over all possible sets, $\{k\{\mathbf{v}_i\}_n\}_u$, for various k values, of k unconnected subsets $\{\mathbf{v}_i\}_n$ of the set $\{\mathbf{n}\}$, of products of functions of these subsets $\{\mathbf{v}_i\}_n$. By unconnected subsets we mean that no member occurs in more than one subset, but every member of the set $\{\mathbf{n}\}$ occurs in one of the k subsets of every set of subsets. We write

$$Q_n(z, \{\mathbf{n}\}) = \sum \{k\{\mathbf{v}_i\}_n\}_u \prod_{i=1}^{i=k} [\rho(z)/z]^{\nu} g_\nu(z, \{\mathbf{v}_i\}_n), \tag{28}$$

for which the inverse is

$$g_\nu(z, \{\mathbf{v}\}) = [z/\rho(z)]^{\nu} \sum \{k\{\mathbf{n}_i\}_\nu\}_\mu (-)^{k-1}(k-1)! \prod_{i=1}^{i=k} Q_n(z, \{\mathbf{n}_i\}_\nu). \tag{29}$$

We define the cluster integrals as

$$b_\nu(z) = \frac{1}{V\nu!} \int\int \cdots \int g_\nu(z, \{\mathbf{v}\}) d\{\mathbf{v}\}, \tag{30}$$

which are, in the limit of infinite V, finite and independent of V for all finite values of ν, in view of (26).

Using (30) in (28) one finds

$$\int\int \cdots \int Q_n(z, \{\mathbf{n}\}) d\{\mathbf{n}\} = n! \sum_{n_\nu \geq 0} (\sum \nu n_\nu = n) \prod_{\nu \geq 1} \frac{1}{n_\nu!} \{V b_\nu(z) [\rho(z)/z]^{\nu}\}^{n_\nu}, \tag{31}$$

since the number of ways that one can arrange n numbered objects in piles, n_ν piles of ν objects each, is $n!/\Pi n_\nu!(\nu!)^{n_\nu}$ with $\sum \nu n_\nu = n$. The normalization (8) of F_n, with (15), shows that

$$\lim_{V=\infty} \left\{ \frac{1}{V^n} \int\int \cdots \int \left[\frac{z}{\rho(z)}\right]^n Q_n(z, \{\mathbf{n}\}) d\{\mathbf{n}\} = [b_1(z)]^n = 1, \right. \tag{32}$$

or

$$b_1(z) = 1, \tag{32'}$$

which fixes the arbitrary constant in $w_1(z, (i))$ so that the normalization (8) is valid.

We must also be able to integrate the function $Q_{n+m}(z, \{\mathbf{n}+\mathbf{m}\})$ over the limited number of coordinates of the set $\{\mathbf{m}\}$. It is somewhat more convenient to write our definitions in terms of the functions $F_n(z, \{\mathbf{n}\})$, related to the Q_n's by the simple proportionality of Eq. (15). We define functions $G_{n\mu}(z, \{\mathbf{n}\}, \{\mathfrak{y}_i\}_m)$ by

$$F_{n+m}(z, \{\mathbf{n}+\mathbf{m}\}) = F_n(z, \{\mathbf{n}\}) \sum \{k\{\mathfrak{y}_i\}_m\}_u \prod_{i=1}^{i=k} G_{n\mu}(z, \{\mathbf{n}\}, \{\mathfrak{y}_i\}_m), \tag{33}$$

for which the inverse is

$$G_{n\mu}(z, \{\mathbf{n}\}, \{\mathfrak{y}\}) = \sum \{k\{\mathbf{m}_i\}_\mu\}_u (-)^{k-1}(k-1)! \prod_{i=1}^{i=k} [F_{n+m}(z, \{\{\mathbf{n}\}+\{\mathbf{n}\mathbf{m}_i\}_\mu\})/F_n(z, \{\mathbf{n}\})]. \tag{34}$$

If the molecules of the set $\{\mathfrak{y}\}$ and those of the set $\{\mathbf{n}\}$ are all distant in the three-dimensional space of the centers of mass, the functions $G_{n\mu}(z, \{\mathbf{n}\}, \{\mathfrak{y}\})$ approach the functions $g_\mu(z, \{\mathfrak{y}\})$ in value.

We make use of this latter fact and write

$$G_{n\mu}(z, \{\mathbf{n}\}, \{\mathfrak{y}\}) = g_\mu(z, \{\mathfrak{y}\}) + \sum \{\mathbf{v}\}_n g_{\nu\mu}(z, \{\mathbf{v}\}_n, \{\mathfrak{y}\}), \tag{35}$$

for which the inverse is

$$\begin{aligned} g_{\nu\mu}(z, \{\mathbf{v}\}, \{\mathfrak{y}\}) &= \sum \{\mathbf{n}\}_\nu (-)^{\nu-n}[G_{n\mu}(z, \{\mathbf{n}\}_\nu, \{\mathbf{n}\}) - g_\mu(z, \{\mathfrak{y}\})] \\ &= (-)^\nu g_\mu(z, \{\mathfrak{y}\}) + \sum \{\mathbf{n}\}_\nu (-)^{\nu-n} G_{n\mu}(z, \{\mathbf{n}\}_\nu, \{\mathfrak{y}\}). \end{aligned} \tag{36}$$

The functions $g_{\nu\mu}$ approach zero in value if any one of the molecules of the set $\{\mathfrak{y}\}$ is sufficiently distant from all members of the set $\{\mathbf{v}\}$.

We may substitute (34) for $G_{n\mu}$ in (36) and obtain

$$\begin{aligned} g_{\nu\mu}(z, \{\mathbf{v}\}, \{\mathfrak{y}\}) = \sum \{\mathbf{n}\}_\nu \sum \{k\{\mathbf{m}_i\}_\mu\}_u (-1)^{\nu-n+k-1}(k-1)! \\ \left\{ \prod_{i=1}^{i=k} F_{n+m}(z, \{\{\mathbf{n}\}_\nu + \{\mathbf{m}_i\}_\mu\})/F_n(z, \{\mathbf{n}\}_\nu) - \prod_{i=1}^{i=k} F_m(z, \{\mathbf{m}_i\}_\mu) \right\}, \end{aligned} \tag{37}$$

or with (35) in (33) one finds

$$F_{n+m}(z, \{\mathbf{n}+\mathbf{m}\}) = F_n(z, \{\mathbf{n}\}) \sum \{k\{\mathfrak{y}_i\}_m\}_u \prod_{i=1}^{i=k} \{g_\mu(z, \{\mathfrak{y}_i\}_m) + \sum \{\mathbf{v}\}_n g_{\nu\mu}(z, \{\mathbf{v}\}_n, \{\mathfrak{y}_i\}_m)\}. \tag{38}$$

In terms of the functions Q, using (15), this becomes

$$\begin{aligned} Q_{n+m}(z, \{\mathbf{n}+\mathbf{m}\}) = Q_n(z, \{\mathbf{n}\}) \sum \{k\{\mathfrak{y}_i\}_m\}_u \prod_{i=1}^{i=k} \{[\rho(z)/z]^\mu g_\mu(z, \{\mathfrak{y}_i\}_m) \\ + \sum \{\mathbf{v}\}_n [\rho(z)/z]^\mu g_{\nu\mu}(z, \{\mathbf{v}\}_n, \{\mathfrak{y}_i\}_m)\}. \end{aligned} \tag{38'}$$

It is seen that with $Q_0 = 1$, Eq. (28) is the special case of (38′) with $n = 0$.

We define

$$b_{\nu\mu}(z, \{\mathbf{v}\}) = \frac{1}{\nu!} \int\int \cdots \int g_{\nu\mu}(z, \{\mathbf{v}\}, \{\mathfrak{y}\}) d\{\mathfrak{y}\}, \tag{39}$$

analogously to the cluster integrals of Eq. (30). Using (39) in (38′) one finds

$$\begin{aligned} \int\int_V \cdots \int Q_{n+m}(z, \{\mathbf{n}+\mathbf{m}\}) d\{\mathbf{m}\} = Q_n(z, \{\mathbf{n}\}) m! \sum_{m_\mu \geq 0} (\sum \mu m_\mu = m) \prod_{\mu \geq 1} \frac{1}{m_\mu!} \{ V b_\mu(z) [\rho(z)/z]^\mu \\ + \sum \{\mathbf{v}\}_n b_{\nu\mu}(z, \{\mathbf{v}\}_n) [\rho(z)/z]^\mu \}^{m_\mu}. \end{aligned} \tag{40}$$

It is seen again that (31) is a special case of (40) when $n = 0$.

DEVELOPMENT IN POWERS OF THE DIFFERENCE OF FUGACITY

Equation (40), if inserted in (19), leads immediately to expressions for the pressure, $P(y+z)=kT\varphi(y+z)$, and the component potentials of average force $w_\nu(y+z, \{\nu\})$ at the fugacity $y+z$, in terms of a power series in y, the coefficients of which are the functions $b_\mu(z)$ and $b_{\nu\mu}(z, \{\nu\})$ at the fugacity z.

Multiplication of Q_{n+m} by y^m in (40) may be accomplished by multiplication of each term $\rho(z)/z$ by y. Division by $m!$ and summation over m (Eq. (19)), removes the restriction on the m_μ's. One finds

$$[\exp V\varphi(y+z)]Q_n(y+z, \{\mathbf{n}\})=[\exp V\varphi(z)]Q_n(z, \{\mathbf{n}\})\sum_{m_\mu\geq 1}\prod_{\mu\geq 1}\frac{1}{m_\mu!}\{Vb_\mu(z)[y\rho(z)/z]^\mu$$

$$+\sum\{\nu\}_n b_{\nu\mu}(z, \{\nu\}_n)[y\rho(z)/z]^\mu\}^{m_\mu}=[\exp V\varphi(z)]Q_n(z, \{\mathbf{n}\})$$

$$\times\exp\{\sum_{\mu\geq 1}Vb_\mu(z)[y\rho(z)/z]^\mu+\sum\{\nu\}_n\sum_{\mu\geq 1}b_{\nu\mu}(z, \{\nu\}_n)[y\rho(z)/z]^\mu\}, \quad (41)$$

for all values of y smaller than the radius of convergence of the series occurring in the last expression. Using (15) and the Eqs. (9) and (13) defining the component potentials of average force, taking the logarithm of (41) and collecting the terms on both sides of the equation that are the same power of V and functions of the coordinates of the same molecules, one finds:

$$\varphi(y+z)=\varphi(z)+\sum_{\mu\geq 1}b_\mu(z)[y\rho(z)/z]^\mu, \quad (42)$$

$$w_1(y+z, (i))/kT+\ln[\rho(y+z)/(y+z)]=w_1(z, (i))/kT+\ln[\rho(z)/z]+\sum_{\mu\geq 1}b_{1\mu}(z, (i))[y\rho(z)/z]^\mu, \quad (43)$$

$$w_\nu(y+z, \{\nu\})/kT=w_\nu(z, \{\nu\})/kT+\sum_{\mu\geq 1}b_{\nu\mu}(z, \{\nu\})[y\rho(z)/z]^\mu. \quad (44)$$

For the special case $z=0$, $\rho(z)/z=1$, Eq. (2), with $y+z=y$, and $\varphi(z)=0$, Eq. (42) becomes the usual equation for the pressure expressed as a power series of the fugacity in an imperfect gas.[3] Under the same conditions Eqs. (43) and (44) permit the calculation of the component potentials of average force in an imperfect gas in terms of a power series in the fugacity. The equations are essentially similar to those derived previously[4] although the form corresponding to (43) and (44) has not been published previously.

As with the special case that $z=0$, the singularities on the real axis of the series (42) correspond to the singularities in the function $\varphi(y+z)$ in the real system.[5]

However, singularities off the real axis of y, or on the real axis with opposite sign, may cause divergence of the series (42) at values of y for which no singularity in $\varphi(y+z)$ exists. Equations (43) and (44) present feasible methods of calculation to extend the evaluation of $\varphi(y+z)$ beyond such radii of convergence. One may use (43) and (44) to evaluate $w_\nu(y'+z, \{\nu\})$ for some value y' inside the radius of convergence. With these functions known, the coefficients $b_\mu(y'+z)$ for the development around the new point $y'+z$ may be evaluated. This may be repeated until a singularity of φ on the real axis is reached.

One might, of course, attempt to calculate around the singularity on the real axis by following this procedure into the complex plane.

Some interesting equations may be obtained by differentiation of (42). We differentiate with respect to y, ν times, and let y approach zero. One finds

$$[\partial^\nu\varphi(y+z)/\partial y^\nu]_{y=0}=\partial^\nu\varphi(z)/\partial z^\nu=(\partial/\partial y)^\nu_{y=0}\sum b_\mu(z)[y\rho(z)/z]^\mu=\nu!b_\nu(z)[\rho(z)/z]^\nu.$$

---

[3] Joseph E. Mayer and S. F. Harrison, J. Chem. Phys. **6**, 87 (1938).
[4] Joseph E. Mayer and Elliott Montroll, J. Chem. Phys. **9**, 2 (1941).
[5] See the discussion of Max Born and Klaus Fuchs, Proc. Roy. Soc. **A166**, 391 (1938).

This may be rewritten as

$$\partial^\nu \varphi(y+z)/\partial y^\nu = \nu! b_\nu (y+z)[\rho(y+z)/(y+z)]^\nu. \tag{45}$$

For the particular case that $\nu=1$ this reduces to a readily obtained thermodynamic equation, in view of (32′) that $b_1=1$,

$$\partial \varphi(y+z)/\partial y = \rho(y+z)/(y+z). \tag{46}$$

We may equate the expression on the right of (45) to that obtained by differentiation of (42) without having y approach zero, obtaining

$$b_\nu(y+z)[y\rho(y+z)/(y+z)]^\nu = \sum_{\mu \geq 1} \frac{\mu!}{(\mu-\nu)!\nu!} b_\mu(z)[y\rho(z)/z]^\mu. \tag{47}$$

For the case $\nu=1$ we obtain

$$y\rho(y+z)/(y+z) = \sum_{\mu \geq 1} \mu b_\mu(z)[y\rho(z)/z]^\mu, \tag{48}$$

which permits the calculation of the density at the fugacity $y+z$ from the properties of the system at the fugacity z.

In the treatment of the monatomic imperfect gas[3,4] it was found to be advisable to make use of the fact that the integrals b_μ could be expressed as a sum of products of what were there called irreducible integrals β_k. This led to an expansion in a power series in the density ρ as an expression for the pressure, the coefficients of which involved these irreducible integrals. The transformation had several advantages. In the first place, it is convenient to have density rather than fugacity as independent variable. Secondly, the calculation of the cluster integrals would actually be performed by primary evaluation of the irreducible integrals, and it seems natural to attempt to express the properties of the system in terms of these integrals.

A third result was more complex in nature. It is possible that the power series in fugacity diverge while those in the density remain convergent, the criterion for the phase transition (divergence of the fugacity series on the real axis) being either that the density series become singular, or that one of them ($\sum k\beta_k\rho^k$) becomes unity in value. The type of transition would be ordinary first order in the former case, and anomalous first order in the second case. It was claimed that the disappearance of the phase transition with rising temperature at the critical point must be preceded by a temperature range in which the anomalous transition is present.[6] The conclusion has been criticized[1] on the justifiable grounds that the physical nature of the coefficients, the irreducible integrals β_k, were not made use of. The criticism, in this form, may be answered, at least partially. The β_k's may be defined as integrals over the coordinates of $k+1$ molecules (divided by the volume) of an integrand which is a function of the potential energy and of T. Especially if component potentials $w_\nu(0, \{\nu\})$ with $\nu \geq 3$ are assumed to exist (which was not assumed in the previous paper) there seems to be no reason why physical systems should not exist in which a wide variety of ratios would occur between the numerical values of the β_k's for different k's.

As the parameter T increases a singularity on the real axis of ρ in the series $\sum k\beta_k\rho^k$ may well disappear into the complex plane at $T=T_c$, and the series remain regular (represent a regular function) to high values of ρ on the real axis above this temperature. If the series approaches a value less than unity when the singularity is approached on the real axis for all $T \leq T_c$ then the density $\rho_0(T)$ at which the singularity occurs will be the density of condensation. T_c will be the upper limit of the temperature at which condensation occurs.

However, if the series approaches a value less than unity at the singularity as T approaches T_c, then $(\partial P/\partial V)_T = -(RT/V^2)(1-\sum k\beta_k\rho^k)$ will not be zero at the critical point. This state of affairs would represent a strange type of critical phenomenon not found in nature. In order to have a critical point of the van der Waals type it is necessary that the value of the function represented

[6] S. F. Harrison and J. E. Mayer, J. Chem. Phys. **6**, 101 (1938).

by $\sum k\beta_k\rho^k$ (approached along the real axis from small ρ values) at the singularity become exactly unity as T approaches T_c, *and* that the value of the derivative $\sum k^2\beta_k\rho^k$ become zero at this point. These criteria can be fulfilled, if at all, only by very special types of potential energy functions, and it appears hardly possible that all critical phenomena are of this type.

The actual state of affairs in real systems seems to be that the value of $\sum k\beta_k\rho^k$ at the singularity increases with T to unity at some temperature T_m lower than the temperature at which the singularity moves into the complex plane. Above T_m an anomalous first-order transition occurs. The experimental evidence is certainly not in contradiction to this view.

Since the critical phenomena in binary liquid mixtures appear to show the same anomalous first-order transition region that is evidenced in the one component gas liquid critical region,[7] it is tempting to try the same introduction of the $\beta_k(z)$'s in the equations derived here, in the prospect of eventually treating two or more component systems.

In order to make the development general, it is necessary to define the new quantities introduced, $\beta_m(z)$ and $h_{nm}(z, \{n\})$, in terms of the $b_\mu(z)$ and $b_{\nu\mu}(z, \{\nu\})$, in which case the development is purely formal and any conclusions drawn about the nature of the approach to singularities would be open to the criticism previously raised. However, in the case that $w_1(z, (i))$ is invariant under translation in the three-dimensional space of the center of mass of the molecule i, which is the case in the liquid and gas, and that $w_\nu(z, \{\nu\})$ for $\nu \geq 2$ is independent of the internal coordinates, then the functions $\beta_m(z)$ and $h_{nm}(z, \{\mathfrak{n}\})$ are calculable as direct integrals of relatively simple functions of the potentials of average force and temperature. In this case the definitions of these functions are given for $\beta_k(0)$ in Eq. (18), reference 3 and for $h_{\mu n}(0, \{\mathfrak{y}\})$ in Eq. (53), reference 4. The definitions given in these articles assume that w_2 alone differs from zero, but the generalization for other cases is fairly obvious. In the general case we may use the definitions:

$$\beta_m(z) = \sum_{m_\mu \geq 0} [\textstyle\sum(\nu-1)m_\mu = m](-)^{\Sigma m_\mu}\mu^{-1}\dfrac{(m-1+\sum m_\mu)!}{m!}\displaystyle\prod_{\mu\geq 2}\frac{[\mu b_\mu(z)]^{m_\mu}}{m_\mu!}, \tag{49}$$

for which the inverse is

$$b_\mu(z) = \frac{1}{\mu^2}\sum_{\mu_m \geq 0}(\textstyle\sum m\mu_m = \mu-1)\displaystyle\prod_{m\geq 1}\frac{[\mu\beta_m]^{\mu_m}}{\mu_m!}, \tag{50}$$

and

$$b_{\nu\mu}(z, \{\nu\}) = \mu b_\mu(z)h_{\nu 1}(z, \{\nu\}) + \sum_{m=2}^{m=\mu} m h_{\nu m}(z, \{\nu\})[\partial b_\mu(z)/\partial\beta_{m-1}(z)]. \tag{51}$$

With these definitions the method used in references 3 and 4 may be readily generalized to apply to the Eqs. (42), (43), and (44). Equation (49) shows that $m\beta_m(z)$ is the negative of the coefficient of y^m in

$$[1+\sum_{\mu\geq 2}\mu b_\mu(z)y^{\mu-1}]^{-m} = y^m[\sum_{\mu\geq 1}\mu b_\mu(z)y^\mu]^{-m}$$

so that

$$\sum_{m\geq 1} m\beta_m(z)x^m = -\frac{1}{2\pi i}\oint\frac{1}{y}\sum_{m\geq 1}x^{-1}[\sum_{\mu\geq 1}\mu b_u(z)y^\mu]^{-m}dy$$

$$= \frac{1}{2\pi i}\oint x\{y[x-\sum_{\mu\geq 1}\mu b_\mu(z)y^\mu]\}^{-1}dy, \tag{52}$$

where the path of integration must enclose the origin of y, and, in order to permit the second expression, must be just outside the curve along which the absolute value of the sum, $\sum\mu b_\mu(z)y^\mu$, exceeds x in value. The integrand has two poles enclosed by this path: one at $y=0$ with residue

[7] Louis D. Roberts and J. E. Mayer, J. Chem. Phys. 9, 852 (1941).

unity, and the other when the sum equals x, that is at y_0 determined by

$$\sum_{\mu\geq 1} \mu b_\mu(z) y_0{}^\mu = x, \tag{53}$$

the residue of which is found by inserting the derivative of the denominator for the denominator to be $-x[\sum \mu^2 b_\mu(z) y_0{}^\mu]^{-1}$. Comparing (53) and (48) we may set $x = y\rho(y+z)/(y+z)$ and find that

$$\sum_{m\geq 1} m\beta_m(z)[y\rho(y+z)/(y+z)]^m = 1 - \{\sum_{\mu\geq 1} \mu^2 b_\mu(z)[y\rho(z)/z]^\mu\}^{-1}[y\rho(y+z)/(y+z)],$$

$$\sum_{\mu\geq 1} \mu^2 b_\mu(z)[y\rho(z)/z]^\mu = [y\rho(y+z)/(y+z)]\{1 - \sum_{m\geq 1} m\beta_m(z)[y\rho(y+z)/(y+z)]^m\}^{-1}. \tag{54}$$

Equation (54) is valid up to values of y for which the function $\varphi(y+z)$ becomes singular, and this y is determined by

$$\sum_{m\geq 1} m\beta_m(z)[y\rho(y+z)/(y+z)]^m = 1, \tag{55a}$$

$$\sum_{m\geq 1} m\beta_m(z)[y\rho(y+z)/(y+z)]^m \text{ singular}. \tag{55b}$$

For the not too trivial proof that the case (55b) as well as (55a) determines the singularity in $\varphi(y+z)$ the reader is referred elsewhere.[5,8]

To proceed we note that from (53)

$$d \ln y_0/dx = \sum_{\mu\geq 1} \mu^2 b_\mu(z) y_0{}^{\mu-1} = x^{-1} - \sum_{m\geq 1} m\beta_m(z) x^{m-1}.$$

Integrating and substituting we find

$$\ln [y\rho(y+z)/(y+z)] = \ln [y\rho(z)/z] + \sum_{m\geq 1} \beta_m(z)[y\rho(y+z)/(y+z)]^m. \tag{56}$$

Similarly, using (53) again, we find

$$(d/dx) \sum_{\mu\geq 1} b_\mu(z) y_0{}^\mu = x(d \ln y_0/dx) = 1 - \sum_{m\geq 1} m\beta_m(z) x^m$$

which can be integrated and substituted to yield

$$\begin{aligned}\varphi(y+z) &= \varphi(z) + \sum_{\mu\geq 1} b_\mu(z)[y\rho(z)/z]^\mu \\ &= \varphi(z) + [y\rho(y+z)/(y+z)]\left\{1 - \sum_{m\geq 1} \frac{m}{m+1}\beta_m(z)[y\rho(y+z)/(y+z)]^m\right\}.\end{aligned} \tag{57}$$

We shall now show that Eqs. (43) and (44) may be transformed into a power series in $y\rho(y+z)/(y+z)$, the coefficients of which are the functions $h_{\nu m}(z, \{\nu\})$. To do this the symbol x is again used for $y\rho(y+z)/(y+z)$ and y_0 for $y\rho(z)/z$. From Eq. (57) it is seen that

$$(\partial/\partial\beta_{m-1})_x \sum b_\mu y_0{}^\mu = (\partial/\partial\beta_{m-1})_x (x - \sum (k/k+1)\beta_k x^{k+1}) = -(m-1)x^m/m.$$

One may, instead, use (53) and (56) to find

$$\begin{aligned}(\partial/\partial\beta_{m-1})_x \sum b_\mu y_0{}^\mu &= \sum (\partial b_\mu/\partial\beta_{m-1}) y_0{}^\mu + (\partial \ln y_0/\partial\beta_{m-1})_x \sum \mu b_\mu y_0{}^\mu \\ &= \sum (\partial b_\mu/\partial\beta_{m-1}) y_0{}^\mu - x^m,\end{aligned}$$

and comparing this with the previous equation, one finds

$$\sum [\partial\beta_\mu(z)/\partial\beta_{m-1}(z)][y\rho(z)/z]^\mu = [y\rho(y+z)/(y+z)]^m/m. \tag{58}$$

[8] Mayer and Mayer, *Statistical Mechanics* (J. Wiley and Sons, 1940), p. 465.

If (48) and (58) are used with (51) in Eqs. (43) and (44) one obtains immediately

$$w_1(y+z,(i))/kT+\ln[\rho(y+z)/(y+z)]=w_1(z,(i))/kT+\ln[\rho(z)/z]+\sum_{m\geq 1}h_{1m}(z,(i))[y\rho(y+z)/(y+z)]^m, \quad (59)$$

$$w_\nu(y+z,\{\nu\})/kT=w_\nu(z,\{\nu\})/kT+\sum_{m\geq 1}h_{\nu m}(z,\{\nu\})[y\rho(y+z)/(y+z)]^m. \quad (60)$$

For the special case that $z=0$, $y+z=y$, $y\rho(y+z)/(y+z)=\rho(y)$, and $\rho(z)/z=1$, Eqs. (54) to (57) reduce to those derived in reference 3, and (59) and (60) reduce to equations derived in reference 4.

SUMMARY AND CONCLUSION

Let us, for brevity, adopt the symbol

$$J_n(z,V)=[\exp V\varphi(z)]\int_V\int\cdots\int Q_n(z,\{\mathbf{n}\})d\{\mathbf{n}\}, \quad (61)$$

in which z is the fugacity, Eq. (1), $\varphi(z)=P(z)/kT$ is proportional to the pressure P, and the Q_n's, Eqs. (15) and (7), are proportional to the distribution functions at the fugacity z. At zero fugacity $\varphi(0)=0$ and in view of (2), and (9) and (10),

$$J_n(0,V)=J_n(V)=\int_V\int\cdots\int\exp(-U_n\{\mathbf{n}\}/kT)d\{\mathbf{n}\}, \quad (61')$$

in which $U_n\{\mathbf{n}\}$ is the potential energy of n molecules as a function of their coordinates $\{\mathbf{n}\}$ of position.

The normal use of the grand partition function leads to Eq. (13) that

$$\exp V\varphi(z)=\sum_{n=0}^{\infty}J_n(V)z^n/n!, \quad (62)$$

a power series in z with positive coefficients that for real systems with molecules having short range repulsion is absolutely convergent to $z=\infty$ for all finite values of the volume V. The first term in the series, J_0, is unity.

Differentiation of (62) leads to an equation for the density ρ in molecules per unit volume,

$$\rho(z)=z(\partial\varphi/\partial z)=\sum_{n=0}^{\infty}nJ_n(V)z^n/n!\Big/\sum_{n=0}^{\infty}J_n(V)z^nV/n!, \quad (63)$$

and

$$\frac{\partial\rho}{\partial z}=\frac{\sum_{n=0}^{\infty}\sum_{m=0}^{\infty}(m-n)^2J_n(V)J_m(V)z^{n+m}/n!m!}{2Vz[\sum_{n=0}^{\infty}J_n(V)z^n/n!]^2}, \quad (64)$$

which shows, in view of the positivity of the coefficients, that neither ρ nor $\partial\rho/\partial z$ can take negative values on the real positive axis of z, which alone is of physical significance.

The first result of this paper is that if the function $\exp[V\varphi(y+z)]$ is developed around the point z as a power series in y the coefficients are the $J_n(z,V)/n!$ of Eq. (61) (compare Eq. (19) with $n=0$) in which the distribution functions of the integrand are proportional to $\exp[-W_n(z,\{\mathbf{n}\})/kT]$, with $W_n(z\{\mathbf{n}\})$ the potential of average force at the fugacity z; and the normalization of the distribution functions are so chosen that their average value in an infinite volume are $[\rho(z)/z]^n\exp[V\varphi(z)]$.

The function $\varphi(z)$ may be expressed as a power series in z, the ν'th coefficient of which, $b_\nu(0)$, is an integral of an integrand which depends only on the potential energy of ν molecules, and the temperature (Eqs. (29) and (30) with $z=0$). The quantities $b_\nu(0)$ depend on the volume V over which the integration is extended, but for finite values of ν they approach finite limits as $V\to\infty$, provided the mutual potentials of the molecules converge rapidly enough to zero at infinite distance.

The quantities $b_\nu(0, V)$ could be defined using any macroscopic but finite V, and the series

$$\varphi_V(z)=\sum_{\nu\geq 1} b_\nu(0, V)z^\nu, \tag{65}$$

used to determine the $\varphi(z)$ defined by (62) at this value of V. The coefficients $b_\nu(0, V)$ of this series would have the value $b_\nu(0)$ of the limit $V=\infty$ except for very large values of ν. Since (62) is absolutely convergent for all z's, if V is finite, it follows that (65) determines a function which is regular except at the zeros of (62), and that (65) is convergent out to the absolute value of z of the zero of (62) nearest to the origin. This zero of course cannot occur on the positive real axis of z.

The function $\varphi_V(z)$ determined by (65) is then regular along the positive real axis of z, as long as V remains finite. If for each ν we extend the range of integration of Eq. (30) to infinity, the coefficient approaches the limiting value $b_\nu(0)$, and the resulting series

$$\varphi(z)=\sum_{\nu\geq 1} b_\nu(0)z^\nu \tag{66}$$

expresses the pressure $P(z)=kT\varphi(z)$ of an infinite thermodynamic system, having singularities on the real positive axis at the values of the fugacity characteristic of the phase transitions. At all these singularities for real positive finite z's, the function $\varphi(z)$ represented by the series (66) approaches the same (positive finite) value as the singularity is approached from either above or below along the real axis.

The slope $\partial\varphi/\partial z=\rho(z)/z$ may approach a higher (positive finite) value if the singularity is approached along the positive real axis from above than if approached from below. In this case the transition is first order. If $\partial\rho/\partial z$ approaches finite values as the singularity is approached either way the transition is normal, if infinite values are approached the transition is anomalous first order.

If the slope of φ, namely, ρ/z, approaches the same value as the singularity is approached from either above or below, then the singularity corresponds to a phase transition of second or higher order, the order depending on which derivative of φ undergoes a discontinuity.

It has been shown that if the function $\varphi(y+z)$ is developed around the point z as a power series in y, and the ν'th coefficient is written $[\rho(z)/z]^\nu b_\nu(z)$, then $b_\nu(z)$ is calculable by the same equation as $b_\nu(0)$, with only the replacement of the potential energy appearing in the expression for the latter by the potential of average force at the fugacity z.

The component potentials of average force, $w_\nu(z, \{\mathbf{v}\})$, Eq. (23), may also be developed as a power series in the fugacity around any arbitrary fugacity. The coefficients of the developments around different fugacities differ only that in each case the potentials of average force at the fugacity around which the development is made enter into the equations. In the special case of zero fugacity the potentials of average force are the potential energies of the molecules.

A Systematic Method of Obtaining the Relations Between Thermodynamic Derivatives

ARTHUR TOBOLSKY
Department of Chemistry, Princeton University, Princeton, New Jersey
(Received August 12, 1942)

An elementary systematic method for obtaining the relations between thermodynamic coefficients is presented. This method is applicable for any desired set of independent variables, and is also easily adapted to obtain the derivatives of any functions of the thermodynamic variables.

A DIFFICULTY invariably encountered by students of physical chemistry and thermodynamics is to find a systematic method for getting the relations between the important thermodynamic derivatives. One can of course use the tables of Bridgman,[1] but in cases where other variables, such as tension and length, enter the thermodynamic formulae, these tables cannot be used without modification.

For the usual systems of chemical thermodynamics, the combined first and second law is:*

$$dE=TdS-PdV. \tag{1}$$

The free energies of Helmholtz and of Lewis and Randall are defined as follows:

$$A=E-TS, \tag{2}$$

$$F=E+PV-TS, \tag{3}$$

$$H=E+PV, \tag{4}$$

so that

$$dA=-SdT-PdV, \tag{5}$$

$$dF=-SdT+VdP, \tag{6}$$

$$dH=TdS+VdP. \tag{7}$$

Since dA and dF are total differentials, we know that they satisfy the Euler relation. From (5) and (6) we can therefore derive the Maxwell relations (8) and (9).

$$(\partial S/\partial V)_T=(\partial P/\partial T)_V. \tag{8}$$

$$(\partial S/\partial P)_T=-(\partial V/\partial T)_P. \tag{9}$$

Since TdS is the heat absorbed in a reversible process, $dQ=TdS$. Remembering the definitions of C_p and C_v; namely,

$$C_p=(dQ/dT)_P, \tag{10}$$

$$C_v=(dQ/dT)_V, \tag{11}$$

it is seen that

$$C_p=T(\partial S/\partial T)_P, \tag{12}$$

$$C_v=T(\partial S/\partial T)_V. \tag{13}$$

The relationships discussed above are of course the essential core of the usual mathematical discussion of thermodynamics. In order to find the relationships between the various thermodynamic derivatives, these relations must be kept in mind. However, we shall discuss below a systematic method for obtaining the other thermodynamic relations, and we shall see that the above relations are the only ones with which we need burden our memory. The method is best explained by example.

Suppose that we wished to express $(\partial H/\partial F)_S$ in terms of more familiar thermodynamic derivatives. First set up the equation

$$dH=XdF+YdS, \tag{14}$$

where X and Y are to be determined. X is of course the quantity we desire.

We next have to specify the variables that we shall consider as independent. A frequent choice is P and T. The fundamental idea of this scheme is to express all the differentials in 12 in terms of dP and dT. When this is done we can equate the coefficients of dV and dT on the right- and left-hand sides and so obtain two simultaneous equations from which we can solve for X and Y. We first substitute in (14), Eqs. (6) and (7).

$$TdS+VdP=X(-SdT+VdP)YdS, \tag{15}$$

[1] See Lewis and Randall, *Thermodynamics*, Chapter 14.
* We shall use the Lewis and Randall nomenclature throughout.

but

$$dS=(\partial S/\partial T)_P dT+(\partial S/\partial P)_T dP, \quad (16)$$

which from (9) and (12) becomes

$$dS=(C_p/T)dT-(\partial V/\partial T)_P dP. \quad (17)$$

Substituting (17 in (15)

$$C_p dT-T(\partial V/\partial T)_P dP+VdP = X(-SdT+VdP) + Y[(C_p/T)dT-(\partial V/\partial T)_P dP]. \quad (18)$$

Equating the coefficients of dP and dT on both sides we have

$$C_p=X(-S)+Y(C_p/T), \quad (19)$$

$$-T(\partial V/\partial T)_P+V=XV+Y\{-(\partial V/\partial T)_P\}. \quad (20)$$

Simultaneous solution of (19) and (20) gives

$$X=\frac{C_P V}{C_P V-ST(\partial V/\partial T)_P}.$$

The extension of the method that we have used to other thermodynamic variables is very straightforward.

Suppose that we were interested in the thermodynamics of rubber where the variables τ and L representing force of tension (or compression) and length, respectively, were important rather than P and V.

The combined first and second law can be written

$$dE=TdS+\tau dL. \quad (21)$$

We define the free energies of Helmholtz and Lewis and Randall as follows:

$$A=E-TS,$$

$$F=E-\tau L-TS$$

so that

$$dA=-SdT+\tau dL, \quad (22)$$

$$dF=-SdT-Ld\tau. \quad (23)$$

From (22) and (23) we get relations corresponding to the Maxwell relations.

$$(\partial S/\partial L)_T=-(\partial \tau/\partial T)_L, \quad (24)$$

$$(\partial S/\partial \tau)_T=(\partial L/\partial T)_\tau. \quad (25)$$

An interesting coefficient in the case of rubber is $(\partial E/\partial L)_T$. Take L and T as independent variables.

$$dE=XdL+YdT, \quad (26)$$

$$TdS+\tau dL=XdL+YdT, \quad (27)$$

$$T[(\partial S/\partial L)_T dL+(\partial S/\partial T)_L dT] +\tau dL=XdL+YdT. \quad (28)$$

Introducing Eq. (24) into (28) and equating coefficients of dL we obtain

$$(\partial E/\partial L)_T=-T(\partial \tau/\partial T)_L+\tau. \quad (29)$$

(From this result we can see that if τ is a constant times the absolute temperature, then $(\partial E/\partial L)_T=0$, which was pointed out by K. H. Meyer. This fact has been very important in the development of the statistical theories of rubber.)

The method described above can be generalized to more than two independent variables, and of course can be used to treat coefficients such as $[\partial(E/T)/\partial(1/T)]_P$ or other derivatives involving functions of the thermodynamic variables. For example, in the theory of fluctuations of density the coefficient $(\partial^2 S/\partial V^2)_E$ is very important. From Eq. (1) $(\partial S/\partial V)_E=P/T$. Applying the methods used above it can readily be shown that

$$(\partial^2 S/\partial V^2)_E=(\partial(P/T)/\partial V)_E=1/T(\partial P/\partial V)_T -1/C_v T^2[(\partial E/\partial V)_T]^2. \quad (30)$$

The second term is taken as zero for gases but is not at all negligible in liquids.

Though schemes have been devised which successfully treat the general problem of obtaining the relations between thermodynamic derivatives,[2,3] the above method can be recommended for simplicity and directness. It is readily adaptable to whatever choice of independent variables may be found convenient.

I wish to thank Professor Henry Eyring who suggested the need for a method of solving the problem suitable for the classroom.

[2] F. Lerman, J. Chem. Phys. **5**, 792 (1937).
[3] P. W. Bridgman, Phys. Rev. **3**, 273 (1914).

The Temperature Dependence of Reaction Rates from the Standpoint of the Broensted-Christiansen-Scatchard Equation

EDWARD S. AMIS AND GEORGE JAFFÉ
Louisiana State University, Baton Rouge, Louisiana

(Received June 18, 1942)

In Section I arguments were presented for the necessity of splitting the log k_∞^* term in the general kinetic equation into a part which represents the rate constant extrapolated to a standard reference state of temperature, dielectric constant and concentration, and into a part giving the temperature dependence. In Section II the repulsive potential between reactants at close distances was formulated and this potential was then incorporated in the general kinetic equation to give the temperature dependence of the reaction rate constant. In Section III this equation was applied to existing kinetic data and found satisfactory. Also the repulsive forces between reactants calculated from the temperature and dielectric dependence of the reaction rate constants were compared with the intermolecular forces between the molecules of noble gases calculated from the second virial coefficients as evaluated by Fowler.

I. INTRODUCTION

LAIDLER and Eyring[1] point out that a term of the form ϕ/kT should be included in the kinetic equation to account for the non-electrostatic effects, which can be treated as repulsions beginning suddenly at the distance of closest approach, modified to take into account van der Waals attractions which may be of considerable importance. A similar term must account for the temperature dependence of the rate in the general kinetic equation[2-4]

$$\log k^* = \log k_\infty^* - z_A z_B \epsilon^2/(DkT(r_A+r_B)) + z_A z_B \epsilon^2 \kappa/(DkT(1+a\kappa)). \quad (1)$$

In this equation ln k_∞^* must be composite containing a term which represents the rate constant extrapolated to a standard reference state of temperature, dielectric constant and concentration, and a term giving the temperature dependence. Although it is generally recognized that the temperature and dielectric constant dependences of reaction rates are quite different, yet Eq. (1) as stated does not indicate this difference. The contrast between these two dependences can be shown as follows: If a reaction between ions is studied as a function of the dielectric constant of the solvent at constant temperature, then from the slope of the curve obtained by plotting $\log k^*_{\kappa=0}$ *versus* $1/D$, r_A+r_B can be obtained, provided that the effect of the solvent is that due to its dielectric constant, i.e., that predicted by electrostatic theory. The values of r_A+r_B obtained in these cases are always reasonable in magnitude and positive in sign. This is true because the slopes of the $\log k^*_{\kappa=0}$ *versus* $1/D$ curves are of the right order of magnitude and of the right sign, i.e., the slopes are negative for ions of like charge sign and positive for ions of unlike charge sign.[5,6] If Eq. (1) were complete, one should be able, by using it, to obtain r_A+r_B from the slopes of plots of $\log k$ *versus* $1/T$. However, irrespective of the signs of the charges on the reactants, the slopes of such plots are always negative as predicted by the Arrhenius equation, so that, for reactants of unlike charge sign r_A+r_B would be negative. The magnitude of r_A+r_B calculated from a temperature dependence will be roughly one-third to one-fourth that obtained from a dielectric constant dependence for ions of like charge sign, but in this case the sign is positive.

From these considerations, it follows that the $\log k_\infty^*$ term must be composite and must embody a non-electrostatic potential which is predominant in determining the dependence of

[1] K. J. Laidler and H. Eyring, Ann. New York Acad. Sci. **39**, 303 (1940).
[2] J. N. Brönsted, Zeits. f. physik. Chemie **102**, 169 (1922); **115**, 337 (1925).
[3] J. A. Christiansen, Zeits. f. physik. Chemie **113**, 35 (1924).
[4] G. Scatchard, J. Am. Chem. Soc. **52**, 52 (1930); Chem. Rev. **10**, 229 (1932).
[5] E. S. Amis and V. K. LaMer, J. Am. Chem. Soc. **61**, 901 (1939).
[6] W. J. Svirbely and A. Schramm, J. Am. Chem. Soc. **60**, 330 (1938).

the rate upon the temperature. The purpose of this paper is the evaluation of this non-electrostatic potential together with a comparison of its magnitude with the value of electrostatic potentials with which we are more familiar.

II. THE KINETIC EQUATION

It follows from the arguments which have been presented above that the mutual potential energy between two reacting particles cannot be restricted to their electrostatic potential energy. In order to obtain the observed temperature dependence of the rate constant a potential must be added which will correspond to the strong repulsive forces that exist for a close approach of the molecules, whether these are charged or not.

Following the line of thought introduced by Brönsted we shall assume that the reaction between two molecules A and B takes place via the formation of an intermediate complex X. Furthermore, we assume that spherical symmetry about each particle exists and that the mutual potential of two molecules A and B, if they are at the distance r, is given by an expression of the form

$$\psi(r)=\varphi_1(r)+\varphi_2(r). \tag{2}$$

Here $\varphi_2(r)$ represents the contribution of the electrostatic forces in the case that A and B are charged (valency z_A and z_B, respectively). Thus, under the usual assumptions, we will have

$$\varphi_2(r)=\epsilon^2 z_A z_B e^{\kappa(a-r)}/(Dr(1+\kappa a)), \tag{3}$$

where κ is the parameter of Hückel and Debye's theory and a the distance of closest approach.

As to the origin and form of the potential $\varphi_1(r)$ nothing need be assumed for our present purpose, except the following two conditions:

1. that φ_1 is independent of the dielectric constant D, and
2. that φ_1 has a positive value for those distances r at which formation of X occurs.

We shall call $\varphi_1(r)$ the non-electrostatic potential though it may be traceable, in ultimate analysis, to forces of electric origin. However, in the latter case, it would have to be assumed that they are independent of the dielectric constant. There is no contradiction in this assumption since, for the short distances involved, the notion of the dielectric constant (of the medium) loses its significance.

With the potential (2) and the concentrations C_A, C_B, the probability of finding a molecule B at a distance between r_0 and r_0+dr_0 from a molecule A will become proportional to

$$C_A C_B \exp(-\psi(r_0)/kT) r_0^2 dr_0. \tag{4}$$

Adopting as the criterion for the formation of X the fact that r should be within these limits the rate of reaction becomes[3,4] (with k^* and K constants):

$$k^*=KT^{\frac{1}{2}}(C_A C_B/C_z)\exp(-\psi(r_0)/kT). \tag{5}$$

Let k_0^* be the rate constant for some standard temperature T_0, and let the unimportant term $T^{1/2}$ be neglected in the usual way, then we obtain our final formula

$$\log k^*=\log k_0^*+\psi(r_0)/kT_0-\varphi_1(r_0)/kT$$
$$-\epsilon^2 z_A z_B \exp(\kappa(a-r_0))/(DkTr_0(1+\kappa a)). \tag{6}$$

It does not seem necessary for the present purpose to reduce k_0 to concentration zero, nor to a standard value of the dielectric constant.

From (6) we obtain, for the dependence on $1/T$

$$a_T=\frac{d\log k^*}{d(1/T)}=-(1/k)[\varphi_1(r_0)$$
$$+\epsilon^2 z_A z_B \exp(\kappa(a-r_0))/(Dr_0(1+\kappa a))], \tag{7}$$

and for the dependence on $1/D$

$$a_D=\frac{d\log k^*}{d(1/D)}$$
$$=-\epsilon^2 z_A z_B \exp(\kappa(a-r_0))/(kTr_0(1+\kappa a)). \tag{8}$$

An inspection of formula (7) will show that a_T will be negative, whatever the charges z_A and z_B are, if the non-electrostatic potential (at $r=r_0$) is sufficiently large compared with the electrostatic potential.

In the case of reactions which conform to electrostatics in their dependence on $1/D$ it should be possible, from (7) and (8) and from the knowledge of a_T and a_D, to derive as well the value of the electrostatic potential $\epsilon^2 z_A z_B/Dr_0$ as

TABLE I. Tests on inequalities (9) and (10).

Reaction	Medium	T	D	a_T	a_D	T/D	a_T/a_D
			A. Ions of like sign				
$S_2O_8^{--}+I^-$	MeOH−H_2O	313.1	73.12	−10140	−624	4.27	16.24
$B\phi B^{--}+OH^-$	MeOH−H_2O	298.1	71.42	−11000	−737	4.18	15.24
$B\phi B^{--}+OH^-$	EtOH−H_2O	298.1	71.42	−11120	−921	4.18	12.08
			B. Ions of unlike sign				
$NH_4^++CNO^-$	MeOH−H_2O	323.1	63.5	− 9370	260	5.09	−36.0
$NH_4^++CNO^-$	Glycol−H_2O	323.1	63.5	−10140	184	5.09	−55.2

TABLE II. A comparison of the non-electrostatic potentials at a distance $r=r_0$ with electrostatic potential between ions

Reaction	Medium	T	D	$\phi_2(r_0)\times10^{+13}$	$\phi_1(r_0)\times10^{+12}$	$\phi_1(r_0)/\phi_2(r_0)$
$NH_4^++CNO^-$	MeOH−H_2O	323.1	63.4	1.83	1.29	7.0
$NH_4^++CNO^-$	Glycol−H_2O	323.1	63.4	1.28	1.39	10.9
$S_2O_8^{--}+I^-$	MeOH−H_2O	313.1	73.12	3.66	1.39	3.8
$B\phi B^{--}+OH^-$	EtOH−H_2O	298.1	73.42	5.27	1.52	2.9
$B\phi B^{--}+OH^-$	MeOH−H_2O	298.1	73.42	4.22	1.51	3.6

that of the non-electrostatic potential $\varphi_1(r_0)$ for the critical distance.

Furthermore, it is easy to derive from (7) and (8) the following two inequalities which connect measurable quantities only:

1. if A and B have charges of the same sign:

$$a_T/a_D > T/D; \tag{9}$$

2. if A and B have charges of opposed sign:

$$a_T/a_D < T/D. \tag{10}$$

III. APPLICATIONS

The first application will be to test the inequalities (9) and (10). Inequality (9) can be tested by the data on the persulfate-iodide reaction in methyl-water media[7] and the brom phenol blue-hydroxide reaction in both ethyl alcohol-water and methyl alcohol-water media.[5] From Table I it can be seen that a_T/a_D is three to four times as large as T/D. The predictions of inequality (10) can be applied to data on the ammonium-cyanate reaction in both methyl alcohol-water[6] and glycol-water[8] media. It is evident that in these cases a_T/a_D is less than T/D, to the extent of the inversion of the sign of a_T/a_D.

In Table II, the potentials $\varphi_1(r_0)$ and $\varphi_2(r_0)$ as well as their ratios are recorded for different sign and valence types of reactants in different media. In all cases the rate dependence on $1/T$ was linear as demanded by both the Arrhenius equation and by Eq. (7). For bivalent-univalent reaction types the value of the non-electrostatic potential, $\varphi_1(r_0)$, is roughly three times as great as the value of the electrostatic potential, $\varphi_2(r_0)$, while in the uni-univalent type $\varphi_1(r_0)$ is from seven to eleven times as great. The electrostatic potential would be expected to be larger for the higher valence types of reactants. The solvent seems to play a rather important part in the ratios of these potentials.

As has been shown above, values of a_T and a_D permit the calculation of $\varphi_1(r_0)$ and $\varphi_2(r_0)$ for reaction rates obeying electrostatics in their dielectric constant dependence. If, however, a_D is not known, $\varphi_1(r_0)$ may still be calculated from a_T by use of Eq. (7), provided that r_0 is known from some other source or provided that the second term on the right of Eq. (7) is neglected as a first approximation. Using this latter method of calculation for reactions between ions and molecules, molecules and molecules, and reactants in the gaseous state, the temperature dependence of the rates should yield values of $\varphi_1(r_0)$ substantially like those for reactions between ions in solution, since this potential arises from repulsive forces between the reactants

[7] E. S. Amis and J. E. Potts, Jr., J. Am. Chem. Soc. **63**, 2883 (1941).
[8] J. Lander and W. J. Svirbely, J. Am. Chem. Soc. **60**, 1613 (1938).

TABLE III. A comparison of the non-electrostatic potential between reactants calculated from the rate dependence on temperature alone and calculated from the rate dependence on both temperature and dielectric constant.

Reaction	Range of Temp.	Range of d.c.	Value used in calculating column 7 of Temp.°C	Value used in calculating column 7 of d.c.	$\varphi_1(r_0)$ from rate dependence on T $\times 10^{+12}$	$\varphi_1(r_0)$ from rate dependence on T and D $\times 10^{+12}$	Media
$S_2O_8^{--}+I^-$[a]	20–40	55.0–76.7	40	73.12	1.39	1.04	EtOH–H_2O
$B\phi B^{--}+OH^-$[b]	5–45	64.5–78.5	25	71.42	1.52	0.93	EtOH–H_2O
$B\phi B^{--}+OH^-$[b]	5–45	64.5–78.5	25	71.42	1.51	1.13	MeOH–H_2O
$NH_4^++CNO^-$[c]	30–60	40.0–63.5	50	63.5	1.39	1.70	Glycol–H_2O
$NH_4^++CNO^-$[d]	30–70	35.0–69.9	50	63.5	1.29	1.32	MeOH–H_2O
$B\phi BOH^-+H_3O^+$[e]	25–45				2.12		EtOH–H_2O
Sucrose$+H_3O^+$[f]	21–41				1.83		EtOH–H_2O
Sucrose$+H_3O^+$[f]	21–41				1.67		Dioxane–H_2O
N_2O_5[g]	25–65				1.73		CCl_4
$*AsO_3^{---}+FeO_4^{--}$[h]	89–120				0.74		H_2O
$*Fe^{+++}+Sn^{++}$[i]	0–25				1.50		H_2O
$2N_2O$[j]	565–852				4.13		Gaseous
C_2H_5OCOCL[k]	150–195				1.99		Gaseous
$2HI$[l]	283–508				3.09		Gaseous
H_2+I_2[l]	283–508				3.06		Gaseous
$H+H_2(P)$[m]	10–100				0.49		Gaseous

[a] See reference 7.
[b] See reference 5.
[c] See reference 8.
[d] See reference 6.
[e] E. S. Amis and J. B. Price, presented to J. Am. Chem. Soc. for publication.
[f] E. S. Amis and F. C. Holmes, J. Am. Chem. Soc. **63**, 2231 (1941).
[g] F. Daniels and E. H. Johnson, J. Am. Chem. Soc. **43**, 53 (1921); see F. H. MacDougall, *Physical Chemistry* (The MacMillan Company, New York, 1936), p. 404.
[h] P. T. Stroup and V. W. Meloche, J. Am. Chem. Soc. **53**, 3331 (1931).
[i] W. F. Timofeew, G. E. Muchin, and W. G. Gurewitsch, Zeits. f. Physik. Chemie **115**, 161 (1925),
[j] C. N. Hinshelwood and R. E. Burk, Proc. Roy. Soc. **A106** 284 (1924).
[k] A. R. Choppin, H. A. Frediani, and G. F. Kirby, Jr., J. Am. Chem. Soc. **61**, 3176 (1939).
[l] M. Bodenstein, Zeits. f. physik. Chemie **29**, 295 (1899); see H. S. Taylor and H. A. Taylor, *Elementary Physical Chemistry* (D. van Nostrand Co., New York, 1937), p. 242.
[m] K. H. Geib and P. Harteck, Zeits. f. physik. Chemie, Bodenstein-Festband, 849–62 (1931); see H. S. Taylor and H. A. Taylor, *Elementary Physical Chemistry* (D. van Nostrand Co., New York, 1937), p. 235.
* k was not extrapolated to $k_\mu = 0$ in these cases.

at very close distances where the influence of the charge and of the dielectric constant is no longer appreciable.

In Table III are recorded the values of $\varphi_1(r_0)$ calculated in the two ways mentioned above and neglecting the second term on the right of Eq. (7) in the second method of calculation. The ionic examples included in the first method of calculation are all the instances recorded in the literature where sufficient data is given for this purpose and where the prerequisite of obedience to electrostatic theory is met. It is observable from Table III that the values of $\varphi_1(r_0)$ calculated from the temperature dependence of the rate correspond closely to the values of this function calculated from the dependence of the rate on both the temperature and dielectric constant. Furthermore, the variation between the two values is that predicted by electrostatics, i.e., $\varphi_1(r_0)$ calculated from a_T and a_D is less than that calculated from a_T, neglecting the electrostatic term, for ions of like sign, and vice versa for ions of unlike sign. It is also evident that for all reactions, whether in solution or in the gaseous state, and irrespective of charge type, the values of $\varphi_1(r_0)$ do not vary by an order of magnitude and in many cases agree in absolute value. It might be mentioned that, in the regeneration by hydrochloric acid of brom phenol blue from the colorless carbinol,[9] even though the reaction did not obey the requirements of electrostatics in its dielectric constant dependence of the rate, yet calculation of $\varphi_1(r_0)$ from the rate dependence upon temperature yielded a value of the non-electrostatic potential which compared favorably with that for the fading reaction the kinetics of which met the requirements of electrostatic theory.

As to the magnitudes of the non-electrostatic potential at the distance of reaction, they are of the expected order. Compared with the electrostatic energies, they are three to ten times as large if reasonable values of r_0 are used. Further-

[9] See Table III, reference *e*.

more, they can be compared roughly with values of the intermolecular energies as calculated from the second virial coefficient. Fowler[10] has evaluated the coefficients λ and μ in the well-known expression

$$\varphi_1(r)=\lambda r^{-s}-\mu r^{-6} \qquad (11)$$

for values of s ranging from 8 to 14 applying Eq. (11) to noble gases. Of the reactions given above that between the ammonium-ion-cyanate ion involves reactants which correspond reasonably well in molecular weight to argon. Using, then, Fowler's constants for argon we obtain for $\varphi_1(r_0)$, with $r_0=2.5\times10^{-8}$ cm as determined from Eq. (1), values between 1.1 and 3.1×10^{-12} when s ranges from 8 to 14. Thus our value of 1.7×10^{-12} is of the same order of magnitude. The good agreement, however, must be considered as fortuitous, as Eq. (11) is very sensitive to a change in r. For this reason the other reactions studied above do not agree nearly as well with Fowler's values, since, for these reactions, Eq. (1) yields values of r_0 between 1.2 and 1.7×10^{-8} cm which are evidently somewhat small if consideration is taken of the large molecular weights of the reactants.

[10] R. H. Fowler, *Statistical Mechanics*, second edition (Cambridge, 1936), p. 306.

OCTOBER, 1942 JOURNAL OF CHEMICAL PHYSICS VOLUME 10

An X-Ray Investigation of the Structure of Lead Chromate*

SELMA BLAZER BRODY
Department of Physics, Bryn Mawr College, Bryn Mawr, Pennsylvania

(Received July 13, 1942)

An attempt to analyze the structure of lead chromate was undertaken, using the Weissenberg x-ray goniometer technique. Positions of the lead and chromium atoms were determined. Although the intensities were carefully corrected for absorption, accurate values of the oxygen parameters could not be determined from the data at hand. Further work is indicated. There is some discussion of the migration of ions in the photoblackening effect which lead chromate exhibits.

BRILL[1] and others[2,3] have established that lead chromate (crocoite) is monoclinic with cell dimensions $a=7.10$A, $b=7.40$A, $c=6.80$A, $\beta=102°27'$. There are 4 molecules ($PbCrO_4$) per cell. The probable space group is $C_{2h}^5-P2_1/n$. These data do not permit lead chromate to be classified with any of the previously determined structures in the oxyacid group of substances,[4] so that a detailed x-ray investigation would seem to be of interest. In addition, a knowledge of the structure is important for an interpretation of the photoblackening process which lead chromate exhibits.

Simple rotation and Weissenberg equi-inclination[5] x-ray photographs were taken about the c and b axes. The indexing of these photographs verified the lattice and space group previously established. Unfiltered copper radiation was used throughout. Intensities were visually estimated. To aid in putting the intensities on a numerical

TABLE I.

Distance vector	Projection	u	v (fractions of cell translations)	w
$(2x\ 2y\ 2z)$	c face	0.43	0.30	
	b face	0.45		0.80
$(\frac{1}{2}\ \frac{1}{2}-2y\ \frac{1}{2})$	c face	$\frac{1}{2}$	0.20	
	b face	$\frac{1}{2}$		$\frac{1}{2}$
$(\frac{1}{2}-2x\ \frac{1}{2}\ \frac{1}{2}-2z)$	c face	0.07	$\frac{1}{2}$	
	b face	0.05		0.70

[5] M. J. Buerger, Zeits. f. Krist. **88**, 356 (1934).

* Submitted to the faculty of Bryn Mawr College in partial fulfillment of the requirements for the degree of doctor of philosophy. Gratitude is expressed to Dr. A. L. Patterson for his guidance and direction of the investigation. A grant made to Bryn Mawr College by the Elizabeth Thompson Science Fund made possible the purchase of much of the apparatus used.

[1] R. Brill, Zeits. f. Krist. **77**, 506 (1931).
[2] Gossner and Mussgnug, Zeits. f. Krist. **75**, 410 (1939).
[3] S. von Gliszczynski, Zeits. f. Krist. **101**, 1 (1939).
[4] See R. W. G. Wyckoff, *The Structure of Crystals* (Chemical Catalogue Company, New York, 1931), second edition, Chap. 16.

scale, two exposures of different times were made at each setting. Use was also made of the relative intensity of reflections from the Cu $K\alpha$ and $K\beta$ components.

The extremely high absorption coefficient of lead chromate ($\mu=1215$/cm for the radiation used) makes it necessary to be very careful in correcting the intensities for absorption. In preliminary work, crystals were used in the form in which they occur in nature, and plane by plane absorption corrections based on the Hendershot[6] method were applied. Even with refinements in the method of making the correction, inconsistencies in the results from these crystals indicated that the best natural crystals which could be found[7] lacked the perfection of form required for a safe application of this method. The artificial crystals available were too small to give satisfactory photographs. It was therefore decided to prepare cylindrical specimens.

A few good single crystals of crocoite of sufficient size were selected. The crystal to be ground was mounted in a goniometer head and set along the appropriate axis with the aid of a two-circle goniometer. It was then transferred with little disturbance of the orientation to a rigid mount in the headstock of a small lathe. A small piece of sandpaper attached at one end to a tool blank and free at the other end served as a grinding tool. A high point on the sandpaper was the actual cutting tool. This paper is stiff enough to furnish the pressure required to cut the soft but brittle crystal, and flexible enough to prevent the frequent breakage attendant upon the use of a rigid tool. The finished cylinders were about $\frac{1}{2}$ mm in diameter and 1–2 mm long. Intensities of reflections from the cylindrical

TABLE II. Parameters in fractions of cell translations.

	x	y	z
Pb	0.220	0.150	0.400
Cr	.215	.150	.896

All values ±0.004.

[6] O. P. Hendershot, Rev. Sci. Inst. **8**, 324 (1937). A discussion of the application of this method will appear shortly.

[7] Crocoite from Tasmania, Brazil, and the Urals was generously supplied by Mr. George Vaux, Mr. Samuel Gordon, and Dr. E. H. Watson. Artificial crystals were obtained from Dr. S. C. Horning.

TABLE III. Observed and calculated structure factors.

$hk0$	$\lvert F_{obs}\rvert$	$F_{Pb}+F_{Cr}$*	$h0l$	$\lvert F_{obs}\rvert$	$F_{Pb}+F_{Cr}$**
200	360	−340	200	390	−343
400	240	208	400	250	211
600	75	− 89	600	85	− 95
800	0	− 5	800	0	2
110	38	46	101	125	−155
210	110	−114	$\bar{1}01$	90	95
310	90	−109	301	230	174
410	240	170	$\bar{3}01$	110	− 19
510	175	133	$\bar{5}01$	160	−163
610	200	−183	$\bar{5}01$	0	− 45
710	130	−129	701	90	133
810	110	168	$\bar{7}01$	35	84
020	73	−117	$\bar{9}01$	30	−106
120	315	−352	002	85	109
220	95	98	202	0	28
320	280	246	$\bar{2}02$	290	−224
420	0	− 61	402	130	−127
520	175	−135	$\bar{4}02$	125	263
620	0	27	602	105	173
720	0	36	$\bar{6}02$	215	−244
820	0	17	802	80	−186
130	46	− 63	$\bar{8}02$	130	201
230	45	− 38	103	135	−171
330	145	158	$\bar{1}03$	320	328
430	29	61	303	110	116
530	210	−201	$\bar{3}03$	175	−182
630	34	− 67	$\bar{5}03$	80	− 57
730	165	202	$\bar{5}03$	120	135
830	22	62	703	20	3
040	243	−248	$\bar{7}03$	80	− 83
140	190	175	$\bar{9}03$	30	33
240	240	217	004	250	−242
340	125	−135	204	260	264
440	130	−147	$\bar{2}04$	170	160
540	35	75	404	135	−232
640	30	66	$\bar{4}04$	90	− 47
740	0	− 22	604	65	175
840	0	4	$\bar{6}04$	25	− 49
150	0	0	$\bar{8}04$	60	116
250	120	104	105	0	22
350	0	0	$\bar{1}05$	30	36
450	155	−172	305	35	− 69
550	0	0	$\bar{3}05$	90	− 87
650	135	199	$\bar{5}05$	45	102
750	0	0	$\bar{5}05$	80	117
060	215	208	$\bar{7}05$	65	−128
160	125	146	006	105	−190
260	205	−183	206	40	112
360	120	−125	$\bar{2}06$	235	235
460	70	126	406	0	− 28
560	53	68	$\bar{4}06$	215	−230
660	1	− 60	$\bar{6}06$	140	186
170	tr.	44	107	80	133
270	tr.	− 27	$\bar{1}07$	80	−120
370	65	−118	307	60	−129
470	24	47	$\bar{3}07$	45	86
570	100	169	$\bar{5}07$	25	− 42
670	1	− 56	008	50	69
080	70	66	208	20	9
180	135	−201	$\bar{4}08$	20	− 57
280	36	− 59			
380	110	163			
480	31	43			
190	0	− 21			
290	25	− 63			

Parameters used in calculating: * Pb $(x_1, y_1)=(0.219, 0.150)$, Cr $(x_2, y_2)=(0.216, 0.150)$; ** Pb $(x_1, z_1)=(0.220, 0.400)$, Cr $(x_2, z_2)=(0.214, 0.896)$.

crystals, corrected for absorption by the method of Bradley[8] were used in the main part of the work.

The general position of $P2_1/n$ is $(x\ y\ z)(\bar{x}\ \bar{y}\ \bar{z})$ $(\frac{1}{2}+x\ \frac{1}{2}-y\ \frac{1}{2}+z)$ $(\frac{1}{2}-x\ \frac{1}{2}+y\ \frac{1}{2}-z)$ and the symmetry of the F^2 series is $P2/m$. A set of atoms of atomic number Z in such a general position will produce an interatomic distance peak in the F^2 series[9] of magnitude Z^2 at each of the general points 4: (*o*) $2x\ 2y\ 2z$ of the space group $P2/m$,[10] and a peak of magnitude $2Z^2$ at each of the special points 2: (*l*) $\frac{1}{2}\ \frac{1}{2}+2y\ \frac{1}{2}$ and 2: (*n*) $\frac{1}{2}+2x\ \frac{1}{2}\ \frac{1}{2}+2z$ of the same group. If two general points $x_1y_1z_1$ and $x_2y_2z_2$ of $P2_1/n$ are occupied, peaks of equal magnitude are produced at the general points 4: (*o*) $S_xS_yS_z$, 4: (*o*) $D_xD_yD_z$, 4: (*o*) $\frac{1}{2}+S_x\ \frac{1}{2}+D_y\ \frac{1}{2}+S_z$, 4: (*o*) $\frac{1}{2}+D_x\ \frac{1}{2}+S_y\ \frac{1}{2}+D_z$ of $P2/m$, where $S_x=x_2+x_1$, $D_x=x_2-x_1$, etc.

Using the intensities of the (*hk*0) and the (*h*0*l*) reflections, properly corrected for polarization and absorption, the projections of the F^2 series on the *b* face and *c* face were computed and plotted. From these maps and from symmetry considerations it was concluded that all atoms must occupy general positions. The only reasonable interpretation of the strongest peaks, corresponding to the lead-lead distances, is given in Table I. This gives a unique set of parameters for the lead atoms, $x_1=0.22$, $y_1=0.15$, $z_1=0.40$.

Because of the high atomic number of lead it can be assumed that the signs of the structure factors are in the main determined by the contributions of the lead atoms, $F_{Pb}(hkl)$. The signs of the contributions $F_{Pb}(hk0)$ and $F_{Pb}(h0l)$ were accordingly determined from the above lead parameters. These signs were combined with the experimentally determined numerical values of the total structure factors and the set of trial *F*'s thus constructed was used in synthesizing the Fourier series for the projected density on the *c* and *b* faces. The chromium atoms were readily located on these maps. Parameters of the lead and chromium atoms obtained from the electron density maps are listed in Table II. The position of the lead atoms is identical with that obtained from the F^2 maps. All peaks due to the lead-chromium distances appear in the right positions and orders of magnitude on the F^2 series maps. The structure factors calculated from these lead and chromium parameters are in good agreement with the observed magnitudes of the *F*'s (Table III). No sign changes are introduced by the contributions of the chromium atoms. Thus the assumption on which the calculation of the *F* series was based is justified.

No values are listed for the oxygen parameters since they cannot be located accurately from the data at hand. The maps give some indication of the positions of the oxygen atoms but the presence of spurious peaks on the maps, probably due to cutting off the Fourier series too soon, indicates that caution must be used in interpreting the weaker peaks. An extension of the data to higher order reflections would be desirable. Although plausible oxygen parameters can be obtained by adjusting the calculated structure factors, this procedure seems worthless without the support of direct evidence since the structure factors are very insensitive to large variations in the oxygen parameters. With the aid of a scale model attempts were made to find possible structures by packing nearly tetrahedral chromate groups about the lead ions. It is difficult to find adequate radii for the lead and chromate radicals in the literature and these attempts were inconclusive. From the lead and chromium positions and from indications of possible oxygen arrangements it seems that the structure is fairly close packed. The coordination number of oxygen atoms about lead is probably 8 or more.

In the light of these findings it would appear that the mechanism of photo-conductivity and photoblackening in lead chromate cannot depend on the migration of ions through a perfect lattice. Migration by means of holes due to lattice defects remains as a possibility. If any migration in a perfect lattice takes place it probably is accompanied by a breakdown of chromate groups and therefore of the lattice as a whole.[11]

[8] A. J. Bradley, Proc. Phys. Soc. **47**, 879 (1935).
[9] A. L. Patterson, Zeits. f. Krist. **90**, 517 (1935).
[10] Notation of *Int. Taf. zur Best. der Krist.*

[11] I am indebted to Dr. Frederick Seitz for a discussion of this interpretation. It was Dr. Seitz' interest in the problem which suggested the research reported here.

Letters to the Editor

THIS section will accept reports of new work, provided these are terse and contain few figures, and especially few halftone cuts. The Editorial Board will not hold itself responsible for opinions expressed by the correspondents. Contributions to this section should not exceed 600 words in length and must reach the office of the Managing Editor not later than the 15th of the month preceding that of the issue in which the letter is to appear. No proof will be sent to the authors. The usual publication charge ($3.00 per page) will not be made and no reprints will be furnished free.

The Carbon-Carbon Bond Strengths in Ethane, Propane, and *n*-Butane

E. R. VAN ARTSDALEN
Department of Chemistry, Lafayette College, Easton, Pennsylvania
August 19, 1942

RECENTLY the carbon-hydrogen bond strengths in methane and ethane were determined from kinetic data by Andersen, Kistiakowsky, and Van Artsdalen[1] who gave values which agree very well with those obtained by Stevenson[2] from measurements of electron impact potentials. In the calculation of the carbon-hydrogen bond strengths the various energy relations were not corrected to absolute zero. When this is done, one finds that the CH_3-H bond strength, in round numbers, is 101 kcal. at 0°K, 102 kcal. at room temperature, as reported, and 103 kcal. at 450–475°K.

The heat of dissociation of carbon-hydrogen bonds may be combined with other established thermal data to calculate carbon-carbon bond strengths in several simple hydrocarbons. From thermal data tabulated by Rossini[3] one obtains the following at 298.16°K:

$$2CH_4=C_2H_6+H_2-15.54 \text{ kcal.}$$

This can be combined with the value of 102 ± 1 kcal. for the strength of the CH_3-H bond and with the value for the heat of dissociation of hydrogen[4] to obtain a value for the CH_3-CH_3 bond strength. Thus at 298.16°K

$$\begin{aligned} 2CH_4&=C_2H_6+H_2 - 15.5 \text{ kcal.}\\ 2CH_4&=2CH_3+2H -204 \text{ kcal.}\\ H_2&=2H \quad -102.9 \text{ kcal.}\\ \hline C_2H_6&=2CH_3 - 85.6 \text{ kcal.} \end{aligned}$$

The probable error is ±2.3 kcal.

This value is in good agreement with that calculated by Stevenson.[2] Trenner, Morikawa, and Taylor[5] obtained 97.6 kcal. employing their value of 108 kcal. for the CH_3-H bond strength. It seems certain that the carbon-carbon bond strength in ethane must be lower than the carbon-hydrogen bond strength in ethane (98 ± 2 kcal.) to account for pyrolytic products. Rice and Johnston[6] estimated from activation energies of free radical formation at high temperature a C–C bond of 74 kcal. Because chain decomposition appears to be less frequent than had been thought, Kistiakowsky[7] suggested that the true bond strength is higher than 74 kcal.

Similar calculations may be made to determine the carbon-carbon bond strength in propane and the center bond in normal butane. The necessary data (heats of formation of the hydrocarbons, C–H bond strengths in CH_4 and C_2H_6, and the heat of dissociation of H_2) are given in the above references. This method of calculating carbon-carbon bonds may be applied wherever the appropriate carbon-hydrogen bonds and heats of formation of the hydrocarbons are known. The following resumé of values for 298.16°K is obtained:

CH_3-CH_3	85.6 ± 2.3 kcal.
$C_2H_5-CH_3$	83.8 ± 3.3 kcal.
$C_2H_5-C_2H_5$	82.4 ± 4.5 kcal.

Lowering of the C–C bond strength with increasing chain length is observed in agreement with expectation. It is noted that a CH_2 increment lowers the bond strength about 1.5 kcal. However, qualitative rather than quantitative significance should be attached to this because of the rather large probable errors.

[1] Andersen, Kistiakowsky, and Van Artsdalen, J. Chem. Phys. **10**, 305 (1942).
[2] D. P. Stevenson, J. Chem. Phys. **10**, 291 (1942).
[3] F. D. Rossini, Chem. Rev. **27**, 1 (1940).
[4] Bichowsky and Rossini, *Thermochemistry* (Reinhold, 1936).
[5] Trenner, Morikawa, and Taylor, J. Chem. Phys. **5**, 203 (1937).
[6] Rice and Johnston, J. Am. Chem. Soc. **56**, 214 (1934).
[7] G. B. Kistiakowsky, J. Phys. Chem. **41**, 175 (1937).

The Partition Function of a Gas of Hard Elastic Spheres

O. K. RICE
University of North Carolina, Chapel Hill, North Carolina
September 8, 1942

TONKS[1] has derived the equation of state of a one-dimensional gas consisting of N hard elastic spheres of radius σ, constrained to move along a line of length l. The partition function, found readily from his work, is

$$Q=[(2\pi mkT/h^2)^{\frac{1}{2}}e(l/N)(1-\theta)]^N, \qquad (1)$$

where $\theta=N\sigma/l$. The factor e^N, occurring because the whole effective length $l(1-\theta)$ can be shared, gives rise to a "communal entropy" of Nk.

In three dimensions Tonks considers separately the dilute and the concentrated gas. For the former he uses an equation of state of the virial type, Eq. T(31). (T refers to Tonks' equations.) For the concentrated gas, Tonks obtains an equation of state, Eq. T(32), by an ingenious argument, which is equivalent to using as the partition function

$$Q=[(2\pi mkT/h^2)^{\frac{1}{2}}ev^{\frac{1}{3}}(1-\theta^{\frac{1}{3}})]^{3N}, \qquad (2)$$

essentially the cube of Eq. (1), with $v^{\frac{1}{3}}$ (v=volume per molecule) taking the place of l/N, and $\theta^{\frac{1}{3}}$ replacing θ. In Eq. (2), $\theta=\sigma^3/2^{\frac{1}{2}}v$; thus the free volume $v(1-\theta^{\frac{1}{3}})^3$ vanishes when the spheres are in contact in a face-centered cubic lattice. To bridge the gap between Eq. T(31) and Eq. T(32), Tonks gives an interpolation formula, Eq. T(33).

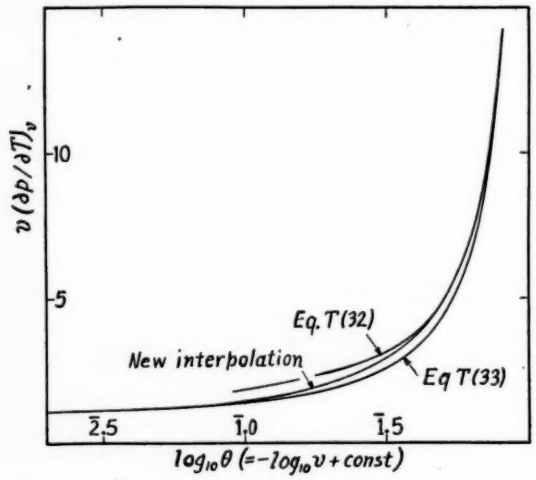

FIG. 1.

In Eq. (2) the factor e^{3N} corresponds to the large communal entropy $3kN$, because lengths are shared in the three directions of space, rather than volume being shared as such. That such a large communal entropy can exist does not seem to have been explicitly pointed out before, though it is implicit in an earlier note by the writer.[2] In the dilute gas, the communal entropy is only kN. Thus the change of entropy per mole from a small volume v_1 to a large volume v_2 will be

$$\Delta S = RT \ln [v_2/v_1(1-\theta^{\frac{1}{3}})^3] - 2R. \quad (3)$$

ΔS can also be calculated by integrating the thermodynamic equation $v(\partial p/\partial T)_v = (\partial S/\partial \ln v)_T$, using Eq. T(33) (see Fig. 1). This gives a ΔS about 1 entropy unit smaller than does Eq. (3), despite the $-2R$ in the latter. A better interpolation is shown in Fig. 1; this assumes that Eq. (2) holds to somewhat lower values of θ than does use of Eq. T(33). The agreement that can thus be obtained shows the essential consistency of Tonks' ideas and seems to offer support to the correctness of the large communal entropy inherent in Eq. (2).

[1] L. Tonks, Phys. Rev. **50**, 955 (1936).
[2] O. K. Rice, J. Chem. Phys. **9**, 121 (1941).

The Partition Function of a Simple Liquid

O. K. RICE
University of North Carolina, Chapel Hill, North Carolina
September 8, 1942

IF we neglect the mutual potential energy of the atoms and consider only the thermal energy, a face-centered cubic solid bears a resemblance to a close-packed gas of hard spheres. We can get an effective value θ_0 for θ of Eq. (2) (preceding note) by equating Q to the thermal part of the partition function for the solid, eT^3/Θ^3 (where Θ is the Debye characteristic temperature). Θ may be obtained as a function of interatomic distance, if the intermolecular potential energy is known.

This may be extended to the liquid, if we consider it to be formed from the solid by introduction of holes through removal of atoms; these holes then contribute to the free volume.[1] If there are N atoms and n holes, we write $\theta = \theta_0 N/(n+N)$, where θ_0 is the value for the solid with the same interatomic distance, obtained as in the preceding paragraph. We substitute θ into Eq. (2), noting also that the molecular volume has been increased by a factor $(n+N)/N$.

This procedure gives only that part of the partition function due to the thermal motion. We must consider, also, the energy necessary in order to produce a hole, already discussed in previous work.[2] But, in addition, in order that these holes should actually be used, it is necessary for the atoms to move past each other, with fluctuations in the distances between nearest neighbors. These fluctuations show up in the atomic distribution curves obtained from x-ray investigations, which show a broader band of nearest-neighbor distances than can be accounted for by thermal motion alone. This results in a further increase in the average potential energy, whose order of magnitude in the liquid can be estimated from the atomic distribution curves. In order that the holes should be effectively used, the increase in entropy gained therefrom must more than counterbalance the increase of energy due to both causes noted above.

These ideas have been applied to argon. In doing this the free energy is minimized using n/N as an additional parameter. The picture appears to work very well in explaining the properties of the liquid at the normal melting point. At 193°K, the theory makes the liquid appear to be too compressible. This seems to be due in large part to two causes. (1) The potential energy curve previously deduced[3] and used in these calculations probably does not rise steeply enough at small distances. (2) It will be recognized that if a close-packed model gas of hard elastic spheres contains only a few holes, these holes cannot be used to increase the freedom of motion, since they are blocked off by surrounding spheres. As the number of holes increases, a point will rather suddenly be reached where they can be shared. In our model of a liquid, some similar effect will occur. This matter will be discussed in a fuller report, in the light of the data and the detailed calculations.

The entropy of the liquid obtained on this model agrees fairly well with that calculated by the method given in a previous note.[1] It is slightly smaller, which is perhaps in the wrong direction, but it increases somewhat more slowly with n/N, and in this respect appears to give a better indication of the behavior of the liquid.

[1] Compare O. K. Rice, J. Chem. Phys. **9**, 121 (1941).
[2] O. K. Rice, J. Chem. Phys. **7**, 883 (1939).
[3] O. K. Rice, J. Am. Chem. Soc. **63**, 3 (1941).